Aromatic Hyperbranched Polymers: Synthesis and Application

Anindita Ghosh, Susanta Banerjee, and Brigitte Voit

Abstract Hyperbranched (hb) polymers have been receiving increasing attention because of their unique architecture that results in an interesting set of unusual chemical and physical properties. Over the past decade quite a number of excellent reviews on hb polymers have been published by different research groups, covering various aspects of this class of polymers. This review will highlight the work on aromatic hb polymers of the last decade, emphasizing general synthetic strategies and recent development of alternative synthetic strategies, and discussing various aspects of hb polymers to demonstrate their wide range of applications.

Keywords Hyperbranched polymers · Polymer applications · Polymer synthesis

Contents

A. Ghosh (✉)
Department of Applied Science, Symbiosis Institute of Technology (SIT), Symbiosis
International University (SIU), Lavale, Pune 412115, India
e-mail: andy.iitkgp@gmail.com

S. Banerjee
Materials Science Centre, Indian Institute of Technology, Kharagpur 721302, India

B. Voit
Leibniz-Institut für Polymerforschung Dresden e. V., Hohe Strasse 6, 01069 Dresden,
Germany

Abbreviations

6F-BPA	4,4′-(Hexafluoroisopropylidene)diphenol
AFM	Atomic force microscopy
BPA	4,4′-Isopropylidenediphenol
BPADA	2,2-Bis[4-(3,4-dicarboxyphenoxy) phenyl]propane dianhydride
BTDA	3,3′,4,4′-Benzophenonetetracarboxylic dianhydride
C-BPA	4,4′-(9-Fluorenylidene)diphenol
$CHCl_3$	Chloroform
Đ	Dispersity (M_w/M_n)
DB	Degree of branching
DMAc	Dimethyl acetamide
DMF	Dimethylformamide
DMSO	Dimethyl sulfoxide
DSC	Differential scanning calorimetry
EB	Elongation at break
FTIR	Fourier transform infra-red spectroscopy
GPC	Gel permeation chromatography
HQDPA	1,4-Bis(3,4-dicarboxyphenoxy)benzene dianhydride
hb	Hyperbranched
M_n	Number average molecular weight
M_w	Weight average molecular weight
NMP	N-Methylpyrrolidinone
NMR	Nuclear magnetic resonance
ODA	4,4′-Oxydianiline
ODPA	4,4′-Oxydiphthalic dianhydride
PAA	Polyamic acid
PL	Photoluminescence
PMDA	Pyromellitic dianhydride
SEM	Scanning electron microscopy
T_c	Crystallization temperature
T_d	Onset decomposition temperature
$T_{d,5\%}$	5% weight loss temperature
$T_{d,10\%}$	10% weight loss temperature
TEM	Transmission electron microscopy
T_g	Glass transition temperature
TGA	Thermogravimetric analysis
THF	Tetrahydrofuran
T_m	Melting temperature
UV	Ultraviolet

1 Introduction to Hyperbranched Polymers

The research activities in the field of hyperbranched (hb) polymers have generated an innovative and impressive number of new hb polymers, together with first applications of these materials. With the availability of synthetic strategies from a wide range of building blocks and with precise control over polymer architecture and functionality, hb polymers have attracted a great deal of attention during the past decade for many interesting applications. New synthetic methodologies have allowed the preparation of highly branched molecules under controlled conditions, and new analytical techniques have allowed the characterization of these materials [1–8]. Numerous unusual and novel properties have been noted for hb and dendritic macromolecules [9–11], and new applications are now appearing at a rapid pace [12–15].

Hyperbranched polymers are promising in practical applications due to their one-pot synthetic route on a large scale, as compared to dendrimers, which require multistep synthesis. Compared with linear polymers, hb polymers have lower viscosity and better solubility due to their abundant functional groups and globular shape. The ease of preparation of hb polymers has led to their incorporation into many copolymers [3, 16]. Copolymerization of linear monomer with branched monomer as a random component generates material with controlled branching that can enhance the properties of linear polymers [17, 18] and also lead to products that have added flexibility [19–22]. Hyperbranched polymers are frequently used as the core of core–shell block copolymers, with the shell block grown from the functional groups of the hb polymer [23–26]. They have also been grown from linear polymers to form diblock [27], triblock [28–30], and graft copolymers [31–33]. It is believed that the terminal groups of hb polymers can greatly affect the macromolecular properties, such as the glass transition temperature, solubility, dielectric properties, hydrophobicity, and thermal stability [34].

Of particular interest from an industrial point of view are the impressive advances that have been made using hb polymers for rheology modifiers, processing aids and, more recently, as functional materials in coatings, catalysts, sensors, biomaterials, emitting materials, nanotemplating applications, and piezo-electric sensors [35–42]. Many hb polymers have already been used as modifiers for different matrix polymers, especially for large-scale engineering plastics. Polymer blending is also a useful approach for combining the advantages of individual components [43]. The different structures of the hb polymers influence the properties of the blends in different ways.

This review is organized in the following way: In the first part, recent developments in the synthesis of various aromatic hb polymers are discussed. In the second part, the applications of hb polymers in polymer processing, including melt modifiers, additives, and blend components as classical examples, are discussed. In addition, the review includes a detailed discussion of new areas that are being explored for the use of hb polymers, such as materials for fuel cell applications, gas separation, optics, and electronics.

## 2 Synthesis of Aromatic Hyperbranched Polymers

Hyperbranched polymers have attracted increasing attention because of their ease of synthesis, high degree of functionality, and material properties. Many strategies have been developed for the preparation of polymers with highly branched structure; in particular, the convenient and cheap one-step polycondensation of AB_x monomer has received significant attention [44, 45]. Many hb polymers have also been prepared via the $A_2 + B_3$ synthetic approach [46, 47]. Kim has reported the synthesis of aromatic hb polyamides from AB_2 and A_2B-type monomers [48]. Monticelli et al. [49] have reported the synthesis of hb aromatic polyamides from an AB_2 monomer, namely 5-(4-aminobenzoylamino) isophthalic acid. Polymerizations were carried out in N-methylpyrrolidinone (NMP) using triphenylphosphite/pyridine as condensing agent. Yamakawa and Ueda developed a 'one-pot–multistep' strategy for the synthesis of aromatic hb polyamides with relatively low dispersities (Đ) of 1.1–1.5 and very high degree of branching (DB) of 80–90% [50, 51]. Their strategy consisted of a repetitive sequence of in situ carboxyl group activation and condensation reactions. Kakimoto and coworkers synthesized hb polyamides [52] using p-phenylenediamine or 4,4′-oxyphenylenediamine as A_2 monomer and trimesic acid as B_3 building block. The structures of these A_2 and B_3 monomers are shown in Scheme 1.

Russo and coworkers have extensively investigated hb polyamides prepared by homopolymerization of 5-(4-aminobenzamido) isophthalic acid or copolymerization of p-phenylenediamine and trimesic acid as supports for the preparation of Pd and Pt nanoparticles [53, 54]. Fang et al. [47, 55] first reported the synthesis of hb polyimides (hb-PIs) from a triamine, tris(4-aminophenyl)amine, and commercially available dianhydrides. The hb-PIs showed a combination of the excellent high temperature characteristics of linear polyimides together with high solubility, low viscosity, and noncrystallinity resulting from the hb structure. Melt polycondensation has been applied for the synthesis of aromatic and aromatic–aliphatic based hb polyesters, leading to broad molar mass distributions and limited molecular weights [56, 57]. Carboxylic acid chloride end-functionalized all-aromatic hb polyesters were prepared from the AB_2 monomer 5-(trimethylsiloxy) isophthaloyl dichloride [56] and the structure of this AB_2 monomer (**1–1**) is shown in Scheme 2.

The hb aromatic polyesters prepared via melt condensation reaction resulted in materials with a very high glass transition temperature (T_g) due to rigidity of the polymer backbones. However, the synthesis of hb polymers with much more facile techniques is still desirable. Kricheldorf et al. [58] synthesized highly branched aromatic polyesters from 3,5-bis(trimethylsiloxy)-benzoyl chloride as an AB_2 type monomer (**1–2**, Scheme 2). Moore and Stupp synthesized linear polyesters [59] by solution condensation using a condensing agent such as 1,3-dicyclohexylcarbodiimide (DCC) and a catalyst [4-(N,N-dimethylamino) pyridinium 4-tosylate] and the method was further utilized for the synthesis of hb polyesters. Blencowe and coworkers reported the synthesis of a rigid hb polyester using coupling agents such as DCC and 1,3-diisopropylcarbodiimide with an AB_2
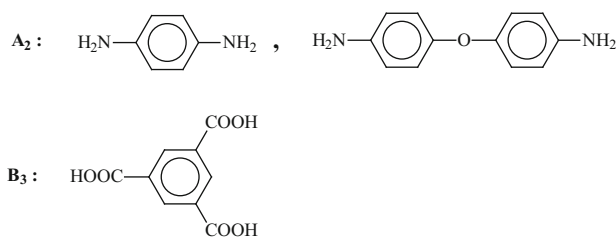
Scheme 1 Structures of A_2 and B_3 monomers used for preparation of hb polyamides [52]
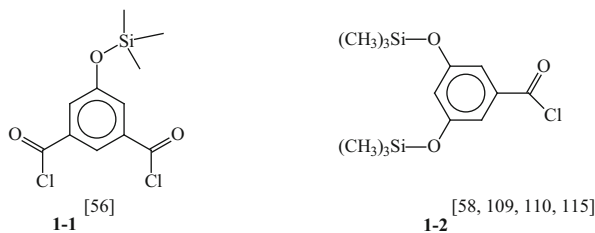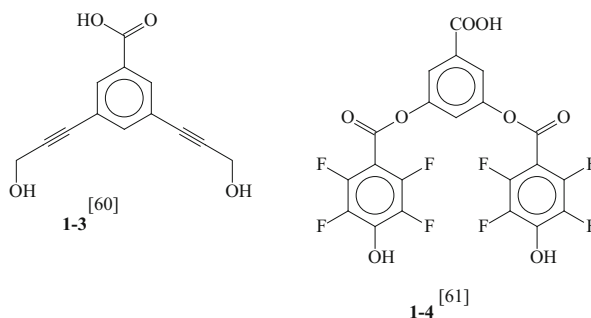

Scheme 2 Structures of AB_2 monomers used for preparing hb aromatic polyesters

monomer, namely 3,5-bis (3-hydroxylprop-1-ynyl)-benzoic acid [60] (**1–3**, Scheme 3). Jen and colleagues [61] reported a fluorinated hb aromatic polyester that was prepared by mild one-step polyesterification of an AB_2-type monomer, namely 3,5-bis(4-hydroxy-2,3,5,6-tetrafluorobenzoate)benzoic acid (**1–4**, Scheme 3), at room temperature using DCC and 4-(dimethylamino)pyridium 4-toluenesulfonate as the condensing agents.

Nucleophilic displacement of an activated dihalo or dinitro compound with an activated bisphenoxide salt at high temperatures has been the most explored method of poly(aryl ether) synthesis [62]. These synthetic strategies were further extended for the preparation of hb poly(aryl ether)s in one-step polymerization from AB_2 monomers containing a phenolic group and two aryl fluorides, which were activated toward nucleophilic displacement by a sulfone, ketone, imide, or heterocycle [63–65]. Miller et al. [63], Hawker and Chu [65], and Shu and Leu [66] reported the synthesis of hb poly(aryl ether ketone)s (hb-PAEKs) via the AB_x method. The structures of AB_2 monomers reported by Hawker and Chu [65] are shown in Scheme 4 (**1–5** and **1–6**). The structures of AB_2 monomers reported by Shu and Leu [66] are shown in **1–7**, Scheme 4.

The synthesis of hb-PAEKs via the $A_2 + B_3$ approach has been reported by many research groups [67, 68]. Choi et al. [69] reported a self-controlled synthesis of hb-PAEKs from diphenyl ether (or 1,4-diphenoxybenene, B_2) and trimesic acid (A_3) via the Friedel–Crafts reaction. Baek and coworkers developed optimized conditions for Friedel–Crafts acylation in poly(phosphoric acid)/phosphorus pentoxide (PPA/P_2O_5) medium for the preparation of hb-PAEKs [70, 71]. Martinez and Hay [72, 73] proposed the efficient synthesis and characterization of hb poly(aryl ether sulfone)s with a K_2CO_3/Mg(OH)$_2$ catalyst system for nucleophilic aromatic substitution. Kim et al. [74] reported the controlled nucleophilic aromatic

Scheme 3 Structures of AB$_2$ monomers used for preparation of hb polyesters [60, 61]
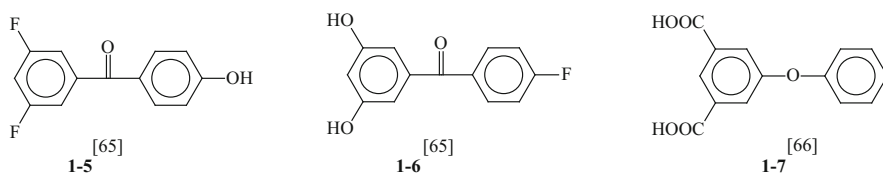
Scheme 4 Structures of AB$_2$ monomers used for preparation of hb-PAEKs [65, 66]

substitution reaction (S$_N$Ar) of BC-type monomer, namely 5-fluoro-2-nitrobenzo-trifluoride [where the reactivity of B (fluoro group) > C (nitro group)], with A or A$_2$-type phenolate for the formation of two aromatic ether linkages. The nitro group activated by the trifluoromethyl group at the *ortho* position had a strong electron-withdrawing capability, enabling the displacement of other leaving groups at the *para* position before it was displaced.

The authors also investigated unusual growth of hb poly(arylene ether)s using 1,1,1-tris(4-hydroxyphenyl ethane as A$_3$-type and 5-fluoro-2-nitrobenzotrifluoride as BC-type monomer by one-pot synthesis with stepwise fluorine displacement followed by nitro displacement [75].

The *trans*-etherification reaction was realized during the polymerization of the above A$_3$ + BC system, leading to various types of growing species whose functional groups were dynamically exchanged during the polymerization. The monomer combination A$_3$ + BC is shown in Scheme 5.

Kim and Webster first prepared hb polyphenylenes from 3,5-dibromophenyl 4-boronic acid and dihalophenyl Grignard reagents by palladium-catalyzed and nickel-catalyzed aryl–aryl coupling reactions, respectively [76]. The structures of 3,5-dibromophenyl 4-boronic acid (**1–8**) and dihalophenyl Grignard reagents (**1–9**) are shown in Scheme 6.

Tang and coworkers [77] used cobalt-catalyzed polycyclotrimerization of aromatic diynes for the preparation of hb polyphenylenes. The representative structures of aromatic diynes used for homopolycyclotrimerizations are shown in Scheme 7.
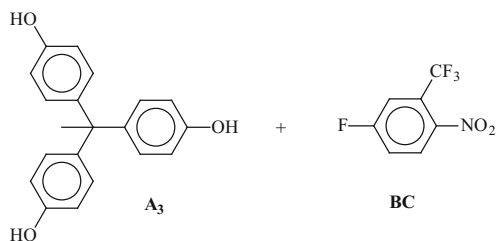
Scheme 5 Monomer combination A_3 + BC used for the synthesis of hb poly(arylene ether)s
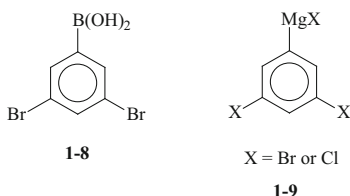
Scheme 6 Structures of 3,5-dibromophenyl 4-boronic acid and dihalophenyl Grignard reagents [76]
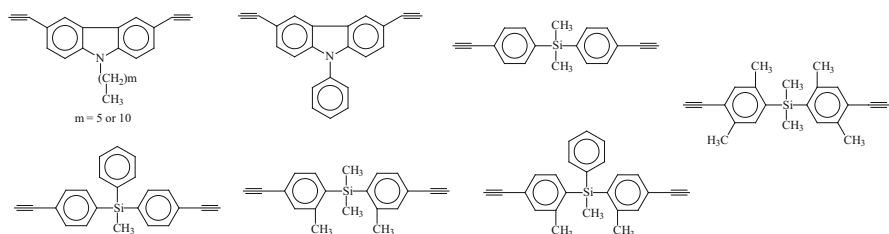
Scheme 7 Representative structures of aromatic diynes used for homopolycyclotrimerizations [77]

2.1 General Synthetic Approaches and Theoretical Aspects

Hyperbranched polymers are more promising for industrial applications than dendrimers because of single-step polymerizations, which are convenient for large-scale production. Hyperbranched polymers were first introduced by Flory in 1952 [78]. Flory presented hb polymers from a theoretical point of view, describing the intermolecular condensation of AB_x-type monomers. There are three types of repeating units, classified as dendritic (D), linear (L), and terminal (T), depending on the number of unreacted B functional groups in the structure of the hb polymers obtained from AB_x or $A_2 + B_x$ type monomers. In 1991, Hawker and Fréchet [79] described the degree of branching (DB) of AB_2 products as a factor for explaining the structure of the hb polymers:

$$DB = (D + T)/(D + L + T). \qquad (1)$$

Because the number of dendritic units is theoretically equal to the number of terminal units at high molecular weights, Hawker and Chu [65] and Frey and coworkers [80] modified the definition as follows:

$$DB = 2D/(2D + L), \tag{2}$$

$DB = 0$ for a linear polymer because there is no branching and $DB = 1$ for a perfect dendrimer because it is completely branched.

   Copolymerization has been widely used with polycondensation reactions to alter or enhance the physical properties and improve the processability of the final polymer. The introduction of the AB monomer allows control of the content of branching units. There are numerous reports in which an AB monomer has been copolymerized with an AB_x type monomer to afford copolymers with varying DB values, where DB is a typical characteristic frequently used to evaluate the irregularity of the structure of hb polymers.

   The DB of the hb polymers resulting from the copolymerization of AB_2 with AB monomers depends on the fraction of branching unit AB_2 according to Eq. (3):

$$DB \;=\; 2rx/\left[r(1-x) + (1+r)^2\right], \tag{3}$$

where x represents the conversion ratio of A groups and r represents the feed fraction of AB_2 monomers in the total.

   The maximum value the DB can reach is 0.5 when the reaction is close to completion for the AB_2 polycondensation system. The DB of the hb polymers resulting from the copolymerization of AB_2 and AB monomers depends greatly on the initial fraction of AB_2 monomer in the total feed. At the end of the reaction, when $x = 1$, Eq. (3) reduces to $DB = 2r/(1+r)^2$.

   Highly branched polymeric structures are also attainable through the polymerization of $A_2 + B_3$ monomers, but at a functional equivalence, when three-dimensional (3D) structures are developed, the polymer becomes a gel or highly crosslinked material that is insoluble in any organic solvent [78, 81]. Hence, polymerization requires careful control of the reaction to produce soluble hb polymers. The polycondensation to prepare hb polymers utilizing the $A_2 + B_3$ approach leads to gelation at the later stage of reactions (at a specific critical conversion and critical concentration) and affects the structure and properties of the final products. The gelation occurs because of the nonlinear propagation of macromolecules through the intermolecular reaction, which depends on the monomer reactivity and molecular steric elements. By choosing the appropriate monomer concentration and composition ratio, or controlling the reaction conversion, the crosslinking can be effectively avoided. A deeper understanding of the kinetics of $A_2 + B_3$ polymerization is valuable for both academic and practical application. Recently, Yang et al. [82] applied a 3D reactive bond fluctuation lattice model to study the kinetics of nonideal $A_2 + B_3$-type hb polymerization with consideration of the intramolecular cyclization, monomer reactivity, and steric elements. This model was further

used to simulate a realistic example of an $A_2 + B_3$ polycondensation system from the work of Voit and colleagues [83, 84], utilizing fitting approximations.

It is well known that avoidance of gelation is crucial in the synthesis of hb polymers. Hence, low monomer concentration, intense stirring, and slow addition speed are used to maintain the lowest local concentration in order to prevent gelation for $A_2 + B_3$-type hb polymerization. Flory's theory of gelation in the polymerization of $A_2 + B_3$ monomers is based on the following requirements for gelation: the equal reactivity of all A groups as well as B groups, the exclusive reactivity of A groups with B groups, and no intramolecular cyclization or chain termination in the process [85]. Thus, if an $A_2 + B_3$ polymerization does not obey these assumptions, gelation can be avoided. Recently, the more facile synthetic approach of $A_2 + BB'_2$ was developed [86–90] because of the more effective avoidance of gelation in this system compared with $A_2 + B_3$. In this approach, monomers are used that contain the same functional groups but with different reactivities, allowing for the formation of an intermediate AB_2 type monomer that is further polymerized to an hb polymer [91].

Litvinenko and coworkers [92, 93], Beginn et al. [94], Dusek et al. [95], Cameron et al. [96], and Galina et al. [97] have discussed the theoretical aspects of the related polycondensation systems in detail. Recently, Zhou et al. investigated the kinetics of the co-polycondensation of AB_2 and AB-type monomers in the presence of multifunctional cores [98].

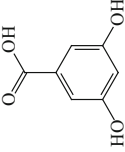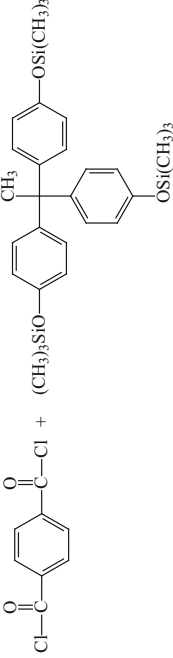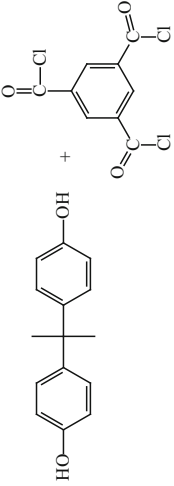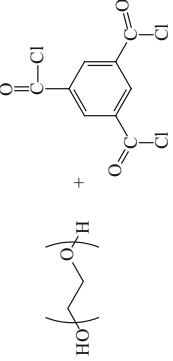## 2.2 Synthesis of Selected Aromatic hb Polymers

Unlike linear polymers, hb polymers are highly branched 3D macromolecules and have inherent internal cavities and abundant terminal groups, which often lead to better processability, compatibility, and solubility [99]. The terminal groups of hb polymers can greatly affect the macromolecular properties, such as the T_g, solubility, dielectric properties, hydrophobicity, and thermal stability. For example, aromatic polyamides (aramids) are well known as high-performance polymers [100]. However, hb structures are introduced [101, 102] in order to improve the poor processability caused by the rigid repeating unit in aramids. As an important engineering plastic, poly(phenylene oxide) has outstanding thermal, mechanical, and dielectric properties [103, 104]. However, its poor moldability, poor solubility, and inadequate adhesive strength limit its application. Compared with linear polymers, hb polymers show lower viscosity and better solubility due to the branching and their abundant functional groups and, therefore, hb poly(phenylene oxide)s, which combine the merits of poly(phenyl oxide) and hb polymers, have been synthesized to expand their application. Linear polyphenylenes [105] are found to be only partially soluble in most common organic solvents as they tend to aggregate in the solid state because of interchain π–π stacking interactions. Introducing the highly branched structure of these materials has made them attractive because of improved solubility and reduced or eliminated strong intermolecular interactions

and aggregation [106]. We will now discuss the synthesis of selected hb polymers such as hb poly(aryl ester)s, hb poly(aryl amide)s, hb polyimides, hb poly(aryl ether)s, hb poly(phenylene oxide)s, hb poly(phenylene sulfide)s, and hb poly (phenylene)s.

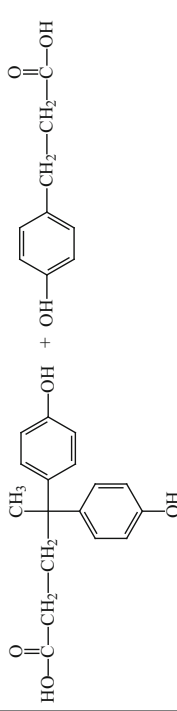### 2.2.1 Hyperbranched Poly(aryl ester)s

Melt polymerization is widely used in preparation of hb poly(aryl ester)s in industry because of the easy one-step process, but the solution polymerization route is more attractive because of the mild polymerization conditions, which reduce the potential for side reactions. Voit and coworkers [107] performed one-pot solution polycondensation of commercially available 3,5-dihydroxybenzoic acid as AB_2 monomer (Table 1, entry 1), at room temperature in the presence of 4-(dimethylamino) pyridinium-4-tosylate as catalyst to suppress the formation of N-acylurea. Different carbodiimides as coupling agents were investigated to find the optimal esterification conditions. To compare the properties of the AB_2 aromatic polyesters produced by different pathways, the solution polycondensation was compared with their well-known analogs synthesized in melt [78, 108]. Because of the mild reaction conditions, completely colorless fully OH-terminated hb aromatic polyester with narrow Đ was obtained. The degree of polymerization could be simply controlled by the reaction time, in contrast to melt polycondensation. The product showed a DB of 60%, which was similar to that of the product previously reported by melt polymerization of 3,5-bis(trimethylsiloxy) benzoyl chloride [78] and was higher in comparison with ideal statistically branched polymers from AB_2 monomers (which should posses a theoretical DB of 50%). The authors attributed the high DB to the activation or deactivation of different reaction sites as a result of different electron densities caused by different substituents formed during the course of the reaction in both melt and solution. Thermal analysis indicated that the hb polyesters were amorphous in nature in contrast to the linear analog poly(m-hydroxybenzoate), which is semicrystalline with a T_g of 145°C and a melting point T_m of 183°C [58]. Previously, Schmaljohann and coworkers [109, 110] used quantitative NMR to analyze the kinetics of the melt polycondensation of 3,5-bis(trimethylsiloxy)benzoyl chloride in detail using the contents of different structural units at different degrees of conversion. A major accelerating effect was a result of preferred formation of the most stable phenolate, which favored the formation of dendritic units as per the previous findings reported in literature [111, 112]. Recently, Khalyavina et al. [113] studied the effect of the DB on the T_g of hb polyesters and observed that the DB did not show much influence on the T_g of the polymers with an identical amount of phenolic –OH groups per unit. For example, the T_g and M_n values of OH-terminated polymers with DB = 8% (M_n = 14,500 Da, T_g = 155°C) and DB = 50% (M_n = 17,000 g/mol, T_g = 152°C), were close to each other. This finding was also in accordance with that observed previously by Wooley et al. [114], where linear, hb, and dendritic polyesters containing an identical amount of phenolic –OH groups per unit showed similar T_g values in the range 197–204°C.

Table 1 Monomer structures and monomer combinations used for the synthesis of hb poly(aryl ester)s

Entry no.	Monomer structures and monomer combinations	Polymerization type	References
1		AB_2	[107]
2		$A_2 + B_3$	[115]
3		$A_2 + B_3$	[116]
4		$A_2 + B_3$	[117]

(continued)

Table 1 (continued)

Entry no.	Monomer structures and monomer combinations	Polymerization type	References
5		$A_2 + B_3$	[118]

Voit and coworkers [115] prepared hb polyesters by solution polycondensation at room temperature from the previously reported monomer, namely 3,5-bis (trimethylsiloxy)-benzoyl chloride (Scheme 2, **1–2**) [109, 110]. Fully soluble aromatic AB_2 hb polyesters with a DB of about 55% in very high yield (~98 %) and of high molar mass ($M_w = 45,000$ Da) were achieved, which was in accordance with results previously reported in the literature [79, 108]. The hb polyesters showed high T_g of 220°C and $T_{d,5}$ of ~380°C. The hb aromatic polyesters prepared by the $A_2 + B_3$ approach were also prepared by Voit and coworkers [115], where the A_2 monomer was terephthaloyl chloride (TCl) and the B_3 monomer was 1,1,1-tris (4-hydroxyphenyl)-ethane (THPE) or THPE modified with 1,1,1-tris(4-trimethylsiloxyphenyl)ethane (TMS) (see Table 1, entry **2** for monomer combination). All the polymerization reactions were conducted at room temperature due to the high reactivity of the TCl. In order to avoid gelation, the polycondensation of TCl (A_2) and THPE (B_3) was performed in dilute solution by slowly adding TCl solution to the THPE solution. The synthesis was carried out using different monomer ratios (A_2:B_3 = 3:2, 1:1, 3:4, and 1:2). The structures of the $A_2 + B_3$ hb polyesters as well as the DB were calculated from the NMR spectra. Well-separated signals corresponding to the different subunits confirmed the hb structure of the $A_2 + B_3$ hb polyester. In general, on approaching the stoichiometric ratio of the functionalities, the molecular weight of the resulting hb polymers increased and, as a result, the T_g and DB also showed an increasing trend. However, at the same time, gelation could not be avoided with higher monomer concentration or when high molar mass products were aimed for. Gelation was observed for higher A_2 ratios (3:2 and 1:1 at a monomer concentration of 57 mmol/L), resulting in insoluble polymers and, hence, gel permeation chromatography (GPC) could not be performed. The T_g values of the polymers obtained were in the range of 199–268°C, which showed an increasing trend with increasing molecular weight. A high T_g of 268°C was realized for M_w as high as 28,500 Da, at an A_2:B_3 molar ratio of 1:1. Interestingly, the melt rheology of $A_2 + B_3$ (3:4) hb polyester from solution polymerization indicated viscous behavior with a shear thinning effect, whereas AB_2 polyester behaved as a completely elastic material.

Hyperbranched poly(aryl ester)s via the polycondensation of A_2 and B_3 monomers were also prepared utilizing the $A_2 + B_3$ approach by Lin and Long [116]. A dilute bisphenol A (A_2) solution was added slowly to a dilute 1,3,5-benzenetricarbonyl trichloride (B_3) solution at 25°C to prepare hb poly(aryl ester) s in the absence of gelation (see Table 1, entry **3** for monomer combination). The molar ratio of A_2:B_3 was maintained at 1:1, and the maximum final monomer concentration was maintained at 0.08 M to avoid gelation. Gelation was not observed, even at longer reaction times of 72 h. Moderate values of M_w of the hb poly(aryl ester)s were obtained in the range of 10,000 and 22,000 Da, with Đ values ranging from 2.45 to 3.48. The molecular weights did not show any increase on increasing the reaction time. The DB was determined to be in the range 47–55%. The hb polymers exhibited lower solution viscosities, as expected, and also exhibited lower T_g values than the linear analogs, ranging from 130 to 150°C,

depending on molecular weight. The authors attributed this to poor chain entanglement of the hb polymers in comparison to the linear analogs.

Tailoring the DB through the synthesis of hb poly(ether ester)s was accomplished by Unal et al. [117]. The polymerizations were conducted at room temperature using the $A_2 + B_3$ approach for the reaction of an acid chloride (1,3,5-benzenetricarbonyltrichloride) with poly(ethylene glycol) (PEG) (see Table 1, entry **4** for monomer combination) in the presence of anhydrous triethylamine (TEA) and using chloroform as solvent. In general, reactions were allowed to proceed for 24 h to ensure complete conversion. When a dilute solution of B_3 monomer was added to a dilute solution of A_2 oligomer, highly crosslinked products were obtained regardless of the rate of addition. In contrast, slow addition of the oligomeric A_2 solution to the B_3 solution yielded branched polymers. The monomer concentration did not show much influence on the molar mass and the Đ of the final products. Commercially available PEG diols of various number-average molecular weights (M_n) controlled the DB. ^{1}H NMR spectroscopy indicated a DB of 69% for a highly branched poly(ether ester) derived from 200 g/mol PEG diol. In general, the molar mass increased with increasing monomer concentration for PEG-600, decreased with increasing monomer concentration for PEG-2000, and changed nonsystematically for the samples derived from PEG-200. Decrease in molar mass with increased monomer concentration for hb poly(ether ester) derived from PEG-2000 was attributed to the limited solubility of the A_2 oligomer and the branched products at higher concentrations. Gelation during the polymerization was also observed at higher monomer concentration for various PEG-diols of M_n 200, 600, and 2,000 g/mol. Molar mass distributions broadened with increasing weight-average molar mass (M_w). The effects of branching and the length of the PEG segments also showed interesting thermal properties of the highly branched polymers, as detected by differential scanning calorimetry (DSC). The branched poly(ether ester)s based on PEG-2000 showed T_g values ranging from -42 to $-51°C$ and a depressed T_m of 40°C, relative to both the A_2 oligomer (PEG-2000) and the linear poly(ether ester) based on PEG-2000, consistent with the reduced crystallization behavior of branched polymers.

A one-pot solution polymerization was performed at room temperature using partially aromatic monomers, namely 4,4-bis(4′-hydroxyphenyl)valeric acid as AB_2 and 3-(4-hydroxyphenyl)propionic acid as AB [118] (see Table 1, entry **5** for monomer combination), in the presence of 4-(N,N dimethylamino) pyridinium 4-tosylate (DPTS) as catalyst and dicyclohexylcarbodiimide (DCC). The dependencies of the DB and the thermal properties of the polymers on the AB:AB_2 monomer ratio were studied. Polyesters with statistical dendritic topology, controlled DB, and $M_w > 35,000$ g/mol were obtained. The DB was found to decrease with an increase in the amount of AB monomers and increasing comonomer ratio in the polymer (r_p = ratio of AB to AB_2) as shown in Fig. 1. Interestingly, the DB for hb homopolyester and branched copolyester at $r_p = 0.46$ was similar (see Fig. 1a), because of the fact that on adding the small-sized linear AB to the more voluminous AB_2 monomers in the reaction mixture, the steric effects decreased, which promoted the formation of dendritic units formed by the AB_2 monomer. The thermal
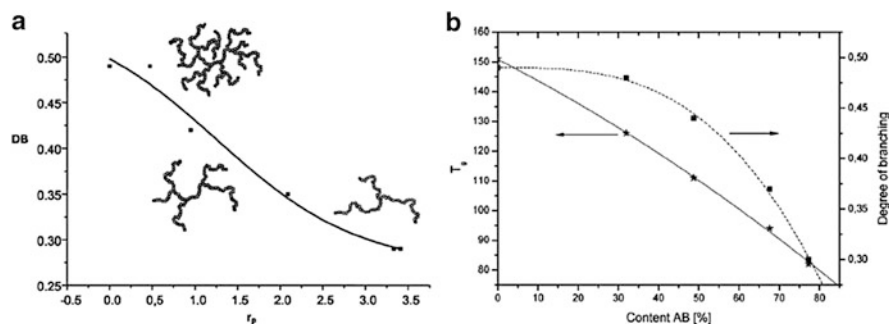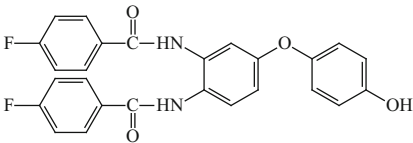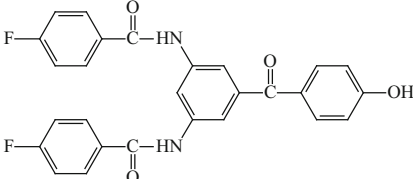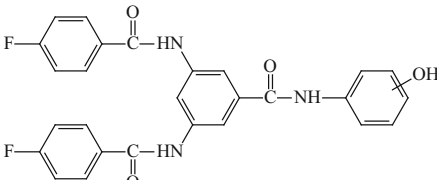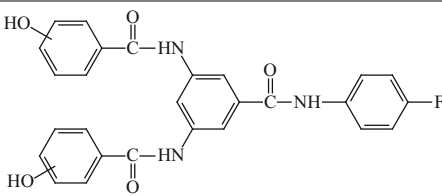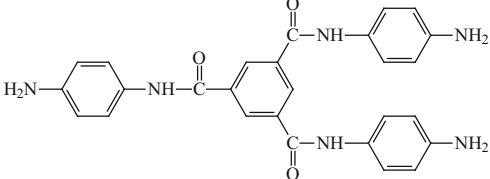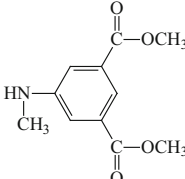
Fig. 1 (**a**) Degree of branching (DB) versus ratio of AB to AB_2 (r_p). (**b**) Influence of the content of AB units on DB and T_g. Reproduced with permission from [118]

behavior strongly depended on the branching of the polymers. Theoretically, with increasing DB, the T_g should decrease but an opposite behavior was observed. The T_g value is also dependent on the flexibility of the polymers. DSC measurements showed a decrease in the T_g with a decrease in the DB, which was ascribed to the higher flexibility of the polymer structures containing an increasing amount of AB units. The T_g of homopolymer resulting from AB_2 monomer was 151°C and that of copolymer resulting from $AB + AB_2$ monomer combinations with $r_p = 0.46$ was 125°C. The hb homopolyester and copolyesters ($r_p = 0$, 0.46, and 0.94–2.00) showed an amorphous behavior. However, the decrease in the DB and increase in the number of linear units in the polymers enabled the formation of crystalline sections. For this reason, the hb copolyester with $r_p = 3.44$ showed a broad melting region, and the T_g ranged from 150 to 220°C with a maximum at 178°C. The dependence of the T_g on the DB and the content of AB units in the copolymer is shown in Fig. 1b. The T_g decreased from 150 to 81°C with increasing AB content in the copolymer as the flexibility of the chains increased, which in turn decreased the T_g. Thermogravimetric analysis (TGA) showed a higher thermal stability for the branched copolyesters, with maximum decomposition temperature in the range 430–450°C, in comparison with the maximum decomposition temperature of 400°C for the hb homopolyester.

2.2.2 Hyperbranched Poly(aryl amide)s and Poly(arylether amide)s
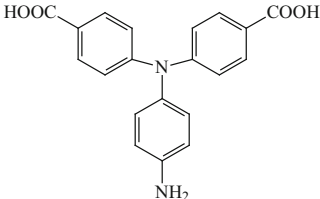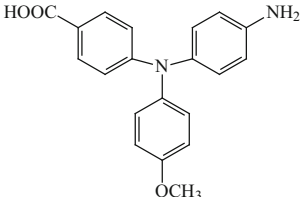
Polymers containing arylamide units have been prepared by forming the amide bonds directly during polymerization or by using monomers that contain amide units and linking them, e.g. by nucleophilic substitution, to form poly(arylether amide)s. for example, Baek and Harris [119] prepared two self-polymerizable AB_2 amide monomers, namely N,N'-bis(4-fluorobenzoyl)-3,4-diamino-4'-hydroxydiphenylether (Table 2, entry **1**) and N,N'-bis(4-fluorobenzoyl)-3,5-diamino-4'-hydroxybenzophenone (Table 2, entry **2**), and polymerized them to afford a hb poly(aryl ether amide) and a hb poly(aryl ether ketone amide). The aryl fluoride-

Table 2 Structures of monomers used for the synthesis of hb poly(aryl ether amide)s and poly
(aryl amide)s

Entry no.	Monomer structures	Type of monomer	References
1		AB$_2$	[119]
2		AB$_2$	[119]
3		AB$_2$	[120]
4		A$_2$B	[120]
5		B$_3$	[121]
6		AB$_2$	[122]

(continued)

Table 2 (continued)

Entry no.	Monomer structures	Type of monomer	References
7	HOOC—⟨structure⟩—COOH, N, ⟨structure⟩—NH$_2$	A$_2$B	[123]
8	HOOC—⟨structure⟩, NH$_2$, N, ⟨structure⟩—OCH$_3$	AB	[125]

terminated hb poly(aryl ether amide) and poly(aryl ether ketone amide) were amorphous and soluble in many common organic solvents, including THF and CHCl$_3$. However, hb poly(aryl ether ketone amide) showed a higher T_g of 269°C compared with that of poly(aryl ether amide), which showed a T_g value of 210°C. The thermal stability evaluated by TGA also showed a similar trend. The $T_{d,5\%}$ values in N$_2$ were recorded as 323°C and 433°C for hb poly(aryl ether amide) and poly(aryl ether ketone amide), respectively. The authors attributed the drastic weight loss at 323°C to the intramolecular formation of imidazole moieties with a concomitant loss of 4-fluorobenzoic acid.

Hyperbranched poly(aryl ether amides) with fluorine or hydroxy end groups were synthesized by In and Kim [120] from AB$_2$ (Table 2, entry **3**) or A$_2$B (Table 2, entry **4**) type monomers via a nucleophilic aromatic substitution (S$_N$Ar) reaction. Monomer syntheses were facilitated by chemoselective amidation reactions, and even a direct synthesis of hb polymer was possible without isolation of the monomer. The resulting hb poly(aryl ether amide)s showed highly branched characteristics, with DB ranging from 43 to 53%. All hb polymers were readily soluble in polar aprotic solvents such as DMF, DMSO, and NMP, regardless of the end groups, due to the high amide contents and longer branching distances between adjacent branching points in the hb polymer backbones. The M_n values measured by GPC were in the range of 46,200 to 112,400 Da. The polymers showed a high T_g of over 220°C and high thermal stability, with $T_{d,10\%}$ over 420°C.

Shabbir et al. [121] aimed to prepare aromatic and semi-aromatic amine-terminated hb polyamides without gelation via direct polymerization of triamine as B$_3$ monomer with different aliphatic and aromatic diacid chlorides (terephthaloyl chloride, isophthaloyl chloride, sebacoyl chloride, and adipoyl chloride) as A$_2$ monomers. An aromatic triamine (B$_3$), 1,3,5-tris(4′-aminophenylcarbamoyl)benzene (TAPCB) (Table 2, entry **5**), was reacted with two aromatic and two aliphatic

diacid chlorides (terephthaloyl chloride, isophthaloyl chloride, sebacoyl chloride, and adipoyl chloride) to yield four hb polyamides. In this work, the ratio A_2:B_3 was set to 2:3 to control the polymerization without catalyst by consideration of reactants and reaction conditions; no free acid chloride groups existed in the polymers, making these amine-terminated polymers. No gelation occurred for the selected reaction temperature and time (0°C for 3 h) with a monomer concentration of 10 mmol. Products containing a large amount of terminal amine groups resulted. The polymers were soluble in polar aprotic solvents at room temperature. The hb polyamides in general showed low molecular weights in the range of 13,000–27,000 Da and DB in the range of 51–55%. Higher molar masses could not be achieved because of the off-stoichiometry chosen to prevent gelation. The T_g values for hb polyamides were in the range of 138–198°C, depending on the rigidity of the polymer structure, the highest being for the hb polyamide containing rigid benzamide units and the lowest for the hb polymer with an alkyl–amide chain. The $T_{d,5\%}$ values recorded in nitrogen for the hb polyamides were in the range of 262–331°C, indicating moderate thermal stability. The hb polyamides studied by X-ray diffraction showed no crystallinity, indicating an amorphous nature that was attributed to the highly branched architecture preventing the packing of macromolecules through hydrogen bonding between the amide groups.

Ohta et al. [122] reported a new approach for controlling the polymerization of AB_2 monomers from a core initiator by utilizing the change in substituent effects between monomer and polymer to suppress statistical self-condensation but favor a type of chain growth. The polymerization of AB_2 monomer (Table 2, entry **6**) was carried out utilizing a mixture of 1.1 equivalents of lithium 1,1,1,3,3,3-hexamethyldisilazide (LiHMDS) and 6.7 mol% of core initiator in the presence of lithium chloride (LiCl), where LiCl helped in reducing the reactivity of the intermediate amide anion. The obtained hb polyamides showed controlled molecular weight and narrow dispersity, $Đ \sim 1.11$, indicating that the controlled polymerization of AB_2 monomer was not only governed by slow monomer addition, but also by the change in substituent effects between the monomer and polymer to suppress self-polymerization.

Liou and coworkers [123] synthesized A_2B type monomer (Table 2, entry **7**) by chemical modification of end functional groups incorporating *para*-methoxy-substituted triphenylamine groups [124], which lowered the oxidation potentials and afforded different electrochromic characteristics. Furthermore, the content of branching units could also be tuned by copolymerization of the A_2B with AB type monomer (Table 2, entry **8**), namely 4-amino-4'-carboxy-4''-methoxytiphenylamine [125]. The aromatic hb polyamide formed by self-condensation of A_2B monomer and the copolymer formed by utilizing the monomer combination $A_2B + AB$ were prepared by the usual polycondensation method using triphenyl phosphite and pyridine. The hb polyamide formed by self-condensation of A_2B monomer was post-functionalized with an amino monomer as the end-capping agent. The high solubility of the hb polyamides in polar aprotic solvents such as NMP, DMAc, DMF, and DMSO and also in THF was attributed to the incorporation of bulky, 3D triphenylamine moieties along the polymer backbone, which

resulted in a high steric hindrance for close packing, and thus reduced their tendency to crystallize. A high T_g in the range of 193–211°C was recorded, depending upon the stiffness of the polymer chain, and DSC thermograms indicated the amorphous nature of the hb polyamides. The $T_{d,10\%}$ of these polymers in nitrogen and air were recorded as 505–550°C and 510–535°C, respectively, indicating good thermal stability.

2.2.3 Hyperbranched Polyimides

Aromatic polyimides represent an important class of high-performance polymeric materials because of their many outstanding key properties, such as high mechanical strength, high modulus, unusual thermoxidative stability, excellent electrical properties, and superior chemical resistance [126, 127]. Hyperbranched polyimides (hb-PIs) show high T_g and superior solubility due to their 3D architecture as well as excellent physical and chemical properties.

Similarly to hb poly(aryl amide)s, the imide function in hyperbranched polyimides can be formed directly through imidation of the respective anhydride (acid)- and amine-containing AB_2 monomers or $A_2 + B_3$ monomer combinations or by polymerization of imide function-containing monomers leading, e.g., to poly (ester imide)s or poly(ether imide)s. Kricheldorf et al. synthesized a poly(ester imide) from a trifunctional imide monomer [128]. Maier et al. synthesized a heterocyclic hb-PI from a monomer containing a maleimide group (A) and an azine group (B_2) through a crisscross cycloaddition polymerization [129]. Moore and coworkers [130] reported the preparation of aromatic hb-PIs through the nucleophilic etherification of a protected AB_2 monomer (**1–10**, Scheme 8). The self-polycondensation was carried out through the nucleophilic etherification of silylated phenol and aryl fluoride in diphenylsulfone at 240°C in the presence of cesium fluoride. Other AB_2-type monomers were also prepared for the synthesis of hb-PIs via nucleophilic etherification, as shown in **1–11**, Scheme 8 [131].

An AB_2-type monomer (**1–12**, Scheme 8) was prepared by Hao et al. [132] by multistep synthesis. The AB_2 monomer was self-condensed to form five hb-PIs by variation of the concentration and reaction temperature. The synthesized hb-PIs showed good solubility in polar aprotic solvents such as in DMF, DMAc, DMSO, and NMP with a DB around 50%. The hb-PIs prepared from the new AB_2 monomer were observed to be soluble in polar aprotic solvents like NMP, DMF, and DMSO. The self-condensation of AB_2 monomer at room temperature, carried out at a dilute concentration of 0.06–0.16, led to low molecular weight oligomers of ~11,100 Da and, hence, polymerization was investigated at higher solution concentration and at a temperature of 50°C. Increasing the solution concentration from 0.06 to 0.32 g/mL showed a limited increase in molecular weight up to 25,500 Da; however, increasing the temperature to 50°C at a dilute concentration of 0.08 g/mL resulted in a marked increase in molecular weight to 173,000 Da. The T_g values of the hb-PIs were found to be in the range of 155–161°C and showed an increasing trend with
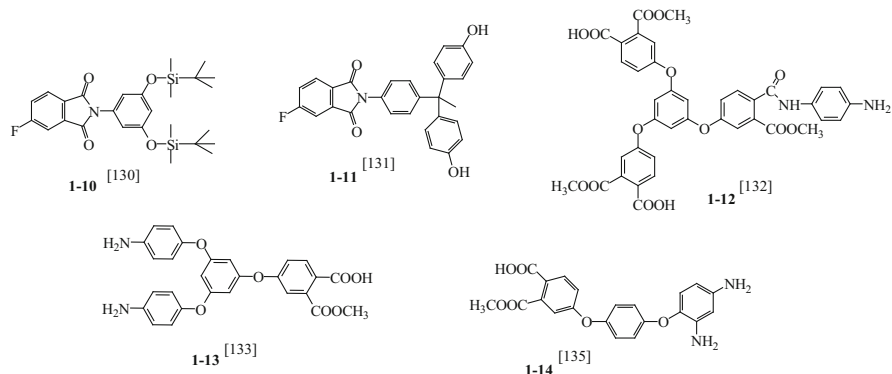
Scheme 8 Structures of some AB_2 monomers used for the synthesis of hb-PIs

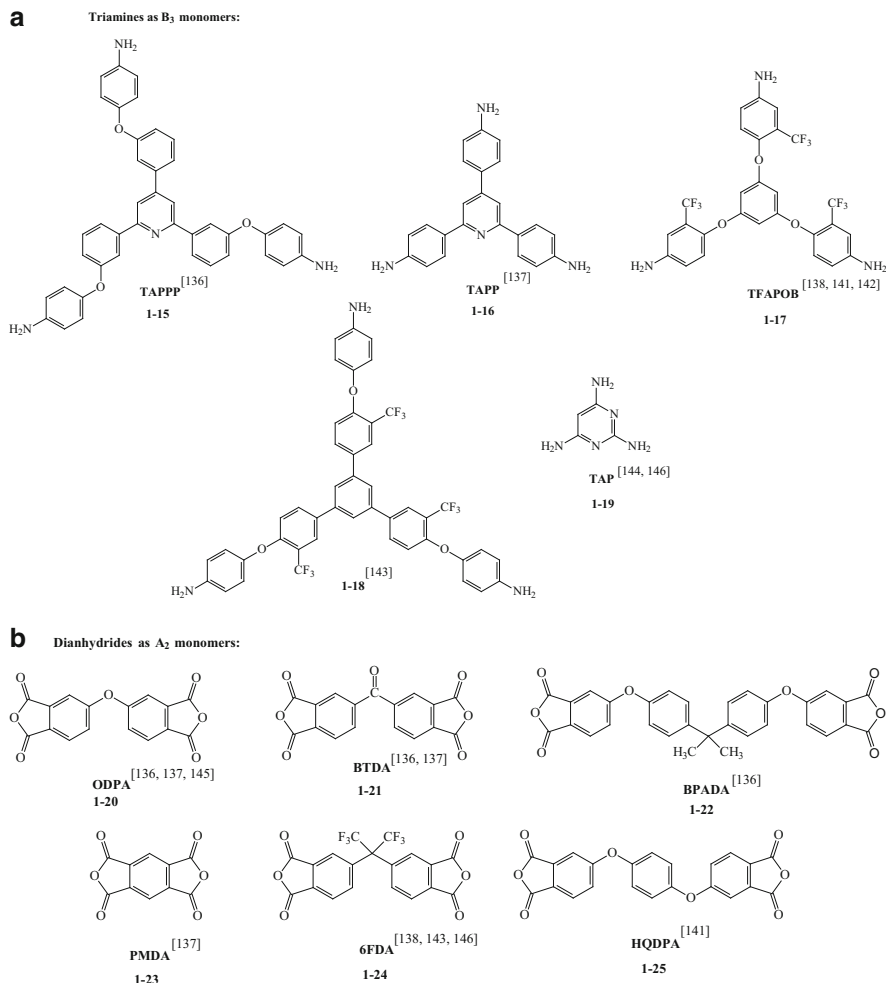increase in molecular weight. The $T_{d,5\%}$ values for the hb-PIs were 445–460°C, indicating high thermal stability.

An AB_2-type monomer (**1–13**, Scheme 8), was synthesized by Yamanaka et al. [133] starting from 3,5-dimethoxyphenol via a polyamic acid methyl ester precursor. The aromatic hb-PIs were prepared by chemical imidization in the presence of acetic anhydride and pyridine. The synthesized polyimides were soluble in polar aprotic solvents and showed thermal stability, with a $T_{d,10\%}$ of 470°C in nitrogen and a T_g of 193°C. In another work by Yamanaka et al. [134], the same AB_2 monomer containing free amine end groups of the precursor was end-capped with acetyl, *n*-heptanoyl chloride, and 4-methylphthalic anhydride. By chemical imidization of these precursors in the presence of acetic anhydride and pyridine, hb-PIs were prepared. The DB of the hb-PIs was ~50% as expected. The hb-PIs showed a $T_{d,5\%}$ above 395°C, and T_g values of 189, 138, and 186°C for the end groups of acetoamide, *n*-heptanoamide, and 4-methylphthalimide, respectively.

Wang et al. [135] prepared a novel ABB' monomer (**1–14**, Scheme 8), namely 4-[4-(2,4-diaminophenoxy)phenoxy] phthalic acid 2-methyl ester, which was polymerized to form the precursor polyamic acid monomethyl ester. The direct polycondensation of the ABB' monomer was carried out to form polyamic acid monomethyl ester as a precursor and had a M_n of 12,000 Da. Chemical imidization in the presence of acetic anhydride and pyridine gave hb-PIs with low DB. The DB of the precursor, as determined by the ^{1}H NMR spectra, was only 7%. They ascribed the low DB to the differences in the reactivities of the amino groups. End modification reactions were accomplished with acetyl chloride, benzoyl chloride, and phthalic anhydride to form end-capped polyimides. The end-group-modified polyimides were soluble in polar aprotic solvents such as DMSO, DMF, and NMP. TGA measurements showed $T_{d,5\%}$ in the range of 400–520°C, and T_g of 200–258°C. The hb-PIs showed film-forming ability, but they were more brittle than analogous linear polymers.

Shen et al. [136] prepared several hb-PIs from a BB'_2-like aromatic triamine monomer, namely 2,4,6-tris[3-(4-aminophenoxy)phenyl]pyridine (TAPPP) (**1–15**

Scheme 9a), with commercial aromatic dianhydrides [4,4′-oxydiphthalic dianhydride (ODPA), 3,3′,4,4′-benzophenonetetracarboxylic dianhydride (BTDA), and 2,2-bis[4-(3,4-dicarboxyphenoxy) phenyl]propane dianhydride (BPADA)] as A_2 type monomers by the $A_2 + B_3$ approach. A different monomer addition order and changes in monomer molar ratios resulted in different hb-PIs. The addition of dianhydride into triamine TAPPP with a monomer molar ratio of 1:1 yielded the amine-terminated hb-PIs, whereas the reverse monomer addition order with a molar ratio of 2:1 gave the anhydride-terminated hb-PIs. The monomer was added slowly to avoid any high local concentration. The amine-terminated hb polyamic acids (hb-PAAs) were thermally imidized in solution at 180°C for 24 h, whereas the anhydride-terminated hb-PAAs were chemically converted into hb-PIs using a mixture of excess acetic anhydride and pyridine. The hb-PIs were obtained in high yields (95–98%). The DB for anhydride-terminated hb-PIs based on ODPA (**1–20**, Scheme 9b), BTDA (**1–21**, Scheme 9b), or BPADA (**1–22**, Scheme 9b) with TAPPP was 100%, indicating a completely branched structure. For amine-terminated hb-PIs, it was impossible to determine the DB by ^{1}H-NMR because the peaks of linear units and terminal units were always in the same range. For the amine-terminated and anhydride-terminated hb-PIs based on BPADA with TAPPP, the M_w was 92,000 and 32,000 Da, respectively. The DSC measurements of the amine-terminated hb-PIs showed T_g in the range of 232–258.5°C and the anhydride-terminated hb-PIs showed T_g in the range of 219–273.5°C. The highest T_g was recorded for BTDA-based hb-PIs and the lowest T_g in the series was detected for BPADA-based hb-PIs because of the flexible ether linkages present in the structure. In the dynamic mechanical analysis (DMA), the T_g values of obtained hb-PI films were in the range of 214–270°C, showing similar values to those detected by DSC. The $T_{d,10\%}$ values for the hb-PIs were in the range of 532–575°C for the amine- and anhydride-terminated hb-PIs, indicating high thermal stability. The hb-PI films showed film-forming ability. Their mechanical properties were evaluated and showed high tensile strength of 83–96 MPa, tensile modulus of 1.8–2.4 GPa, and low elongation at break (EB) of 5–7%.

Chen et al. [137] employed microwave irradiation for the preparation of amine- or anhydride-terminated hb-PIs. A $BB′_2$-type triamine monomer, namely 2,4,6-tris (4-aminophenyl)pyridine (TAPP) (**1–16**, Scheme 9a), was synthesized under microwave irradiation to prepare a series of amine- and anhydride-terminated triphenylpyridine-containing hb-PIs by $A_2 + BB′_2$ polymerization. Several commercially available aromatic dianhydrides, namely pyromellitic dianhydride (PMDA, **1–23**, Scheme 9b), BTDA, and ODPA, were used as A_2 type monomers to react with the $BB′_2$ type aromatic triamine (TAPP). The addition of dianhydride to triamine with a monomer molar ratio of 1:1 yielded the amine-terminated polymer, whereas the reverse monomer addition order with a molar ratio of 2:1 gave the anhydride-terminated polymer. Slow monomer addition was used to avoid any high local concentration. The authors kept the total solid content below 0.08 mol/L for the amine-terminated polymer and 0.06 mol/L for the anhydride-terminated polymer to prevent insoluble gels. During the whole polymerization, continuous microwave irradiation was employed to enhance the reactivity and

a   Triamines as B₃ monomers:

TAPPP[136]
1-15

TAPP[137]
1-16

TFAPOB[138, 141, 142]
1-17

TAP[144, 146]
1-19

[143]
1-18

b   Dianhydrides as A₂ monomers:

ODPA[136, 137, 145]
1-20

BTDA[136, 137]
1-21

BPADA[136]
1-22

PMDA[137]
1-23

6FDA[138, 143, 146]
1-24

HQDPA[141]
1-25

Scheme 9 Structures of (**a**) triamines as B₃ monomers and (**b**) dianhydrides as A₂ monomers commonly used for the synthesis of hb-PIs

shorten the reaction time. The amine-terminated hb-PAAs were thermally imidized in solution in the presence of *m*-xylene at 170°C, whereas the anhydride-terminated hb-PAAs were chemically converted into hb-PIs using a mixture of excess acetic anhydride and pyridine at 40°C. All resulting hb-PIs were obtained in high yields (95–98 wt%). The model compounds of terminal and linear analogous units were not easy to obtain separately because of their multiple isomers and it was difficult to determine the DB. The amorphous polyimides were soluble in polar aprotic solvents at room temperature or upon heating. The amino- and anhydride-terminated hb-PIs showed $T_{d,10\%}$ values of 568–583°C, indicating high thermal stability. The BTDA- and ODPA-based hb-PIs showed high T_g values of 311–339°C. The

thermally cured solution-cast films evaluated for mechanical properties showed tensile strength and modulus of 53–89 MPa, and 1.0–1.2 GPa, respectively, with low EB of up to 7%.

Gao et al. [138] synthesized fluorinated hb-PIs from a triamine monomer, namely 1,3,5-tris(2-trifluoromethyl-4-aminophenoxy)benzene (TFAPOB) (**1–17**, Scheme 9a), as B_3 monomer (shown in Scheme 2) and 4,4-(hexafluoroisopropylidene)diphthalic anhydride (6FDA, **1–24**, Scheme 9b) as A_2 monomer to form fluorinated hb-PIs by the $A_2 + B_3$ approach. Here, 3,5-ditrifluoromethylphenyl was used as an end-capping reagent. The synthesis route was similar to the conventional two-step method for the synthesis of linear polyimides, but with a different monomer addition order. Molar ratios of the dianhydride monomer and triamine monomer resulted in different hb polymers. The addition of dianhydride to triamine TFAPOB with a monomer molar ratio of 1:1 yielded the amine-terminated polymers, whereas the reverse monomer addition order with a molar ratio of 2:1 gave the anhydride-terminated polymers, as also reported by Chen et al. [137]. All hb-PIs exhibited moderate molecular weights with broad distributions. The anhydride-terminated hb-PI and amine-terminated hb-PI showed T_g values of 232°C and 243°C, respectively, in DSC. They ascribed the difference in T_g values to the appearance of hydrogen bonds in amine-terminated hb-PI and the different content of 6FDA residues in the two polymers [139]. The authors observed that hb-PI showed a birefringence as low as 0.002 at 650 nm, which was attributed to the presence of triamine monomers that reduced the orientation of the bonds in the polymer backbone and thereby reduced the birefringence. Liu et al. [140] used a nonideal $A_2 + B_3$ polymerization approach to obtain fluorinated hb-PIs based on TFAPOB. A series of aromatic ether dianhydride monomers with different flexible linear lengths were used to overcome the poor mechanical properties of globular branched macromolecules. In general, by increasing the linear part of the dianhydride monomer, the entanglements of polymer chains were enhanced and the mechanical properties of fluorinated hb-PIs were further improved.

Gao et al. [141] synthesized –CF$_3$-terminated hb-PI by condensation of a triamine monomer, 1,3,5-tris(2-trifluoromethyl-4-aminophenoxy) benzene (TFAPOB) (**1–17** Scheme 9a), and a commercially available dianhydride monomer, 1,4-bis(3,4-dicarboxyphenoxy) benzene dianhydride (HQDPA, **1–25**, Scheme 9b), using the $A_2 + B_3$ approach. Here, 3,5-ditrifluoromethylaniline was used as an end-capping reagent. In addition, the physical and gas transport properties of CF$_3$-HQDPA were compared with those of the non-trifluoromethyl-terminated fluorinated hb-PI analog. The authors found that the introduction of –CF$_3$ groups at the end of hb polyimide increased oxygen and nitrogen permeability, whereas the selectivity decreased in the presence of the terminal groups. The B_3 monomer TFAPOB (**1–17**, Scheme 9a) was further utilized by Zhang and colleagues [142] together with 4,4′-oxydiphthalic anhydride (ODPA) as A_2 monomer to form fluorinated hb-PIs by the $A_2 + B_3$ approach. Fluorinated hb-PIs end-capped with metallophthalocyanines were prepared by the reaction of dicyanophenyl end-capped fluorinated hb-PI with excessive amounts of 1,2-dicyanobenzene and

the corresponding metal (Cu, Zn, Ni) salt in quinoline. Because of the paramagnetic copper and nickel ions, ^{1}H-NMR analysis was not possible for structural elucidation; however, the UV–vis absorption spectrum supported the chemical structure of metallophthalocyanine-containing hb-PIs. The metallophthalocyanine-containing hb-PIs also showed good solubility in polar aprotic solvents and $CHCl_3$ and their M_n varied from 25,300 to 31,800 Da. The T_g values of these polymers were in the range of 217–225°C and the $T_{d,5\%}$ varied from 440 to 487°C.

Banerjee et al. [143] synthesized a triamine monomer B_3 (**1–18**, Scheme 9a) with the aim of preparing fluorinated hb-PIs by the $A_2 + B_3$ approach using commercially available dianhydrides as A_2 monomers. However, during solution imidization of the amide acids that formed by the reaction of the dianhydrides and B_3 monomer, an appreciable amount of gelation was observed for all the molar ratios, except when 6FDA was used as dianhydride for reaction molar ratio of 1:1 and the solution concentration was maintained at 2.7 wt%. Due to the considerable amount of gelation during solution imidization, further characterization was not explored.

Previously, Park et al. [144] prepared hb-PIs by the polymerization of $A_2 + B_2B'$ monomers. No gelation occurred during the polymerization although the monomer conversions surpassed the theoretical gel points, which was attributed to the unequal reactivity of the amino groups present in 2,4,6-triaminopyrimidine TAP as B_2B' monomer (**1–19**, Scheme 9a). Peter et al. [145] prepared a series of hb-PI membranes by copolymerization of 4,4′-oxydiphthalic anhydride (ODPA), 2,4,6-triaminopyrimidine (TAP), and 4,4′-oxydianiline (ODA) at various molar ratios of comonomers. No gelation occurred during polymerizations, probably because of the different reactivities of the amino groups at the 2- and 4-/6- positions in TAP. These hb-PIs were further explored for gas separation studies.

Recently, Chen et al. [146] also prepared a series of free-standing transparent hb-PI membranes by the $A_2 + B_2B' + B_2$ polymerization approach using 6FDA as A_2 monomer, TAP as B_2B' monomer, and ODA as B_2 monomer. Here too, no gelation occurred during polymerization because of the different reactivities of the amino groups present in the TAP monomer. The DB of the prepared hb-PIs increased from 0 to 69% with increase in the content of branching unit TAP. The T_g decreased in the range of 313–266°C with increasing the content of TAP, which the authors attributed to a lowering of molecular weight [147] with increasing TAP content, which in turn led to higher segment mobility of the macromolecules and, hence, lower T_g values. The TGA measurements revealed that the $T_{d,5\%}$ decreased from 559 to 432°C with increase in the TAP content. These hb-PI membranes were further studied for gas separation applications.

2.2.4 Hyperbranched Poly(aryl ether)s

High molecular weight poly(aryl ether)s can be prepared typically from arylhalogenides and phenols in the presence of weak bases such as potassium carbonate in dipolar aprotic solvents [148–150]. The water formed during the

reaction is removed azeotropically with toluene to promote the polymerization. The S_NAr reaction generally requires a leaving group activated with an electron-withdrawing group at the *ortho* or *para* position. Typical leaving groups are fluorine, chlorine, and nitro groups. Fluorine as a leaving group shows good reactivity due to its small size and high electronegativity.
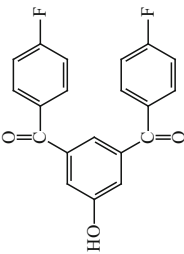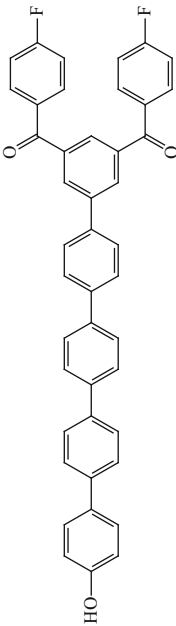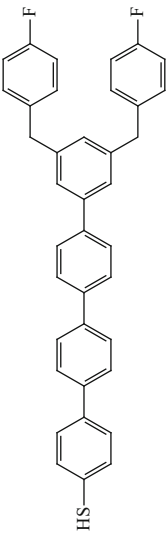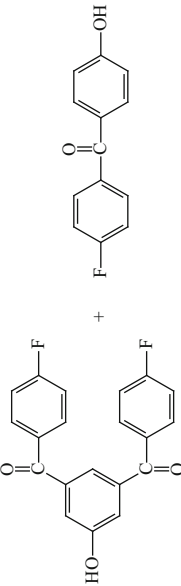
Hyperbranched Poly(aryl ether)s with a Ketone Moiety

Kricheldorf et al. [151] prepared 3,5-bis(4-fluorobenzoyl)phenol from 5-hydroxyisophthalic acid and 5-methoxyisophthalic acid via Friedel–Crafts acylation of fluorobenzene with 5-methoxyisophthaloyl chloride. The 3,5-bis (4-fluorobenzoyl)phenol as AB_2 monomer (Table 3, entry **1**) was polycondensed under various reaction conditions utilizing different solvent mixtures and temperature ranges (DMSO + toluene/140–145°C, NMP + toluene/150–155°C, sulfolane + toluene/150–155°C, sulfolane + xylene/170–175°C). In NMP, the molecular weights of the poly(aryl ether ketone)s were slightly lower than those obtained in DMSO. With sulfolane and either toluene or xylene, the reaction temperature could be raised to 150–155 or 170–175°C, respectively, but the lowest molecular weights were obtained using this solvent. The M_w values were in the range of 7,000 to 12,500 Da. Copolymerizations were carried out using 4,4′-difluordiphenyl sulfone (DFBP) as a comonomer in varying ratios, leading to the formation of star-shaped polymers with a diphenyl sulfone star center. The results were compared with those obtained from 'linear polycondensations' based on DFBP and 4-*tert*-butylcatechol or bisphenol A. The hb poly(aryl ether ketones) (hb-PAEKs) prepared from DFBP had low molecular weights and contained high fractions of cyclic poly(ether ketone)s. The authors concluded that for hb polymers, cyclization competes with propagation at any stage of the polycondensation at any concentration and that for polycondensations with AB_n-type monomers, in general, star-shaped polymers having a cyclic core and hb star arms are formed.

Previously, Morikawa [152] prepared hb-PAEKs with various numbers of phenylene units in the backbone. A representative structure of the AB_2 monomer containing phenylene units is shown in Table 3, entry **2**. The values of T_g for the hb-PAEKs were in the range of 188–218°C and increased with an increasing number of the phenylene units.

Recently, Maken and coworkers [153] prepared AB_2-type monomers, namely 4-thio-3′,5′-bis(4-fluorobenzal)biphenyl,4-thio-3″,5″-bis(4-fluorobenzal)-*p*-terphenyl and 4-thio-3‴,5‴-bis(4-fluorobenzal)-*p*-quarterphenyl (Table 3, entry **3**), starting from 3,5-bis(4-fluorobenzoyl)phenol. The AB_2 monomers were prepared by repeating a series of conversions of the hydroxy group to the triflate, crosscoupling of the triflate with (*p*-methoxythiophenyl) boronic acid, reduction of the carbonyl groups, and subsequent conversion of the methylthio group to a thiol group. The AB_2 monomers self-condensed to form different hb-PAEKs and the T_g was 175, 197, or 215°C, depending on whether the repeat unit structure contained biphenyl, terphenyl, or quadriphenyl units in the polymer backbone.

Table 3 Monomer structures and monomer combinations used for the synthesis of hb poly(aryl ether ketone)s

Entry no.	Monomer structures and monomer combinations	Type of polymerization	References
1		AB$_2$	[151]
2		AB$_2$	[152]
3		AB$_2$	[153]
4		AB$_2$ + AB	[154]

5		$A_2 + B_3$	[155]
6		$A_2 + BB'_2$	[156]

Baek and Tan [154] improved the procedure for preparation of 3,5-bis (4-fluorobenzoyl)phenol (AB$_2$ monomer) at the intermediate step by the use of an acetyl group instead of a methyl group as the protecting group for the hydroxyl function of the AB$_2$ monomer. Alkaline hydrolysis of the intermediate 3,5-bis (4-fluorobenzoyl)phenyloxyacetate led to the desired AB$_2$ monomer, 3,5-bis (4-fluorobenzoyl)phenol. High molecular weight products ($M_w = 23,900$– 49,800 Da) were obtained from that monomer. The T_g value of the hb-PAEK was recorded to be 159°C, which was higher than the previously reported T_g by Miller et al. (140–143°C) [63]. The hb homopolymer showed a bimodal molecular weight distribution that was also observed for other related linear hb systems. The AB$_2$ monomer was also copolymerized with AB monomer, namely 4-fluoro-4'- hydroxybenzophenone, in weight ratios AB$_2$:AB of 1:3, 1:1, and 3:1 to afford the respective hb-PAEKs with variable degrees of branching. The monomer combination AB$_2$ + AB is shown in Table 3, entry **4**. For 1:1 and 3:1 copolymers, the T_g value was 213°C and 164°C, respectively, indicating an increase in T_g with increase in the AB monomer content. The 1:3 copolymer (i.e., at 75 wt% of AB content) was semicrystalline in nature and showed a well-defined melting endotherm at 340°C, but no T_g was observed.

Trimesic acid and phenyl ether were in-situ polymerized as A$_2$ and B$_3$ mono- mers, respectively, in a Friedel–Crafts acylation in the presence of 10 wt% multiwalled carbon nanotubes (MWCNTs) by Baek and coworkers [155] to afford nanocomposites of hb-PAEK and MWCNT (hb-PAEK-g-MWNT). The feed ratios of A$_2$ and B$_3$ monomers varied from 2:3 to 2:1 in a mildly acidic medium. The monomer combination A$_2$ + B$_3$ is shown in Table 3, entry **5**. By simply varying the A$_2$:B$_3$ monomer feed ratio, the polarity of the resulting nanocomposites was altered, changing from highly ionizable (theoretically 100% COOH end groups when A$_2$: B$_3$ = 1:1) to relatively nonpolar (theoretically 100% phenoxy end groups when A$_2$: B$_3$ = 2:1). Because of the globular molecular architecture of hb polymers, the morphology of the nanocomposites resembled 'mushroom-like clusters on MWCNT stalks.' The hb-PAEK-g-MWCNT nanocomposites showed good solu- bility in polar aprotic solvents. The T_g of the nanocomposites was 276–325°C and $T_{d,10\%}$ was recorded to be 477–498°C in air, indicating high temperature stability.
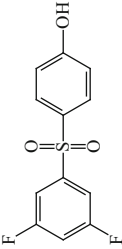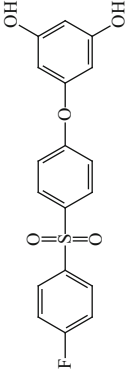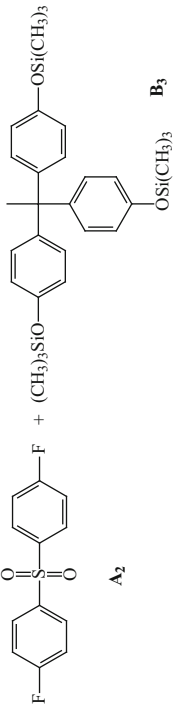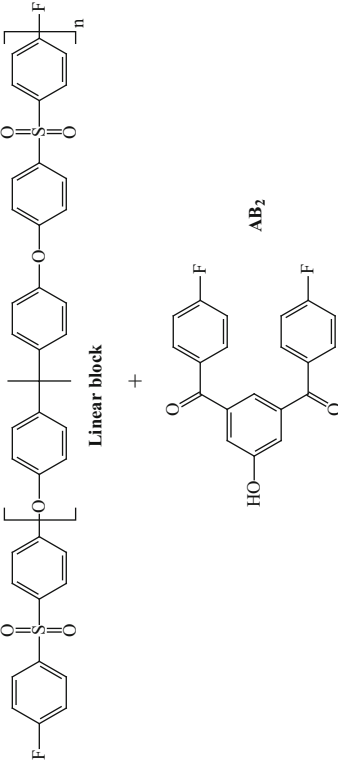
Li et al. [156] prepared hb poly(aryl ether ketone)s by the A$_2$ + BB$'_2$ approach using hydroquinone (A$_2$ monomer) and 2,4',6-trifluorobenzophenone (BB$'_2$ mono- mer). The monomer combination A$_2$ + BB$'_2$ is shown in Table 3, entry **6**. When the feed molar ratio of A$_2$ to BB$'_2$ was less than or equal to 1 (A$_2$:BB$'_2 \leq 1$ or OH: F ≤ 0.67), aryl fluoro-terminated hb poly(aryl ether ketone) (F-hb-PAEK) was obtained. When the feed molar ratio of A$_2$ to BB$'_2$ was greater than or equal to 2 (A$_2$:BB$'_2 \geq 2$ or OH:F ≥ 1.33), phenolic –OH terminated hb poly(aryl ether ketone) (OH-hb-PAEK) was obtained. The chemical structure of F-hb-PAEK and HO-hb-PAEK was confirmed using FTIR and ^{1}H-NMR spectroscopy. In the A$_2$ + BB$'_2$ approach, the reaction of the B group (fluorine located at *para* position of the C=O group) of BB$'_2$ and the A group of A$_2$ monomer was much faster than that of B' group (fluorine located at *ortho* position of the C=O group) of BB$'_2$ and the A group of A$_2$ monomer. Hence, in the initial stage of the reaction, the dimers

AB'_2 were formed predominantly as new monomers, and such dimers further polymerized with each other to form the hb polymer. The DB of F-hb-PAEK was more than 50%, whereas that of OH-hb-PAEK was 100%. Other copolymers were also prepared by using 4,4′-oxydiphenol, bisphenol A, or dihydroxydiphenyl as A_2 monomers. All the hb polymers exhibited good solubility in common organic solvents. The T_g values of the hb polymers varied in the range of 146–176°C, depending on the structure of the A_2 monomers.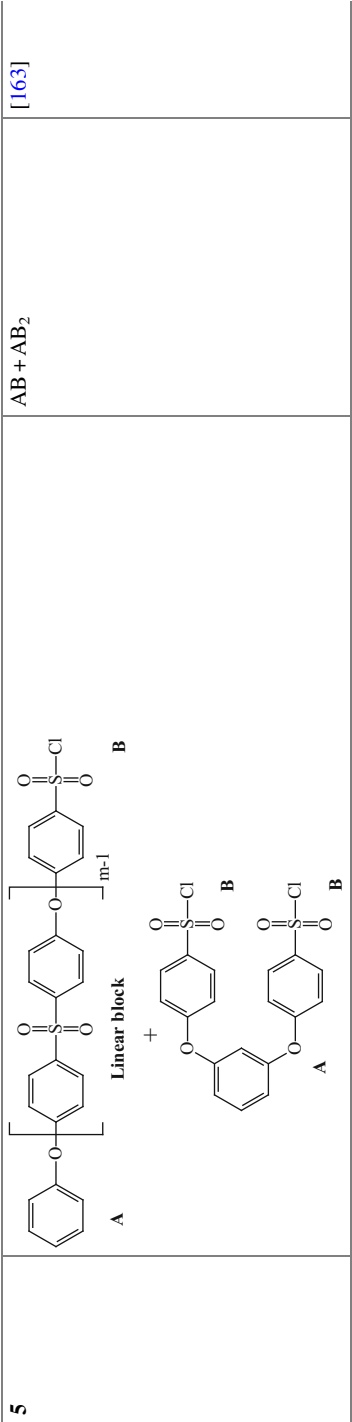 The T_g of OH-hb-PAEK was higher than that of F-hb-PAEK. This difference was attributed to the appearance of hydrogen bonds and the different contents of hydroquinone in the two types of hb polymers. The highest T_g was recorded for the copolymer containing the rigid diphenyl moiety and the lowest T_g was recorded for the copolymer containing isopropylidene groups on account of the flexibility and increased free volume in the polymer. The $T_{d,5\%}$ values of all the hb polymers were above 500°C in nitrogen, indicating high thermal stability.

Hyperbranched Poly(aryl ether)s with a Sulfone Moiety

Himmelberg and Fossum [157] synthesized a new AB_2 monomer, namely 3,5-difluoro-4′-hydroxydiphenyl sulfone) (Table 4, entry 1), by the reaction of 3,5-difluorophenylmagnesium bromide with 4-methoxyphenylsulfonyl chloride, followed by deprotection of the phenol group with HBr in acetic acid. The polymerization of AB_2 in the presence of core molecules, namely 3,4,5-trifluorophenylsulfonyl benzene or tris(3,4,5-trifluorophenyl)phosphine oxide, yielded hb poly(aryl ether sulfone)s, (hb-PAESs) with M_n values ranging from 3,400 to 8,400 Da and Đ values ranging from 1.5 to 4.8. The DB of the hb-PAESs was determined by ^{19}F-NMR spectra of the polymers and found to be in the range 51–70%, which was higher than the 50% usually observed for AB_2-type polymers. No satisfactory explanation was provided by the authors for the higher DB values. The polymerizations were accomplished using two different solvents, namely DMSO and NMP. The hb-PAESs synthesized using DMSO or NMP showed relatively low M_n values of 4,070 Da (Đ = 4.00) and 7,170 Da (Đ = 2.84), respectively. The presence of cyclic oligomeric species, formed by an intramolecular cyclization process, was a contributing factor for the relatively low molecular weights, which were attributed to the tetrahedral geometry of the AB_2 monomer. The intramolecular cyclization was restricted by conducting polymerization at higher concentration, leading to higher Đ values. However, all the M_n values observed for the polymerization reactions of 3,5-difluoro-4′-hydroxydiphenyl sulfone were also relatively low in comparison with the M_n values of the polymers prepared from a similar monomer with a ketone analog [65]. The authors were of the opinion that the low M_n values were due to the presence of core molecules that placed an upper limit on the molecular weight, or due to the formation of small cyclic structures that consumed monomer leading to additional core molecules. The T_g values for the hb-PAESs were in the range of 205–222°C with $T_{d,10\%}$ as high as 500°C under nitrogen.

Table 4 Monomer structures and monomer combinations used for the synthesis of hb poly(aryl ether sulfone)s

Entry no.	Monomer structures and monomer combinations	Type of polymerization	References
1	(structure: aryl ether sulfone with OH and two F)	AB_2	[157]
2	(structure with OH, OH and F)	AB_2	[158]
3	A_2: F—sulfone—F + (CH$_3$)$_3$SiO—...—OSi(CH$_3$)$_3$ B_3	$A_2 + B_3$	[160]
4	Linear block + AB_2 (HO—...—F, F)	Linear block + AB_2	[162]

| 5 | | AB + AB$_2$ | [163] |

Jikei et al. [158] reported the synthesis of a new AB_2 monomer (Table 4, entry **2**) with a sulfone linkage and prepared hb-PAESs and studied their properties. It was found that the reaction conditions affected the DB of the resulting polymers. Self-condensation of the AB_2 monomer to form hb-PAES was explored in three different ways: First, self-condensation of the AB_2 monomer was performed in the presence of a base such as K_2CO_3 in a DMAc/toluene solvent system. Second, the AB_2 monomer was polymerized using cesium fluoride (CsF) in DMAc as solvent by stirring the mixture at 160°C for 10 h. Third, self-condensation of the AB_2 monomer was performed by using low monomer concentration in the presence of DMAc as solvent in a highly diluted solution. The structure of the AB_2 monomer was elucidated by ^{1}H-NMR and ^{13}C-NMR spectra and the peaks confirmed the proposed structure.

The self-condensed polymer prepared in three different ways showed an absolute M_w (determined by GPC-MALLS in NMP) in the range 27,000–270,000 Da. The DB of the hb-PAES prepared at a temperature of 160°C with CsF was higher (DB = 39%) than that of hb-PAES prepared with K_2CO_3 (DB = 17%) although both showed the same T_g value of 217°C. The difference in DB was attributed to the difference between the solubility of dissociated phenolate anions mediated by K_2CO_3 and that of phenolate-ion-like intermediates mediated by CsF [159] for the polymerization reaction. Both the hydroxyl groups of the AB_2 monomer were converted to the corresponding phenolates but the solubility of the diphenolates in the reaction medium was very low compared with the monophenolate. This increased the possibility of reaction between the monophenolate and the AB_2 monomer resulting in the formation of the linear units and causing a lower DB of 17%. In comparison, the phenolate-ion-like intermediates showed better solubility in the reaction medium, leading to a higher DB of 39%. Interestingly, when the heating–cooling scan of the hydroxyl-terminated hb-PAES (DB = 39%) was carried out five times in air at temperatures ranging from 50 to 300°C, the T_g increased from 217 to 236°C and the polymer sample became insoluble in all of the organic solvents, indicating thermal crosslinking. The hb-PAES prepared with K_2CO_3 with DB = 17% also showed an increase in the T_g, but the effect on the increasing trend of T_g was predominantly weaker than for the hb-PAES with DB = 39%. This finding indicated that the increasing trend in T_g was dependent on the DB of hb-PAES. However, the nitrobenzene-terminated hb-PAES did not show the increase in T_g after the heating–cooling scans from 50 to 260°C (repeated five times) in air. The hydroxyl-terminated hb-PAES prepared with CsF showed an improvement in thermal stability after heating at 300°C for 30 min in air and the $T_{d,5\%}$ and $T_{d,10\%}$ were recorded as 406 and 424°C, respectively, due to thermal crosslinking reactions at high temperature. The hydroxyl groups in the hb-PAES were end-functionalized by p-fluoro nitrobenzene to yield nitrobenzene-terminated hb-PAES, which showed a T_g value of 183°C that was lower than the T_g of the hydroxyl-terminated hb-PAES (T_g = 217°C). This difference was attributed to the strong intra-and intermolecular interactions occurring between the hydroxyl groups present in hydroxyl-terminated hb-PAES.

Kricheldorf et al. [160] prepared hb-PAESs from 1,1,1-tris(4-hydroxyphenyl) ethane (THPE) as B_3 and 4,4′-difluorodiphenyl sulfone (DFDPS) as A_2 monomers, either by polycondensation in DMSO with the elimination of water or via the silyl method in NMP. All polycondensations based on silylated THPE were conducted in NMP. The monomer combination of $A_2 + B_3$ monomers is shown in Table 3, entry **3**. The reaction temperature of most experiments was kept at 140–145°C to allow for a comparison with the experiments performed in DMSO and to keep minimum chain scission. The silyl method required longer reaction times than the standard method because the concentration of active end groups (phenoxide ions activated by K_2CO_3) was significantly lower when silylated monomers were used. However, when an exact 1:1 stoichiometry was used, an increase in reaction time from 24 to 48 h did not significantly enhance the molecular weight, whereas a higher temperature for 24 h was more successful. With an exact 1:1 stoichiometry, crosslinking was avoidable. For the silyl method, even an excess of DFDPS of 10 mol% did not result in crosslinking, but larger excess of DFDPS yielded gels after a short reaction time of 2 h.

Lin et al. [161] reported the preparation of hb polymers, with moderately branched, slightly branched, and linear topologies by phenol end-capped telechelic poly(arylene ether sulfone) oligomers as A_2 and tris(4-fluorophenyl) phosphine oxide as trifunctional monomer B_3. When bisphenol A and low molar mass oligomers were used as A_2, pronounced cyclic reactions led to branched products without gelation. The significance of the cyclic reactions decreased as the molar mass of the A_2 oligomers was increased. When moderate molar mass oligomers were used as A_2 monomers, a kinetic excluded volume effect resulted in a low branching efficiency. An increase in the concentration of A_2 oligomer significantly improved the branching efficiency.

Osano et al. [162] reported the synthesis of hybrid linear–dendritic 'ABA'-type architectures, where A and B were hb poly(ether ketone)s and linear poly(ether sulfone)s, respectively. They prepared an AB_2 monomer [3,5-bis(4′-fluorobenzoyl) phenol] to construct the hb segments, in an attempt to provide better control of the resultant hb structures than by utilizing the $A_2 + B_3$ approach. The monomer combination of linear block and AB_2 monomer for the formation of ABA-type architecture are shown in Table 4, entry **4**. Unreacted terminal groups of the ABA polymers were capped by *tert*-butylphenol and sodium 4-hydroxybenzene sulfonate. Such a flexible approach could allow different functional groups on the polymer chain ends simply by replacing the functional group on the phenol in the last part of the synthesis.

Kakimoto and coworkers [163] prepared multiblock linear–hb copolymers by a two-step method involving polymerization of the AB monomer, namely [4-(phenoxy)benzenesulfonyl chloride], to generate the linear block followed by addition of the AB_2 monomer 4,4′-(*m*-phenylene-dioxy)-bis(benzenesulfonyl chloride) in large molar excess (AB_2:AB = 19:1) to generate the hb block. The monomer combinations of linear block AB and AB_2 are shown in Table 4, entry **5**. The thermal properties of multiblock linear–hb polymers were compared with the homo-linear and homo-hb polymers.

The advantage of such a multiblock linear–hb architecture lies in its simplicity, ability to control the ratio of linear to hb blocks, and the avoidance of the potential degradation of the macromonomer sulfonyl chloride by clean-up procedures. The DB of such polymers was difficult to calculate from the ^{1}H-NMR spectra because of the broad, overlapping peaks. The overall AB$_2$:AB monomer molar feed ratio for the entire procedure was 1.35 for 15 min and 0.39 for 1 h for linear–hb block polymerization. The thermal stability of the multiblock hb–linear polymers was intermediate to that of the homo-linear and homo-hb polymers. The linear polymers showed $T_{d,10\%}$ at nearly 500°C, independent of molecular weight, and the hb polymer showed $T_{d,10\%}$ above 343°C. The multiblock hb–linear polymers showed $T_{d,10\%}$ values between 500 and 343°C, based on the weight ratio of linear to hb polymer. The DSC thermograms showed a single T_g of ~200°C for all multiblock hb–linear polymers, which was higher than that measured for the linear homopolymers ($T_g = 133–154$°C), indicating a homogenous product formation with no phase separation. A homo-hb polymer of molecular weight 30,000 Da showed no indication of a T_g below 250°C; however, a homo-hb polymer of only 8,400 Da showed a T_g at 181°C. Multiblock hb–linear products prepared with a linear reaction time of 15 min and hb reaction time of 6–12.5 h had $M_w = 26,600$–34,600 Da and did not showed any film-forming ability, similar to homo-hb polymers. Multiblock hb–linear products prepared with a linear reaction time of 1 h and longer hb reaction time (6–12.5 h) had $M_w = 53,500$–145,600 Da and showed film-forming ability, but the mechanical properties could not be evaluated due to brittleness of the hb polymer films.

Hyperbranched Poly(aryl ether)s with a Phosphine Oxide Moiety

The phosphine oxide group is an exceptionally good electron-donating group and facilitates the subsequent coordination with various metal ions or the formation of relatively strong hydrogen bonds. In addition, polymers incorporating phosphorus are known to have flame retardance and oxygen plasma resistance.

Lee et al. [164] prepared AB$_2$ and BA$_2$ monomers, namely bis(4-fluorophenyl)-4'-hydroxyphenylphosphine oxide and bis(4-hydroxyphenyl)-4'-fluorophenylphosphine oxide, that were converted to the corresponding hb poly(arylene ether phosphine oxide)s (hb-PAEPOs) with hydroxyphenyl and fluorophenyl end functional groups. The hb polymers were prepared by self-condensation of AB$_2$ (**1–26**, Scheme 10) or BA$_2$ monomers (**1–27**, Scheme 10) utilizing NMP/toluene as solvent in the presence of K$_2$CO$_3$ as base. The hb-PAEPO with hydroxyphenyl end functional groups showed a lower intrinsic viscosity ($\eta = 0.15$ dL/g), and thus a lower molecular weight, in comparison to the hb-PAEPO with fluorophenyl end functional groups ($\eta = 0.44$ dL/g) because of the low solubility of the phenolate ion during polymerization. The T_g values for the obtained polymers were 230 and 266°C, which showed an increasing trend with increase in η values. The fluorophenyl-terminated hb polymer was soluble in CHCl$_3$, but the hydroxyphenyl-terminated polymer was not soluble in CHCl$_3$ even though it had
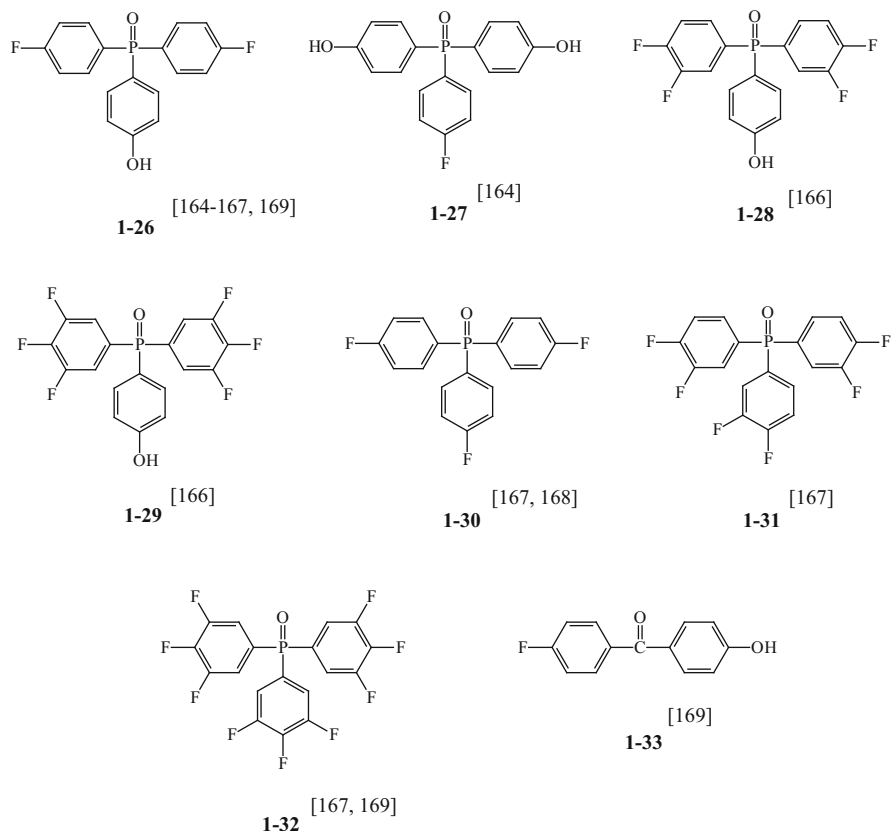
Scheme 10 Structures of monomers and core molecules used for the synthesis of hb-PAEPOs

a lower molecular weight than the fluorophenyl-terminated polymer, indicating that the properties of the hb polymers were dependent on the end functional groups as well as on their molecular weight. The prolonged polymerization of the AB_2 monomer yielded insoluble product, presumably due to the intermolecular reaction. However, the polymerization of BA_2 monomer at the same polymerization conditions produced relatively low molecular weight polymer due to the poor solubility of the corresponding phenoxide salt.

The AB_2 monomer, 4-(fluorophenyl)-4′,4″-(bishydroxyphenyl) phosphine oxide (**1–26**, Scheme 10), was synthesized by Lin and Long [165] by polymerizing the AB_2 monomer with various catalysts, such as K_2CO_3 or $Cs_2CO_3/Mg(OH)_2$, in the presence of dry and distilled DMSO as a solvent. All hb-PAEPOs were readily soluble at room temperature in polar aprotic solvents and basic water. Because of the highly irregular, branched 3D structures, gel permeation chromatography (GPC) did not provide an accurate measurement of molecular weight. Higher monomer concentrations in DMSO resulted in higher molecular weight but with

lower yields. The $Cs_2CO_3/Mg(OH)_2$ catalyst resulted in higher molecular weights than similar reaction conditions employing K_2CO_3 but resulted in lower yields of about 45%, which the authors attributed to the formation of insoluble, high molecular weight products. DSC measurements indicated no thermal transitions for the hb-PAEPO below 350°C, with the exception of a transition at 100°C that the authors attributed to the presence of residual water. They were of the opinion that the abundance of phenolic end groups was capable of efficient hydrogen bonding with other polar compounds.

A series of AB_2 monomers, namely bis-(4-fluorophenyl)-(4-hydroxyphenyl) phosphine oxide (**1–26**, Scheme 10), bis-(3,4-difluorophenyl)-(4-hydroxyphenyl) phosphine oxide (**1–28**, Scheme 10), and 4-hydroxyphenyl-bis-(3,4,5-trifluorophenyl)phosphine oxide (**1–29**, Scheme 10), were synthesized and characterized by Bernal et al. [166]. The AB_x monomers were self-condensed to form hb-PAEPOs according to the procedure reported by Hawker and Chu [65]. Spectral analysis of the resulting polymers indicated DB of 57% with M_w ranging from 22,400 to 52,500 Da and Đ in the range of 2.44–3.60. The polymerization time required to achieve reasonable molecular weights was decreased from 20 h to less than 6 h and then to 4.5 h by the introduction of additional fluorine atoms to some of the monomers, and a M_w of 33,000–22,400 Da was obtained. The hb-PAEPOs showed only a very weak endothermic baseline shift at approximately 300°C in DSC scans up to 450°C. TGA measurements of hb-PAEPOs showed high thermal stability at 545–590°C under nitrogen atmosphere and 475–480°C in air atmosphere.

Bernal et al. [167] further extended their work and prepared hb-PAEPOs with controlled molecular weights and narrow Đ by the polymerization of bis-(4-fluorophenyl)-(4-hydroxyphenyl)phosphine oxide in the presence of three core molecules. Polymerization reactions of bis-(4-fluorophenyl)-(4-hydroxyphenyl)phosphine oxide (**1–26**, Scheme 10) in the presence of 3, 5, and 10 mol% of tris(4-fluorophenyl)phosphine oxide (**1–30**, Scheme 10), tris(3,4-difluorophenyl)phosphine oxide (**1–31**, Scheme 10), and tris(3,4,5-trifluorophenyl)phosphine oxide (**1–32**, Scheme 10), respectively, were carried out in NMP at reflux in the presence of K_2CO_3, with reaction times of 8 h. The more reactive the core toward nucleophilic aromatic substitution, the more control was provided over the final molecular weight and the resultant Đ. Polymers showed M_n values ranging from 3,270 to 8,100 Da for polymerization reactions in the presence of core molecules. The highly fluorinated core, tris(3,4,5-trifluorophenyl) phosphine oxide (**1–32**, Scheme 10), yielded polymers with molecular weights approaching the theoretical values and narrow Đ values as low as 1.25 were obtained. The DB also decreased significantly with increase in concentration of the core molecule from 3.5 to 10 mol%.

Czupik and Fossum [168] prepared hb-PAEPOs via an $A_2 + B_3$ polymerization technique with tris(4-fluorophenyl) phosphine oxide (**1–30**, Scheme 10) as B_3 monomer, using a variety of bisphenols, namely 4,4′-isopropylidenediphenol (BPA), 4,4′- dihydroxybiphenyl (DHB), and 4,4′-dihydroxybiphenyl ether

(DHBE), as A_2 monomers. They studied the effects of the reactivity of the A_2 monomer, the A:B ratio, the mode of addition, the solvent, and the concentration on the final molecular weight, Đ, and DB. Soluble hb-PAEPOs with M_w up to 299,000 Da were obtained. When BPA was added to a solution of tris (4-fluorophenyl) phosphine oxide over a period of 5.7 h, the M_w of the resulting polymer increased slowly until all of the BPA was added, and then the M_w increased dramatically to 299,000 Da with a Đ of 24.2. If a solution of tris(4-fluorophenyl) phosphine oxide was slowly added to a solution of BPA over a period about 4 h, only 85% of tris(4-fluorophenyl) phosphine oxide could be added before the gel point was reached. If tris(4-fluorophenyl) phosphine oxide was added slowly to BPA over 3.5 h at twice the concentration (i.e., A_2:B_3 = 2:1), the entire solution of tris(4-fluorophenyl) phosphine oxide could be added before the gel point was reached. These results indicated that soluble, moderate molecular weight hb-PAEPOs with Đ values of about 3.0 were achieved with a molar ratio of 2:1 (A_2:B_3) if the reaction was stopped at an appropriate time. Slow addition of DHB to a solution of tris(4-fluorophenyl) phosphine oxide and of tris(4-fluorophenyl) phosphine oxide to a solution of DHB resulted in significantly lower molecular weight products, with M_w values ranging from 7,800 to 12,600 Da and Đ of about 2. When DHBE was added slowly to a solution of tris(4-fluorophenyl) phosphine oxide, M_w values were similar to those observed for BPA and DHB, which increased with an increase in reaction time. Reactions in which the A_2 component was added slowly resulted in lower DBs, ranging from 20 to 50%, whereas the slow addition of the B_3 component provided samples with DBs of approximately 75%. Reactions performed under highly diluted conditions were independent of the mode of monomer addition and afforded completely soluble products with M_w values in the range of 9,000–12,100 Da and Đ values as low as 2.2.

Fossum and coworkers [169] reported the synthesis and characterization of soluble, branched copoly(aryl ether ketones) with a phosphine oxide moiety with controlled molecular weights and relatively low Đ values, prepared via the copolymerization reactions of AB (**1–33**, Scheme 10) and AB$_2$ (**1–26**, Scheme 10) in the presence of a highly reactive core molecule, tris-(3,4,5-trifluorophenyl)phosphine oxide (**1–32**, Scheme 10). Many of their findings were compared with previously reported results [170]. Initial reactions were performed with AB:AB$_2$ molar ratios of 75:25, 90:10, and 95.5 in the presence of 3 mol% of core molecule, at a final reaction temperature of 200°C. The final molecular weight could be easily controlled by varying the amount of core molecule added to the reaction mixture. For example, for AB:AB$_2$ with 95:5 mol%, when 5 mol% of core molecule was utilized in the polymerization reaction compared to 3 mol%, a corresponding decrease in the M_n value (4,010 Da compared with 6,820 Da) was observed for the same polymerization temperature of 200°C. At each polymerization temperature, the ratio of AB:AB$_2$ also showed a significant impact on the Đ of the samples. Samples prepared at the same reaction temperature, for example at 200°C, with AB:AB$_2$ ratios of 75:25, 90:10, and 95:5 possessed Đ values of 2.2, 2.6, and 4.1, respectively. The combined effects of reaction temperature, the ratio of AB:AB$_2$, and the
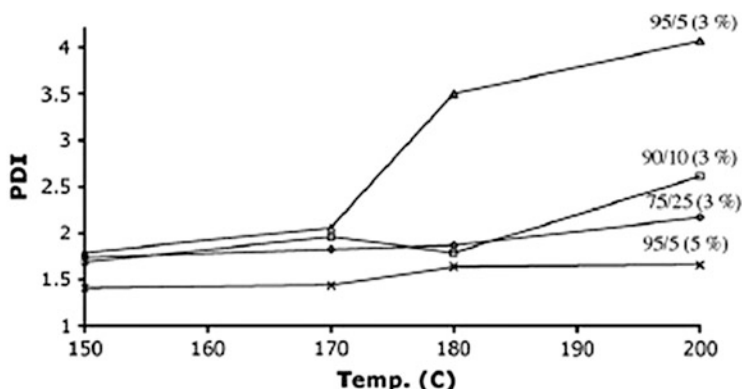
Fig. 2 The combined effects of reaction temperature, the ratio of AB to AB$_2$, and the mol% of the core molecule on the final polydispersity (*PDI*) of hb-PEK copolymers. Reproduced with permission from [169]

percentage of core molecule on the final $Đ$ of hb-PEK copolymers are shown in Fig. 2.

The substantial increase in $Đ$ values with the increase of AB$_2$ in the ratio of AB: AB$_2$ was attributed to the greater number of end groups present in the growing polymer chains, thus favoring the reaction of monomer with growing polymer rather than starting a new polymer chain. Fossum and coworkers also observed that the effect of reaction temperature was not that significant for 5 mol% of core molecule in comparison to that observed at 3 mol%. This finding was attributed to the fact that the total number of end groups in the system was higher when a higher mol% of core was utilized. Furthermore, for hb polymer prepared under similar reaction conditions, with AB:AB$_2$ molar ratio of 75:25 mol% containing 3 mol% of core molecule, both T_c (229°C) and T_m (278°C) were measurable in comparison to a similar polymer product prepared without a core molecule, which was completely amorphous. Samples prepared under the same reaction temperature of 200°C, with AB:AB$_2$ ratios of 75:25 containing 3 mol% of core molecule, showed much lower M_n and dispersity ($M_n = 5,400$ Da, $Đ = 2.2$) compared with a similar polymer sample prepared without the presence of a core molecule ($M_n = 13,000$ Da, $Đ = 11$). Fossum and coworkers assumed that the polymer samples prepared in the presence of core molecule were more homogeneous in nature, leading to better packing into crystalline regions and, hence, a T_m of 205°C. A similar polymer sample prepared under the same reaction conditions without the core molecule was completely amorphous in nature and did not show any T_m, which the authors attributed to self-plasticification, thus preventing the formation of crystalline regions. The M_n values of these systems could be controlled by altering the percentage content of core molecule, providing an efficient method for generating materials for a thorough study of structure–property relationships.

**Scheme 11** Structure of AB$_2$ monomer with ketone-imide moiety [131]
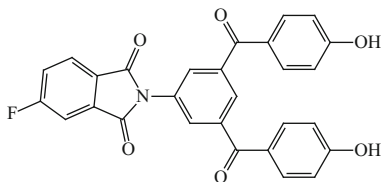
Hyperbranched Poly(aryl ether) with a Keto-imide Moiety

Baek et al. [131] synthesized an AB$_2$ monomer containing a preformed aromatic imide moiety and *para*-carbonyl functions to facilitate the formation of phenolate nucleophiles using K$_2$CO$_3$ as base. The AB$_2$ monomer, *N*-[3,5-bis (4-hydroxybenzoyl)benzene]-4-fluorophthalimide (shown in Scheme 11) was prepared from 4-fluoroisophthalic anhydride and 3,5-bis(4-hydroxybenzoyl)aniline. The AB$_2$ monomer was then polymerized via the aromatic fluoride-displacement reaction to afford the corresponding hydroxyl-terminated hb poly(aryl ether keto-imide) (hb-PAEKI). Functionalization of the resulting hb poly(arylene-ether-ketone-imide) was accomplished by modifying the chain ends with allyl bromide, propargyl bromide, or epichlorohydrin to afford allyl-terminated, propargyl-terminated, or epoxy (glycidyl)-terminated hb polymers, respectively. All hb-PAEKIs were soluble in common organic solvents. The hydroxyl-terminated hb PAEKI showed a T_g of 224°C due to hydrogen bonding whereas its derivatives exhibited lower T_g values that ranged from 122 to 174°C. Preliminary thermal study of the allyl ether-terminated hb polymer as a toughening additive for high-performance thermosets was conducted. The allyl-terminated hb-PAEKI was blended with a bisphenol A-based bis(maleimide) in various weight ratios. The results from DSC studies indicated that the presence of allyl-terminated hb-PAEKI significantly affected the T_g and cure behavior of bisphenol A-based bis(maleimide) when added up to 32 wt%.

Baek and coworkers [171] also synthesized a phthalonitrile-terminated hb-PAEKI that was end-functionalized with allyl groups, which could serve as a good processing aid and property enhancer for a bismaleimide resin. Furthermore, the authors blended it with a phthalonitrile (PN) resin based on [4,4'-bis (3,4-dicyanophenoxy)biphenyl] because PN resins are known to show excellent thermal and oxidative stability, together with flame retardant properties, and have attracted a great deal of attention as matrices for composite applications in the vicinity of an aircraft or submarine engine.

Fossum and coworkers were very curious to prepare hb-PAEKIs from the same AB$_2$ monomer [172] on an industrial scale via a cost-effective route. They concluded that the introduction of phenol groups via the nucleophilic aromatic substitution reaction of aryl fluorides with K$_2$CO$_3$ afforded a very low-cost and efficient alternative to demethylation of the methoxy groups using either pyridine hydrochloride or BBr$_3$ when a large excess of reagent is used. The yields and selectivity of the reactions were also improved significantly utilizing the nucleophilic aromatic
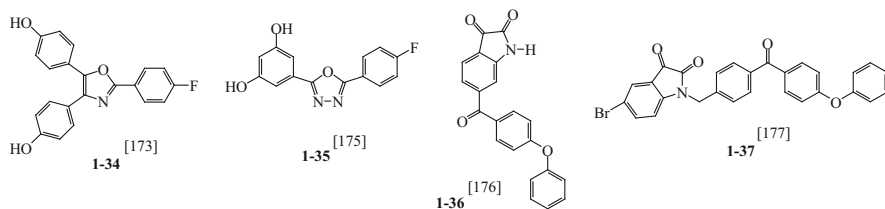
Scheme 12 Structures of monomers containing oxazole, oxadiazole, and oxindole moieties

substitution reaction of aryl fluorides with potassium hydroxide as a low cost reagent.

Hyperbranched Poly(aryl ether)s with Oxazole, Oxadiazole, and Oxindole Moieties

Gong et al. [173] synthesized and characterized an ABB′-type monomer containing a pair of phenolic groups and an aryl fluoride, which was activated toward displacement by the attached oxazole ring. The ABB′ monomer (**1–34**, Scheme 12) was self-condensed to form a hb poly(aryl ether oxazole) (hb-PAE-Ox) with terminal phenolic groups. The DB of hb-PAE-Ox was approximately 50%. The polymer was thermally stable and readily soluble in polar organic solvents. The terminal phenolic groups were easily functionalized, yielding hb hb-PAE-Oxs with a variety of ester-terminated and ether-terminated chain ends using different end-capping agents. Physical properties such as the T_g and solubility of the hb-PAE-Oxs depended significantly on the nature of the chain ends. It is known that for hb polymers the transition from the polar hydroxyl function to nonpolar aliphatic end groups results in a decrease in T_g because of the reduction in the extent of intermolecular interactions in the polymeric molecules [174]. The hb-PAE-Ox, which has polar hydroxyl terminal groups, showed a T_g value of 274°C. Polymers with less polar terminal groups, such as ester and ether groups, showed T_g values of 197 and 154°C, respectively. A further decrease in T_g to 124 and 119°C was observed for polymers when the length of the alkoxyl chain of the terminal ester or ether groups increased. The different chain ends also led to differences in solubility. The phenolic-terminated polymers were soluble in polar solvents such as DMSO and DMF, whereas the ester-terminated polymers were only partially soluble in DMF and insoluble in DMSO; the ether-terminated polymers were totally insoluble in both polar solvents. Conversely, in relatively nonpolar solvents such as CH_2Cl_2 and $CHCl_3$ polymers with ester- and ether-terminated chain ends were very soluble, whereas the polymers with a hydroxyl-terminated chain end were insoluble.

An AB_2 monomer (**1–35**, Scheme 12) was synthesized by Wu and Shu [175] for preparation of a hb poly(aryl ether oxadiazole) (hb-PAE-Oxd) with terminal phenol functionalities. The AB_2 monomer contained two phenolic groups and a single aryl

fluoride group that was activated toward nucleophilic displacement by the attached oxadiazole ring. The hb-PAE-Oxd showed a DB of 44%. The terminal phenolic groups were further post-functionalized with ether and ester chain ends using different end-capping agents to yield hb-PAE-Oxds. The nature of the chain-end groups showed a significant influence on the T_g and solubility. The hb-PAE-Oxd containing polar hydroxyl terminal groups showed T_g of 286°C, whereas the T_g values of hb-PAE-Oxds that contained less polar terminal groups, namely ether and ester groups, were 183 and 220°C, respectively. A further decrease in T_g to 121 and 146°C was observed for polymers with increasing length of the alkoxyl chain of the terminal ether or ester groups.

Hyperbranched poly(aryl ether oxindole)s (hb-PAE-Oxns) with a DB of 100% were prepared by Fu et al. [176] from an isatin-based AB$_2$ monomer (1–36, Scheme 12) by one-pot polymerization without using toxic organometallics nor chromatographic purification. The hb-PAE-Oxns soluble in apolar solvents were able to encapsulate a hydrophilic dye from the same polymer.

Kowalczuk et al. [177] synthesized an AB$_2$-type monomer (1–37, Scheme 12) that was self-condensed to give the hb poly(aryl ether oxindole) (hb-PAE-Oxn) with a DB of 100% and showed good solubility in common organic solvents such as CHCl$_3$ and THF. In general, the synthesis of the monomers for the preparation of hb-PAE-Oxn required toxic chemicals. However, in this work, the AB$_2$ monomer was prepared by only three steps: Friedel–Crafts acylation of 4-methylbenzoyl chloride with diphenyl ether to yield benzophenone, which was brominated by treatment with N-bromosuccinimide leading to benzyl bromide, and alkylation with 5-bromoisatin to yield the respective AB$_2$ monomer purified simply by precipitation from diisopropyl ether. The isatin functional groups were then end-capped with phenol and acylated using 2-bromoisobutyryl bromide, yielding a macroinitiator that was used for the synthesis of star polymers. The molar mass and dispersity of the synthesized bromopropionyl-functionalized poly(arylene oxindole) core showed $M_n = 20,000$ Da and Đ = 1.7. The hb core polymer exhibited a high T_g of about 250°C, which was similar to the previously obtained linear analogs ($T_g \sim 250$–300°C) [178].

Hyperbranched Poly(aryl ether)s with a Phenylquinoxaline Moiety

Baek and Harris prepared AB$_2$ (1–38, Scheme 13) and A$_2$B (1–39, Scheme 13) monomers [179] and self-polymerized them to very high molecular weight hb poly (phenylquinoxaline)s (hb-PPQs). The phenol-terminated hb-PPQs were only soluble in strong organic acids, whereas the aryl fluoride-terminated hb-PPQs were soluble in most common organic solvents. The hb-PPQs were treated with allyl bromide to afford an allyl ether-terminated hb-PPQ, which was also soluble in most organic solvents. The aryl fluoride hb-PPQs had a much higher M_w of ~2,643,000 Da and a much broader molecular weight distribution (Đ ~ 60) than the phenol-terminated hb-PPQs ($M_w = 322,000$ Da, Đ = 3.7) and allyl-terminated hb-PPQs ($M_w = 243,000$ Da, Đ ~ 4). The results indicated that phenol-terminated
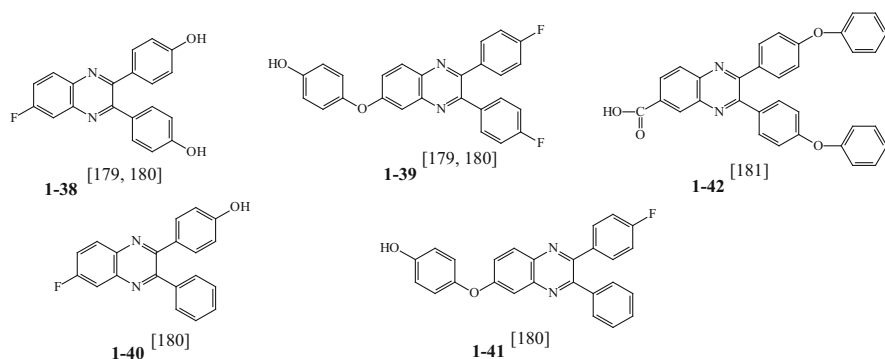
Scheme 13 Structures of monomers used for the synthesis of hb-PPQs

hb-PPQs formed aggregates in solution due to the formation of hydrogen bonding and showed limited solubility in organic solvents. The aryl fluoride-terminated hb-PPQs, on the other hand, had a much more extended and open conformation and showed good solubility in most common organic solvents. The lower T_g (225°C) of aryl fluoride-terminated hb-PPQs compared with phenol-terminated hb-PPQs ($T_g = 255$°C) was attributed to the extra flexible units in the repeating unit, no hydrogen bonding, and its apparent extended and open conformation. The phenol-terminated hb-PPQ and the aryl fluoride-terminated hb-PPQ showed $T_{d,5\%}$ at 511 and 575°C, respectively, in nitrogen, indicating high thermal stability. The reduced thermal stability of phenol-terminated hb-PPQs was attributed to the lower stability of the terminal phenol groups.

Baek and Harris also synthesized AB (**1–40**, Scheme 13) and BA (**1–41**, Scheme 13) monomers [180] in addition to the previously synthesized AB$_2$ and A$_2$B monomers [179]. The AB and AB$_2$ monomers were copolymerized to afford different degrees of linear units in hydroxyl-terminated hb-PPQs. Similarly, BA and A$_2$B monomers were copolymerized to afford different types of fluorine-terminated hb-PPQs. In the case of hydroxyl-terminated hb-PPQs, properties such as solubility, solution viscosity, T_g, and polymer degradation temperature were greatly influenced by the number of hydroxyl groups on the surface. However, the properties of fluorine-terminated hb-PPQs were much less influenced by the number of fluorines on the surface. The copolymers of AB and AB$_2$ were soluble in most aprotic solvents and phenolic solvents and T_g values ranged from 239 to 274°C. Copolymers of BA and A$_2$B were also soluble in most aprotic solvents and phenolic solvents. The hydroxyl- and fluorine-terminated hb-PPQs showed $T_{d,5\%}$ values ranging from 511 to 568°C in air and from 556 to 588°C in nitrogen, respectively, indicating that thermal degradation depended on the surface functional groups at the chain ends. The enhanced thermal stabilities of fluorine terminated hb-PPQs could be attributed to the fluorine terminal groups on the macromolecule surfaces.

A new phenylquinoxaline-containing AB$_2$ monomer (**1–42**, Scheme 13) was designed and synthesized by Baek and Tan [181] and the corresponding polymer

was synthesized at the optimal temperature of ~130°C using PPA and P_2O_5 (4:1). During the optimization study, the evolution of polymer density was realized by visualizing the existence of a changeover in the macromolecular architecture from a 'fanlike' conformation at the early stage of polymerization to a denser, globular conformation at higher molecular weights. The authors also showed that the subsequent chain-end functionality transformation for the resulting hb-PPQ could be performed either in a one-pot process or a batch process. The resultant hb-PPQs were thermally stable, with a $T_{d,5\%}$ of over 500°C in air.

Fluorinated hb Poly(arylene ether)s

Fluorine-containing polymers [182] are of special interest because they provide attractive properties such as low optical loss, birefringence, dielectric constant, and moisture absorption. On the other hand, poly(arylene ether)s are well-known aromatic polymers of high T_g, excellent thermal stability, and mechanical strength. Researchers have reported that perfluoroalkyl groups as a pendant unit or in the main chain activate fluoro displacement by phenoxides [183]. Since electron-withdrawing perfluoroalkyl groups cannot participate in resonance stabilization, activation by this group is expected due to the stabilization of the negative charges at the 2- or 4-position by a negative inductive effect [184, 185]. The steric congestion due to the bulky trifluoromethyl group ($-CF_3$) may also facilitate the formation of a stable Meisenheimer complex with the release of steric strain [186]. The presence of a pendent $-CF_3$ group in polymers increases the fractional free volume and lowers the dielectric constant while increasing its solubility without forfeiture of thermal stability [187–190]. The pendent $–CF_3$ group also decreases the crystallinity and serves to increase the free volume of the polymers, thereby improving gas permeability [191, 192] and electrical insulating properties [193]. The continued search for new activating groups for nucleophilic aromatic substitution leading to the formation of poly(arylene ether)s has been a very active area of polymer research, and in this regard fluorinated hb poly(arylene ether)s (F-hb-PAEs) with pendant $–CF_3$ groups are noteworthy in terms of their interesting properties observed.

An AB_2 monomer containing pendent $-CF_3$ groups (**1–43**, Scheme 14), namely 2,4 bis-(4-fluoro-trifluoromethylphenyl)phenol, was synthesized by Banerjee [194] utilizing Pd-initiated coupling, which was self-condensed to yield fluorinated hb poly(arylene ether) (F-hb-PAE) with an $M_n = 8,200$ Da and Đ = 1.2, indicating a highly regular structure. The F-hb-PAE was soluble in a wide variety of organic solvents and also in acetone. F-hb-PAE showed reasonable thermal stability, with $T_{d,5\%}$ in air of about 379°C and a T_g of 132°C. However, it was not possible to calculate the DB from NMR spectra due to several aromatic units between the branching points that restricted the analysis between a linear and a terminal unit.

An AB_2 monomer containing pendent $-CF_3$ groups (**1–44**, Scheme 14), namely bis-(4-fluoro-3-trifluoromethylphenyl)-4′-hydroxyphenylphosphine oxide, was synthesized by Satpathi et al. [195]. On self-condensation, this AB_2 monomer led
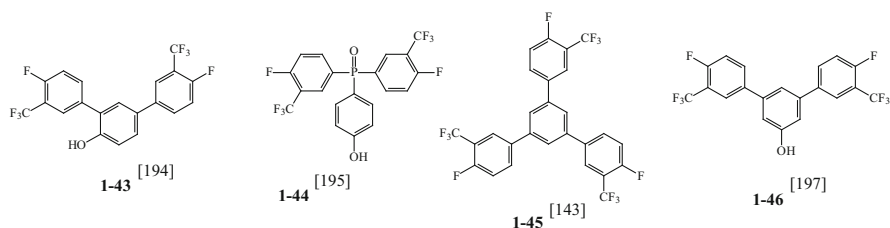
Scheme 14 Structures of monomers used for the synthesis of F-hb-PAEs

to fluorinated hb poly(arylene ether phosphine oxide) (F-hb-PAEPO) of much higher molar mass ($M_w \sim 6,16,000$ Da).The F-hb-PAEPO showed a T_g value of 225°C; the $T_{d,10\%}$ in nitrogen and air were found to be 508°C and 448°C, respectively. Due to missing entanglements, no free-standing films could be prepared from the F-hb-PAEPO and no mechanical properties could be recorded. An interesting finding was observed from ^{19}F-NMR spectra that indicated partial loss of 4-fluoro groups from unreacted B sites, as also observed previously by Fossum and coworkers [167] but was not explained. This effect was also manifested on the DB of the F-hb-PAEPO, which was approximated to 53 or 59% using the equations given by Frechét or Frey, respectively, but the DB should be ~50% without unwanted side reactions. Satpathi and coworkers ascribed this to the lability of these activated fluorine atoms under basic polymerization conditions. Under basic conditions of the polycondensation reaction, this fluorine was not only replaced by the phenolate under formation of ether bonds but probably also by the water that was generated by the deprotonation of the hydroxyl groups, which was not removed fast enough by azeotropic distillation, and this finding was supported by a model reaction. Herbert et al. showed that activation of the fluorine by the phosphine oxide group in the *para* position could further accelerate this reaction [196].

Banerjee et al. synthesized a new trifluoromethyl-activated trifluoro monomer by Pd-initiated coupling of 1,3,5-tribromobenzene with 4-fluoro-3-trifluoromethyl-phenylboronic acid to afford 1,3,5-tris(4-fluoro-3-trifluoromethylphenyl)benzene as B$_3$ monomer (**1–45**, Scheme 14) [143]. The B$_3$ monomer was reacted with three different bisphenols, namely 4,4′-isopropylidenediphenol (BPA), 4,4-′-(hexafluoroisopropylidene) diphenol (6F-BPA), and 4,4′-(9-fluorenylidene) diphenol (C-BPA), as A$_2$ monomers in different molar ratios (A$_2$:B$_3$ = 1:1, 1.5:1, or 2:1) leading to several fluorinated hb poly(arylene ether)s (F-hb-PAEs). At a functional equivalence of A$_2$:B$_3$ (i.e., 3:2 molar product) very high molecular weight products were obtained without significant gelation. In order to prevent gelation, a slow mode of addition of B$_3$ monomer for a period of 3 h was adopted to prevent any high local concentration at any time during polymerization, and the solid content was kept as low as 2.7 wt%. For 1:1 and 2:1 (A$_2$:B$_3$) molar ratios, reactions proceeded smoothly without any noticeable gel formation since both contained a significant excess of one type of functionality. However, despite the highest reactivity of BPA (strongly nucleophilic) toward the B$_3$ monomer in the

series, there was no gelation even at a functional equivalence (A_2:B_3 = 1.5:1). Theoretically, the gel point is reached in such a system at a functional group conversion of about 71% whereas, interestingly, a very high molar mass product (714,200 Da) was achieved in high yields, which clearly indicated a high monomer conversion and this was also manifested by spectral analysis. Polymerization in a highly diluted system, as well as slow monomer addition, helps to prevent macroscopic gelation to some extent according to the previous findings in literature [83, 84]; however, there could be a tendency to intramolecular cyclization due to favorable monomer configuration, which might help in shifting the gel point to higher conversion or prevented it totally. Some gelation was observed in the case of F-hb-PAEs resulting from 6F-BPA or C-BPA towards B_3 monomer (i.e., A_2:B_3 = 2:1 molar ratio) under similar reaction conditions. It was also observed that the gel content increased with increase in reaction time, particularly when the reaction temperature was 180°C. To avoid the problem of gelation, the F-hb-PAEs based on 6F-BPA or C-BPA with A_2:B_3 = 1.5:1 were prepared by maintaining the reaction temperature at only 165°C. All the polymers were soluble at room temperature in common organic solvents such as NMP, DMF, and DMAc, but were insoluble in DMSO. The ^{19}F-NMR signals revealed very high DB for these F-hb-PAEs (>70% and approaching almost 100%). GPC analysis of the F-hb-PAEs polymers prepared from 1:1 or 2:1 molar reaction of A_2 and B_3 monomers showed relatively low molar masses with values as low as 10,900 Da and narrow Đ values as low as 1.45 due to the presence of excess reactive functional groups, resulting in termination of the polycondensation. The 1.5:1 molar reaction resulted in very high molecular weight polymers, up to 2,840,000 Da, with Đ as high as 7.94. The 1.5:1 and 2:1 molar F-hb-PAEs exhibited higher T_gs than the 1:1 molar products. The phenoxy-terminated products, i.e., the 2:1 molar reaction products, showed a higher T_g (180–249°C) than the 1:1 molar reaction products (T_g ~147–232°C). The F-hb-PAE prepared from C-BPA and B_3 monomer with 1.5:1 molar ratio of A_2:B_3 did not show any T_g up to 350°C and showed a $T_{d,10\%}$ as high as 595°C, indicating very high thermal stability. Besides, the polymers showed more than 50% char residue even above 700°C under nitrogen atmosphere.

A new AB_2 monomer [3,5-bis(4-fluoro-3-trifluoromethylphenyl)phenol] containing pendent –CF_3 groups (1–46, Scheme 14) was prepared by Ghosh et al. [197] utilizing Suzuki coupling of 4-fluoro-3-trifluoromethylphenylboronic acid and 3,5-dibromophenol. The self-condensation of the AB_2 monomer led to F-hb-PAEs of low molecular weight and high molecular weight (see Scheme 15 for hb structures), depending on the solution concentration and reaction time. In general, a high solution concentration and long reaction time led to high molecular weight products. The M_w of the AB_2 self-condensation product was further increased to 231,300 Da with a Đ of 2.0 when the solution concentration was increased to 10 wt%. The fluorinated hb copoly(arylene ether)s 2a, 2b, 2c, 3a, 3b, and 3c (see Scheme 15 for hb structures) were prepared by the AB_2 + A_2 approach. The synthesized AB_2 monomer was reacted with two different commercial bisphenols, namely BPA and 6 F-BPA, at three different molar ratios (AB_2: A_2 = 1:1, 3:2, 2:1) to form fluorinated hb copoly(arylene ether)s. Here, the reactions
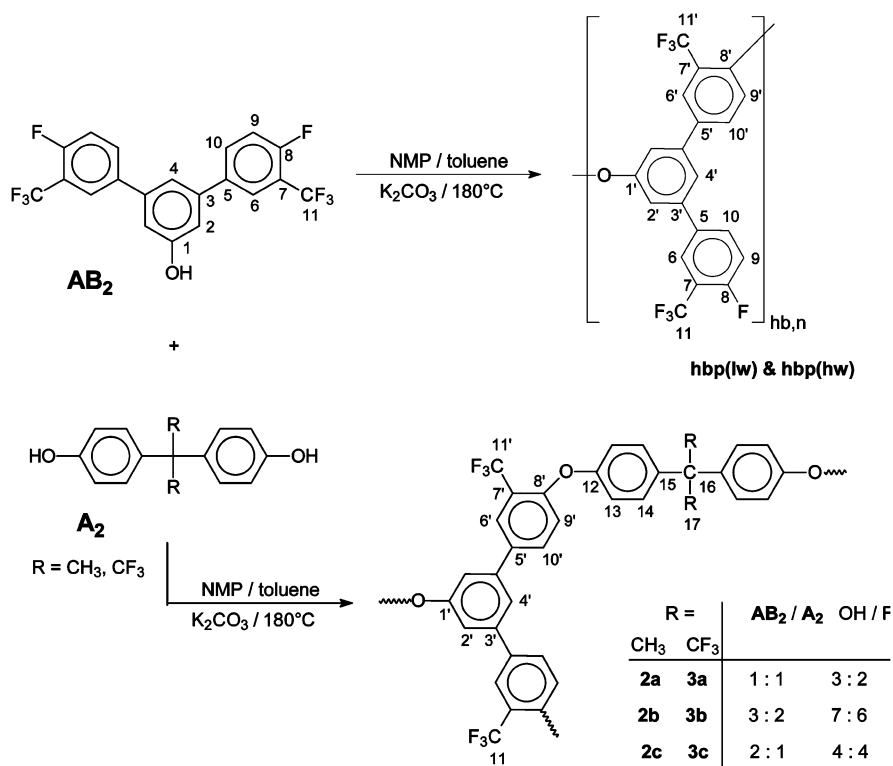
Scheme 15 Reaction scheme and structure of the hb poly(arylene ether)s. Reproduced with permission from [197]

were carried out at lower solution concentration of about 4 wt% to avoid any gelation, and some changes were also made in terms of reaction temperature and reaction time, such as 150°C for 8 h and then at 180°C for another 3 h. These changes were required to avoid any gelation in the 2:1 molar reactions of AB_2 and A_2. The calculation from ^1H-NMR spectra for hbp(lw) showed $DB_{Frechet}$ value of 0.5, whereas DB_{Frey} gave a value of 0.44. As the molecular weight increased for high molecular weight F-hb-PAE, broadening of the ^1H-NMR signals prevented an accurate determination of the content of linear, dendritic, and terminal subunits. For the polymers **2c** and **3c**, there were broad and overlapping signals; however, the copolymer structures could be confirmed. For the fluorinated hb copoly(arylene ether) samples with excess of A groups (**2a, 2b, 3a,** and **3b**), additional signals due to unreacted A sites of the AB_2 and A_2 monomer, respectively, were observed.

Both refractive index (RI) and multi-angle laser light scattering (MALLS) detectors were used in GPC measurements to determine the molecular weight of the F-hb-PAEs synthesized using different monomer ratios. Extremely high molecular weight products were obtained without gelation for 2:1 molar reactions, with M_w values of ~3,730,000 and ~4,470,000 Da using BPA and 6 F-BPA as A_2

Fig. 3 DSC plots of fluorinated hb copoly(aryl ether) (**2a–c** and **3a–c**; see Scheme 15 for structures) and fluorinated hb homopoly(aryl ether)s, where *hbp(lw)* signifies hb poly(aryl ether) of low molecular weight and *hbp (hw)* signifies hb poly(aryl ether) of high molecular weight. Reproduced with permission from [197]
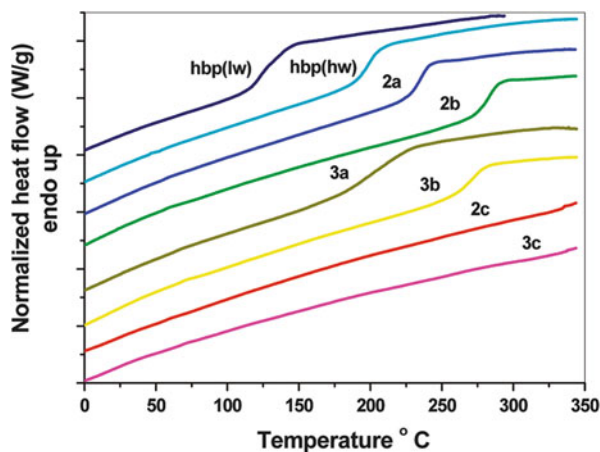

monomers, respectively. The authors stated that for the molar ratio AB_2:$A_2 = 2$:1, i.e., at a stoichiometric equivalence, only half of the A functional groups contributed to potential gelation whereas the other half underwent self-condensation of the AB_2 monomer, and shifted the critical conversion from ~70% to nearly 90% without affecting the molar mass of the product. This observation was somewhat in accordance with the previous theoretical finding by Voit and coworkers on the 'diluting' effect on the critical functionality ratio of adding A_x to AB_2 [198]. The F-hb-PAEs showed excellent thermal stability and very high T_g values. The AB_2 self-condensed F-hb-PAE showed a T_g as high as 199°C and $T_{d,10\%}$ as high as 573°C in N_2, whereas the extremely high molar mass products of the $AB_2 + A_2$ approach did not show any T_g up to 350°C and $T_{d,10\%}$ as high as 554°C. The DSC plots of the fluorinated hb homopoly(aryl ether)s and copoly(aryl ether)s are shown in Fig. 3.

2.2.5 Hyperbranched Poly(aryl amine)s with a Triazine Moiety

Mahapatra and Karak [199] prepared triazine-containing hb polyamines (hb-PAms) by the $A_2 + B_3$ polymerization approach. The methylene-containing hb-PAm (the monomer combination is shown in Scheme 16a) showed a lower T_g of 230°C due to the presence of the flexible methylene linkage compared with the sulfone-containing hb-PAm (monomer combination shown in Scheme 16b), with a T_g of 240°C as per DSC measurements. The solubility studies revealed that the hb-PAms were soluble only in polar aprotic solvents, which the authors attributed to the presence of polar –NH– groups and rigid triazine moieties. Flame retardancy studies revealed that the resulting sulfone-containing hb-PAm showed higher flame retardancy in terms of the limiting oxygen index (LOI), with a value as high as 42 compared with that of the methylene-containing hb-PAm with a LOI value of 32. The authors attributed the higher LOI of the sulfone-containing hb polyamine to the presence of sulfur as a nonflammable element compared to the

a

b
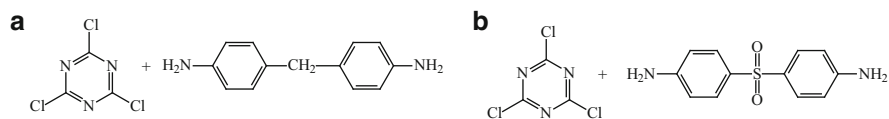
Scheme 16 Structures of monomer combinations used for the synthesis of triazine-containing hb-PAms [199]

1-47   [200]   **1-48**   [201]   **1-49**   [203]
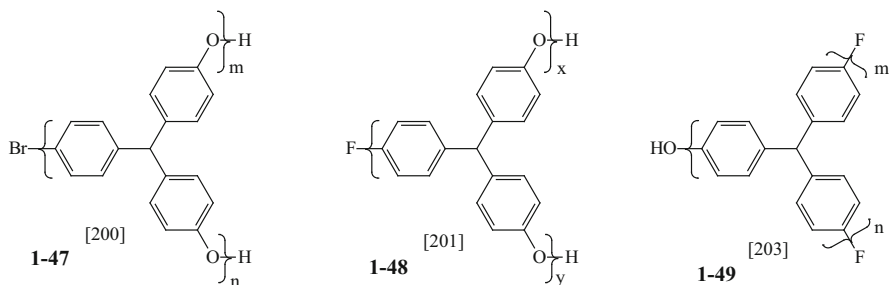
Scheme 17 Structures of hb-PPOs with different end-functionalities

methylene-containing hb-PAm, which might form flammable methane, ethane or similar type of flammable molecule upon combustion.

2.2.6 Hyperbranched Poly(phenylene oxide)s

Zhang et al. [200] prepared an AB_2 monomer, namely 4-bromo-4′,4″-dihydroxytriphenylmethane, through a modified Ullmann reaction. The monomer was treated with K_2CO_3 or NaOH as a base and copper chloride (CuCl) as a catalyst in solvents such as DMSO or sulfolane to form hb poly(phenylene oxide)s (hb-PPOs) with phenolic terminal groups (**1–47**, Scheme 17). The sulfolane/NaOH system at a higher temperature of ~210°C led to more rapid polymerization with a higher DB (71%), in comparison to polymers prepared in the presence of DMSO/K_2CO_3 at a temperature of 170°C, which showed a DB of 48%. The phenolic terminal groups were modified into a variety of functional chain ends, namely methoxy, 1-butoxy, ethyleneoxy, or diethyleneoxy units, which were coupled with the aryl hydroxyl branch-end. The nature of the chain-end groups showed significant influence on the solubility of the hb-PPOs. The hb-PPOs were insoluble in chloroform, whereas the modified hb-PPOs were soluble in chloroform. Due to the presence of the branched structure and the large number of polar phenolic terminal groups, the resulting samples exhibited higher T_g values, between 130°C and 153°C, compared to linear PPOs with T_g values of about 95°C. The resulting hb polymers showed high thermal stability, with $T_{d,5\%}$ above 258°C in N_2 and above 280°C in air.

Lv et al. [201] designed and synthesized an AB_2-type monomer, namely 4-fluoro-4′,4″-dihydroxy triphenyl methane. Through the homopolymerization of

the monomer, hb-PPO with terminal phenolic groups (**1–48**, Scheme 17) was obtained. Here, the aryl bromide was replaced with aryl fluoride group because in the previous studies [200], hb-PPOs prepared from 4-bromo-4′,4″-dihydroxyltriphenylmethane by the Ullmann reaction had some limitations such as promotion of branching via Ar–CH₃ groups during high temperature processing by the unreacted amine and copper salts and also difficulty in removal of copper salts [202]. Hence, the aromatic nucleophilic substitution reaction was used to replace the Ullmann reaction to synthesize hb-PPO free of the amine and copper salts for environmental safety. Aromatic nucleophilic substitution (S_NAr) is a very effective method among the various reactions that involve a leaving group activated with an electron-withdrawing group that produces an aromatic ether linkage [74, 120]. The fluorine was chosen as a leaving group due to its good reactivity on account of its small size and high electronegativity. Moreover, the fluorine group can offer many desirable properties such as low polarity, low moisture absorption, and good solubility.

A new AB_2 monomer, namely 4-hydroxyl-4′,4″-difluorotriphenylmethane, was successfully synthesized by Luo et al. [203] via a Friedel–Crafts alkylation of phenol from 4,4′-difluorodiphenylmethanol. A series of fluoro-terminated hb-PPOs (F-hb-PPOs, **1–49**, Scheme 17) was prepared by self-condensation leading to different molecular weights, with M_n values varying from 2,000 to 6,800 Da and Đ of 1.7–4.8. It was found that the molecular weight and Đ of the F-hb-PPOs increased with monomer concentration and reaction time. The solubility of the F-hb-PPO was different from the hb-PPO synthesized in a previous study [200], which the authors attributed to the large number of terminal groups leading to the greater solubility of hb polymers. The DB of the F-hb-PPOs decreased from 0.63 to 0.53 as the molecular weight increased. This was attributed to differences in reactivity between the two B groups of AB_2 monomer due to the steric hindrance. The authors were of the opinion that one B group of the AB_2 monomer reacted with an A group and the other B group in the same AB_2 had lesser chance of reacting with the A group. As the molecular weight increased, the hb architecture became larger and the terminal B groups on the outside surface became increasingly crowded. The crowding or the steric hindrance inhibited the reaction between the second B group and the A group, resulting in a more linear architecture and thus lowered the DB. The T_g of the F-hb-PPOs increased with increasing molecular weight, up to 164°C when the M_n was over 6,800 Da. The increase in T_g was ascribed to the highly branched molecular architecture, which could inhibit the mobility of chain segments. The F-hb-PPOs showed excellent thermal stability, with $T_{d,5\%}$ values up to 559°C.

The trifluoromethyl group can act as an effective activating group for fluoro displacement. Ghosh et al. synthesized a new trifluoromethyl-substituted AB-type monomer, namely 4-fluoro-3-trifluoromethylphenyl phenol [204], which was copolymerized with the AB_2 monomer [197] in molar ratio 1:1 to yield a fluorinated hb copolymer by the AB + AB_2 polymerization approach. The representative structure of the hb copolymer is shown in Scheme 18. The DB could not be evaluated from spectral analysis; however, assuming a random copolymerization of the

Scheme 18 Representative
structure of the fluorinated
hb copolymer [204]
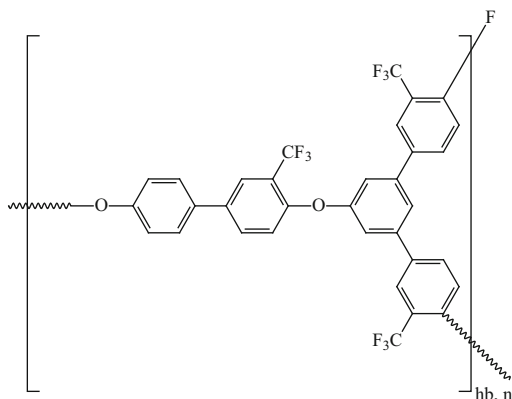
monomers and a full conversion of A groups, the DB should be approximately 44%
as calculated theoretically by Frey and Holter for a 1:1 molar ratio of AB:AB_2
[205]. The hb copolymer exhibited M_w of 144,100 Da. The hb copolymers
exhibited good solubility in common organic solvents such as in THF, CH_2Cl_2,
and $CHCl_3$ compared with a linear polymer that was prepared by self-condensation
of the AB monomer for comparison. The hb copolymers showed excellent thermal
stability, with $T_{d,10\%}$ up to 522°C in air and T_gs as high as 187°C.

2.2.7 Hyperbranched Poly(phenylene sulfide)s

Mellace et al. [206] reported the preparation and characterization of hb poly
(phenylene sulfide) (hb-PPS) utilizing 3,4-dichlorobenzenethiol as the AB_2 mono-
mer. Furthermore, polymerization of 3,4-dichlorobenzenethiol as AB_2 monomer
with 1,3,5-trichlorobenzene as a multifunctional core (B_3 monomer) was utilized to
prepare hb-PPS by the $AB_2 + B_3$ approach. Polymerization of commercially avail-
able 3,4-dichlorobenzenethiol was accomplished utilizing anhydrous K_2CO_3 as a
base in the presence of DMF or NMP as solvent. The monomer combination is
presented in Scheme 19. When DMF was used as solvent, the reaction was carried
out at 100°C for 24 h and in NMP the reaction was carried out at 150°C for 8.5 h.

   The polymer resulting from AB_2 monomer (see structure of AB_2 monomer in
Scheme 19) showed a reasonably high M_w (~17,000 Da), with a Đ value of 2.0
when polymerization was accomplished in DMF as solvent. Addition of 1 core
molecule for every 50 monomers gave a polymer with a M_w of 8,400 Da and Đ of
1.2 in DMF, and a polymer with a M_w of 13,000 Da and Đ of 1.3 in NMP. DSC
revealed that the hb-PPS was amorphous, with a T_g between 60 and 90°C in
comparison to linear PPS with a T_g value of 85°C. No T_m was observed up to
375°C for hb-PPS. They attributed the low T_g values (similar to the linear analogs)
to a change in the nature of the intermolecular interactions as a result of the large
number of terminal chlorines, or to the nonsymmetrical branching [207, 208]. The

Scheme 19 $AB_2 + B_3$
monomer combination for
preparation of hb-PPS [206]
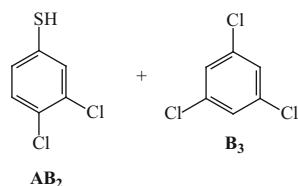
hb-PPSs reported by Mellace and co-workers had both nonsymmetrical branching and a nonsymmetrical arrangement of the chlorines on the terminal groups, which might have resulted in the reduction in T_g. A crystallization temperature T_c was not observed for hb-PPSs by annealing, even when the polymer samples were heated to 300°C, in contrast to the linear PPS that showed T_c of ~225°C. The lack of crystallinity was due to the highly branched nature of hb-PPS. The hb-PPS samples showed an onset temperature for decomposition (T_d) between 400 and 445°C, compared to 480°C for linear PPS. The author attributed the slightly reduced thermal stability to the large numbers of chain ends, which had a tendency to evolve volatiles at a lower temperature, or to effect of chlorination of the terminal and linear groups in the polymer, leading to more rapid chain-cleavage.

A detailed study on the thermal degradation of hb-PPS was accomplished by Bo et al. [209] utilizing thermal decomposition kinetics by applying the Kissinger [210], Friedman [211, 212], and Ozawa–Flynn methods [213]. The values of activation energy were constant with increasing degree of conversion. Through analyzing the activation energies obtained by the three methods, it was found that the values were close to each other for Kissinger, Friedman, and Flynn–Wall–Ozawa methods and the values were 183, 189, and 194 kJ mol^{-1}, respectively. The Coats–Redern method [214–216] was also chosen for determining the activation energy and showed a value of 184 kJ mol^{-1}. These values strongly suggest that the solid-state thermal degradation mechanism followed by hb-PPS is a phase boundary controlled reaction mechanism. Oxidation of the hb-PPS to hb poly(phenylene sulfone) was also accomplished by Mellace et al. [206] with hydrogen peroxide in acetic acid. The resulting sulfone polymers were insoluble in all common solvents. DSC analysis of the hb poly(phenylene sulfone) polymer revealed a T_g of ~155°C, which was higher than for hb-PPS ($T_g = 85$°C) and lower than for the linear aromatic polysulfones, which usually show high T_g values of above 200°C. The hb poly(phenylene sulfone) did not show any detectable T_m due to its branched architecture.

Xu et al. [217] decorated the core of hb-PPS with benzyl, phenyl, and naphthyl groups and investigated the effects of the core structures on the fluorescence properties of hb-PPS. Two hb-PPSs were synthesized (batch 1: polymerization time = 7 h, $M_n = 1,900$ Da, and $Đ = 1.4$; batch 2: polymerization time = 16 h, $M_n = 4,500$ Da, and $Đ = 1.2$). Under the same reaction conditions, three different molecules naphthyl, phenyl, or benzyl were attached to the central thiol (−SH) group as shown in Scheme 20.
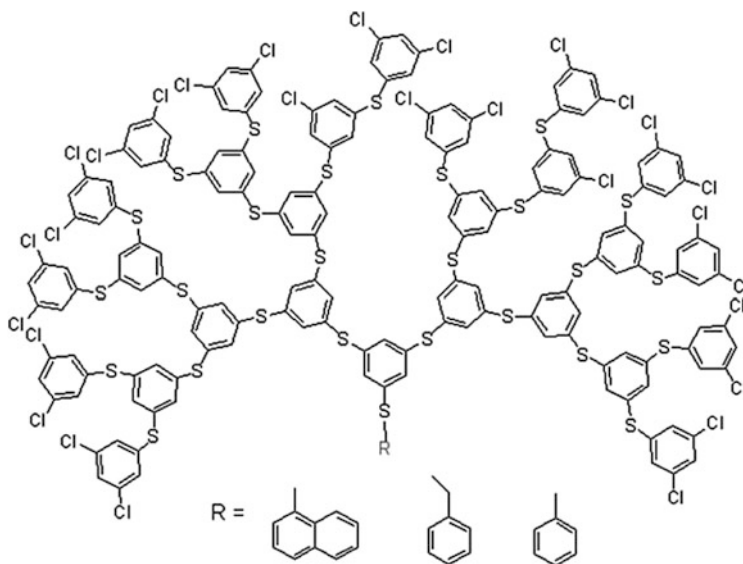
Scheme 20 Schematic structure of core-functionalized hb-PPS. Reproduced with permission from [217]

Both the phenyl-cored and the naphthyl-cored hb-PPS gave rise to a fluorescence peak at about 500 nm due to excimers formed by intermolecular packing, which results in a high degree of fluorescence polarization due to encumbered molecular rotation. Phenyl and naphthyl groups could form conjugated structures with the hb-PPS backbones through sulfide bridges, whereas the benzyl group showed almost no effect on the fluorescence properties of hb-PPS. The naphthyl-cored hb-PPS showed drastic fluorescence enhancement of about 10- to 18-fold higher than the original hb-PPS, indicating that the core structures are conjugated with the hb backbones and might have important effects on the structural rigidity of the hb backbones [218]. The naphthyl core was more restricted in its intramolecular rotations in comparison to the phenyl core, which could easily rotate. DSC analysis showed that the T_g of naphthyl-cored hb-PPS increased to 93°C in comparison with the T_g of 55°C for neat hb-PPS; however, no significant change in T_g was found for benzyl- or phenyl-cored hb-PPS. DSC results indicated that naphthyl-cored hb-PPS showed a higher T_g because of the strengthened intermolecular packing, leading to strengthened planar rigidity, proving that the focal group might have an important effect on the electronic structure of highly branched hb-PPS conjugated polymers.

2.2.8 Hyperbranched Polyarylenes

Acetylene cyclotrimerization is a well-established method for the effective transformation of triple bonds to benzene rings. Acetylenic polymerization has emerged

as a useful technique for the synthesis of advanced specialty polymers with novel molecular structures and unique functional properties. Polycyclotrimerizations of diyne molecules are anticipated to result in the formation of hb polyarylenes [219–221]. The polycyclotrimerization of aromatic diyne uses only a single A_2-type monomer. The A_2-type diyne monomers are stable at room temperature in the absence of a catalytic species. The polymers have been found to exhibit a variety of unique properties such as high luminescence with fluorescence quantum yields up to unity and high thermal stability up to 500°C [222]. Triple bond-mediated metathesis or insertion, coupling, addition, and cyclization have also been explored for synthesis of acetylenic polymers with different chain structures and dimensionalities such as poly(arylene ethynylene), polydiacetylene, polyarylene, and poly (1,2,3-triazole) as well as their substituted derivatives [223, 224].

Hyperbranched Polyphenylenes

Hyperbranched polyphenylenes (hb PPhs) are nonconducting polymers because extended π-conjugation is hindered due to their tightly packed and strongly twisted phenylene units. Different linear or branched PPh have been explored by several research groups [76, 225–227]. The polymers are synthesized utilizing Diels–Alder cycloaddition [228] of phenylated cyclopentadienones with phenylated alkynes and subsequent decarbonylation leading to hb structures with high thermal stability and better processability. Previously, Tang and colleagues prepared hb-PPhs using diyne polycyclotrimerization initiated by transition metal catalysts [229] and base-catalyzed alkyne polycyclization [230].

Hyperbranched PPhs were synthesized by Voit and coworkers [231] utilizing the Diels–Alder reaction with subsequent decarbonylation based on the $A_2 + B_3$, AB $+ AB_2$, and AB_2 approaches. All the polymer backbones were based on hexaphenylbenzene units that were linked in different ways depending on the monomer structure and the Diels–Alder adduct that was formed during the course of the polymerization reaction, which was conducted for 48 h. The structures of the monomers and monomer combinations are shown in Scheme 21. For structural characterization of different hb-PPhs, ^{1}H-NMR and ^{13}C-NMR was carried out. It was difficult to assign terminal, linear, and dendritic substructures due to signal overlap for AB_2 and $AB_2 + AB$-type polymers. For $A_2 + B_3$ polymers, signals for both ^{1}H-NMR and ^{13}C-NMR spectra were clearly distinguishable and it was possible to assign terminal, linear, and dendritic substructures.

The $A_2 + B_3$ polymerization was carried out at different molar ratios of A_2 and B_3 monomers (A_2:B_3 = 1:1, 3:2, 2:1, and 3:1). The molar masses of polymers obtained by the $A_2 + B_3$ approach were lower ($M_w = 2,500–68,000$ Da, as recorded by refractive index detector) than those of AB_2 polymers ($M_w = 47,000–660,000$ Da, as recorded by light scattering detector) due to the off-stoichiometric functional ratios. For AB_2-type polymerization, a higher molar mass was attained at longer reaction times. All the AB_2 polymers showed a bimodal weight distribution whereas all the polyphenylenes derived from the A_2 and B_3 monomers showed a
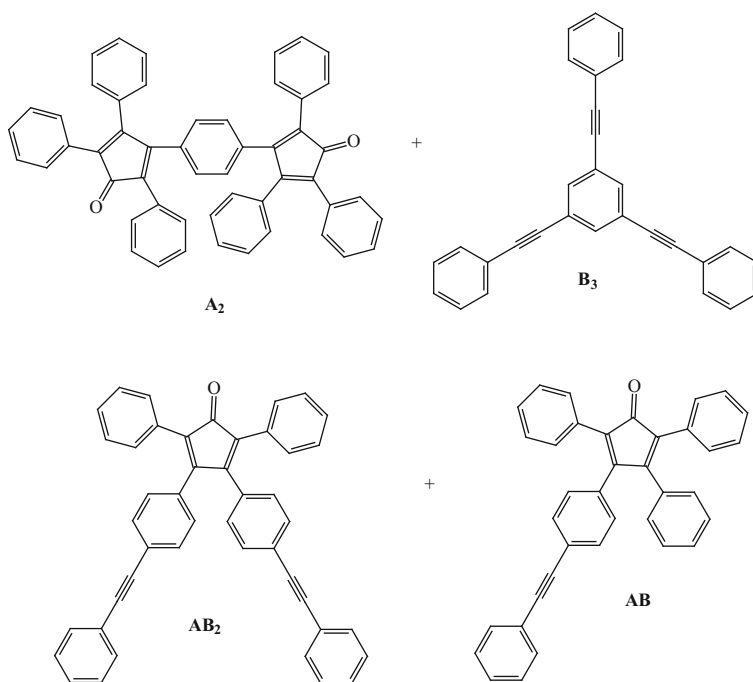
Scheme 21 Structures of monomers and monomer combinations used for the synthesis of hb-PPhs [231]

monomodal distribution. The molar masses of polymers resulting from the $AB_2 + AB$ approach (AB_2:AB = 3:1 and 1:1) decreased with an increase in the AB monomer content (M_w = 74,000–20,000 Da, as recorded by light scattering detector). All the hb-PPhs showed good solubility in common organic solvents, including chloroform and toluene. The polymer of molar mass M_w = 95,800 Da and Đ of 9.5 synthesized by self-condensation of AB_2 monomer also showed film-forming ability using very slow evaporation from a chloroform solution over several weeks [232]. Scheme 22 shows the structure of hb-PPh from AB_2 monomer and of a small rolled-up film of hb-PPh. It is noteworthy that the $A_2 + B_3$ system showed no crosslinking at functional equivalence (A_2:B_3 = 3:2) although the monomer conversions crossed the theoretical gel points. Voit and colleagues ascribed this behavior to the steric hindrance of the bulky hexaphenylbenzene units after two of the B groups of monomer B_3 were converted, resulting in polymers with a high percentage of linear units. The synthesized hb-PPhs did not show any T_g up to 360°C and TGA measurements showed $T_{d,10\%}$ of 550–600°C, indicating high thermal stability.

Suitable crosslinking chemistry for the hb-PPh with reactive alkynyl functionalities derived from the AB_2 approach, utilizing azide–alkyne click reaction by 1,3-dipolar cycloaddition, was utilized to check the suitability of such polymers as dielectric material in microelectronics. For polymers to be used for optoelectronic
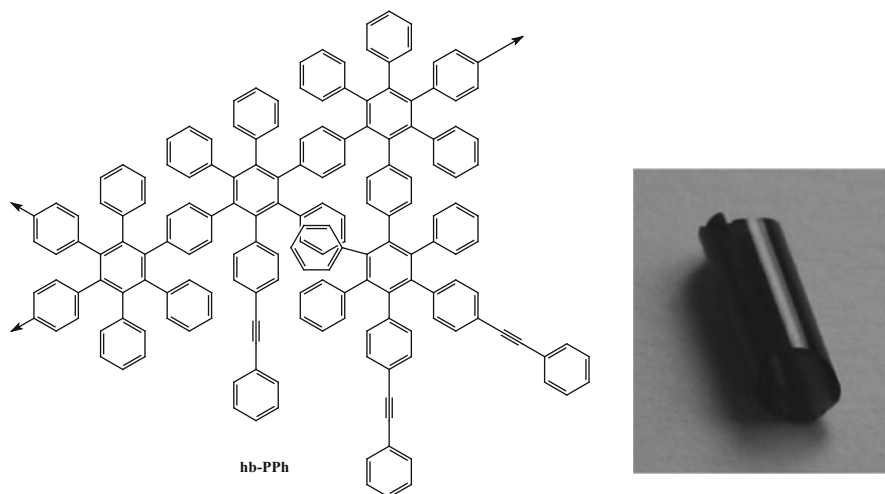
Scheme 22 Structure of hb-PPh from an AB$_2$ monomer (*left*) [231]. Small rolled-up film of hb-PPh of wall thickness ~0.5 mm (*right*). Reproduced with permission from [232]

application a metal-free reaction for curing is the preferred route because the removal of the Cu residues after click coupling of alkyne–azide moieties using Cu(I) catalyst is quite difficult, and small residues might be detrimental for a material to be used in microelectronic applications. Again, high temperatures for curing, such as above 200°C, should be avoided because of potential degradation of some active substances. In this regard, a small molecule, namely 1,3,5-tris (azidomethyl)benzene (TAMB), was prepared by Pötzsch and Voit [233] and successfully used to crosslink the hb-PPh matrix both thermally and photochemically. The mechanisms of these two crosslinking reactions were different; in thermal curing, triazole units were formed between the acetylene groups of hb-PPh and the azide group of the crosslinker in a 1,3-dipolar cycloaddition reaction. In the photochemical curing, a reactive nitrene group was formed upon photolysis of the azide group, which further reacted with the benzene rings in hb-PPh to form an azanorcaradiene derivate and after rearrangement an azepine unit. Films of hb-PPh and TAMB (9:1) were made by drop-casting the 5 wt% toluene solution onto glass substrates and either thermally crosslinking at 180°C for 6 h or exposing to UV light for 2 h. Scheme 23c shows neat hb-PPh film , where immediate film dissolution is observed in CHCl$_3$ yielding a greenish solution that is typical for hb-PPh. In comparison, for the thermally or photochemically crosslinked films, no film dissolution in CHCl$_3$ took place even after several days, indicating that these films were sufficiently crosslinked. Atomic force microscopy (AFM) in tapping mode revealed homogeneous surfaces of thin film, which explains why the thin film morphology remained unaffected by the crosslinking reactions.

The selectivity of thiol addition to a diphenylacetylene (DPA) system was studied recently by Voit and coworkers [234]. When thiophenol was used, no trace of bis-adduct was observed even when a large excess was used, which was
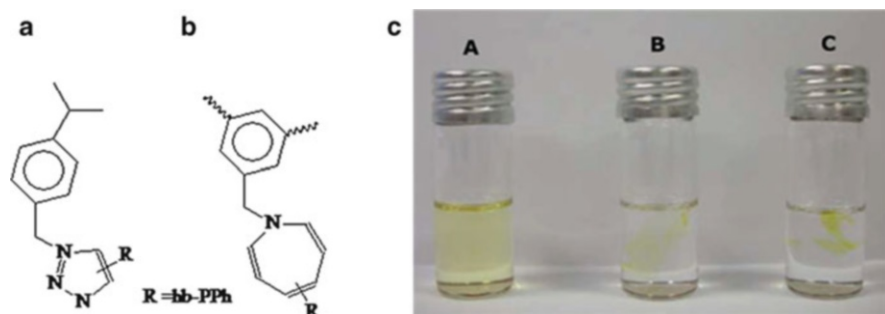
Scheme 23 (**a**) Thermal curing by formation of triazole unit. (**b**) UV curing by formation of azepine unit. (**c**) Films of hb–PPh in CHCl$_3$: pristine film (*A*); thermally crosslinked film (*B*); and UV crosslinked film (*C*). Reproduced with permission from [233]
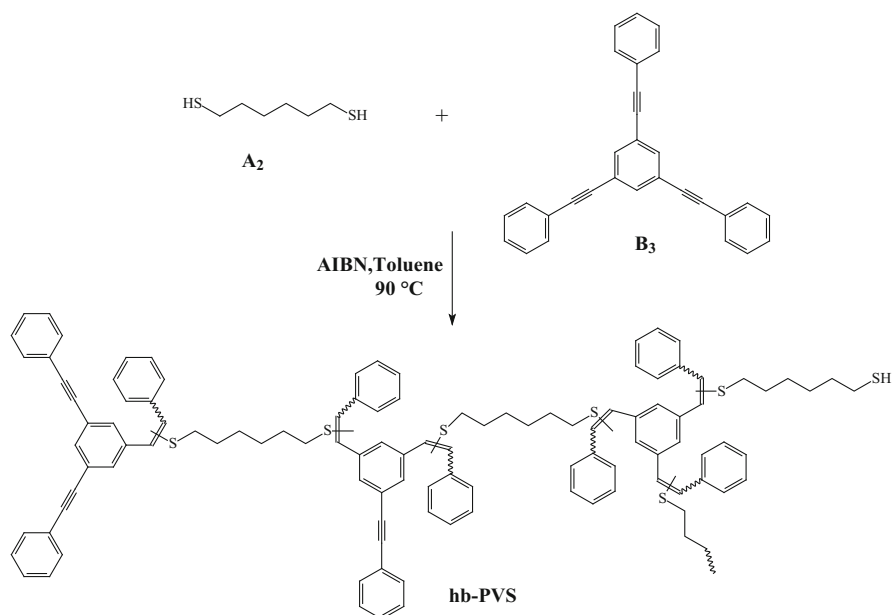
Scheme 24 Synthesis of hb poly(vinyl sulfide) (hb-PVS) with a sketch of the hyperbranched structure showing all potential units that may appear in the final polymer, depending on the molar ratio of A$_2$ and B$_3$. Reproduced with permission from [234]

attributed to the steric hindrance of a second thiol addition to the vinyl sulfide. This selective and efficient mono-addition reaction was applied for the preparation of hb poly(vinyl sulfide)s (hb-PVSs) via the A$_2$ + B$_3$ approach starting from 1,3,5-tris (phenylethynyl)benzene B$_3$ monomer and hexane-1,6- dithiol as A$_2$ monomer (as shown in Scheme 24). Polymerization was therefore conducted with a 1:1 molar ratio of thiol and alkyne functional groups using thermal initiation. The hb-PVS showed $T_{d,5\%}$ of 350°C and T_g of 68°C. The resulting polymer exhibited

excellent solubility in common organic solvents and showed a high refractive index of 1.70 at 589 nm, which was attributed to the presence of sulfur and phenyl rings in the (hb-PVS) [235]. The vinyl sulfides and residual end groups also provided suitable crosslinking sites. The authors concluded that such interesting properties, including good processability and the potential for secondary crosslinking, might be useful for application as suitable coating materials for optical devices.

Utilizing the methodology of selective thiol radical mono-addition to phenyl–acetylene derivatives, Voit and coworkers [236] recently synthesized a series of high refractive index hb polymers (refractive index of 1.68–1.75 with low optical dispersions of 0.004) by using different dithiol and trialkyne monomers. The hb structures produced materials with better performance in terms of light reflection and chromatic dispersion compared with linear analogs that were also synthesized for comparison.
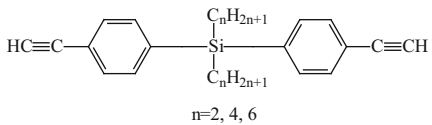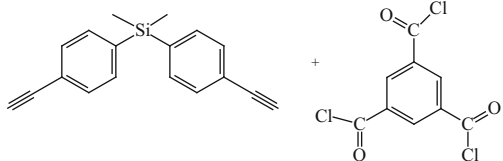
Conjugated Hyperbranched Polyarylenes

A variety of potential optical and electronic applications have been proposed for conjugated polymers, and the perspective has stimulated dynamic research activities on macromolecules with extended π-conjugations [237]. The frontier of research on conjugated polymers is now moving from linear to dendritic and hb structures [238, 239]. In general, such polymers are prepared by transition-metal-catalyzed alkynepolycyclotrimerization involving a single monomer species, such as acetylenic monomers, and do not suffer from stoichiometric imbalance [240]. Tang and coworkers explored polycyclotrimerization of aromatic diynes and succeeded in the homopolycyclotrimerization of organic and organometallic diynes and their copolycyclotrimerization with aromatic and aliphatic monoynes [241, 242].

Liu et al. [243] prepared soluble and processable hb poly(silylenephenylene)s (hb-PSPs) (Table 5, entry 1) by the polycyclotrimerization of A_2-type monomers initiated by a single-component catalyst $TaBr_5$. Spectroscopic analyses assisted by mathematical modeling revealed that ~75% of the triple bonds were cyclotrimerized into benzene rings via a [2+2+2] cyclotrimerization mechanism. The hb-PSPs were completely soluble in common organic solvents. The polymers showed $T_{d,5\%}$ of 480°C, possessed a unique σ–π conjugated electronic structure, and emitted strong violet-blue light upon photoexcitation. The triple bonds on the peripheries allowed the thin films of the polymers to be readily photocrosslinked, generating fluorescent photoimages in high resolutions.

Tang and coworkers [244] further synthesized a series of conjugated hb polyarylenes (hb-PAs) containing carbazole and/or fluorene chromophores by the homo- and copolycyclotrimerization of diynes with monoyne by different transition-metal catalysts and investigated their thermal and optical properties. Alkyne polycyclotrimerizations are effected by TaX_5-Ph_4Sn (X = Cl, Br) and $C_pCo(CO)_2$-$h\nu$ catalysts, yielding soluble hb-PAs with high molecular weights (M_w up to ~1.6×10^5 Da). The homopolymer showed $T_{d,5\%}$ as high as 560°C. All

**Table 5** Monomer structures and monomer combination used for the synthesis of conjugated hb polyarylenes

Entry no.	Monomer structures and monomer combination	References
1	$HC\equiv C-$ ... Si ... $C\equiv CH$, C_nH_{2n+1}, $n = 2, 4, 6$	[243]
2		[246]

the copolymers started degrading at slightly lower temperatures due to the incorporation of aliphatic 1-octyne into the polymer structure. In general, the hb-PAs prepared from $TaCl_5$-Ph_4Sn and $C_pCo(CO)_2$ showed quantum yield values of 50 and 53%, respectively, whereas the hb-PAs obtained from $TaBr_5$-Ph_4Sn showed a quantum yield value as high as 90%. The authors suggested that the poorer π-conjugation along the all-*meta*-substituted benzene ring might partially block the radiative decay pathways of the excited species and, consequently, lower the quantum yield value.

Organometallic hb-PPhs containing ferrocene groups to be utilized for magnetic ceramics were synthesized by Tang and colleagues [245] by designing a diyne monomer carrying a ferrocene moiety as single crystals. Scheme 25 shows the reaction scheme and structures of the monomer and hb-PPh. The authors successfully developed ruthenium- and rhodium-based catalysts to bring the polymerization reactions under control. The hb-PPh recorded by DSC showed a peak at 240°C during the first heating scan due to the thermally induced crosslinking associated with the alkyne polymerization; however, during the second heating scan no exothermic peak was realized indicating that the thermal curing process was irreversible. The (hb-PPh) started to lose weight at temperatures above 300°C.

For metallization, hb-PPh was admixed with octacarbonyldicobalt to form a cobalt complex. Refractive index values were measured for the neat hb-PPh and for the hb-PPh cobalt complex, indicating refractive index values of 1.704–1.681 together with low optical dispersion for the hb-PPh-cobalt complex, as verified by the high value of the Abbe number. The authors concluded that these materials could act as precursors to magnetic ceramics with high magnetizabilities.

Recently, Tang and coworkers [246] reported a new method for the formation of conjugated hb polymers with diyne monomer [bis(4-ethynylphenyl)dimethylsilane] and benzene-1,3,5-tricarbonyl trichloride as branching unit using the $A_2 + B_3$ polymerization approach (Table 5, entry **2**) by the rhodium (Rh)-catalyzed decarbonylative reaction for the formation of hb poly(arylene chloro-vinylene)s. The molar ratio selected for polymerization of A_2:B_3 was 4:3 (A:B = 8:9) so as to
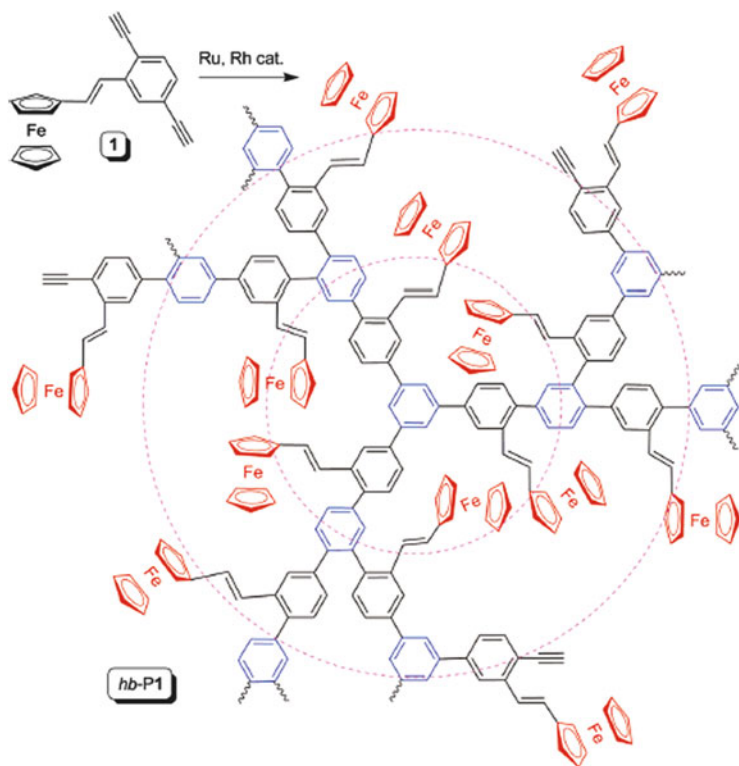
Scheme 25 Polymerization of (*E*)-1-[2-(2,5-diethynylphenyl)vinyl]ferrocene (*1*) to hyperbranched polyphenylene (*hb-P1*) with ferrocenyl groups attached to its repeat branches as pendant groups. Reproduced with permission from [245]

render an excess of alkyne functionalities at its peripheries for post-functionalization. The polymers showed good solubility in common organic solvents. The DB value of hb polymer was determined to be 30%. The authors attributed the low DB to the stoichiometric imbalance of the two mutually reactive groups during polymerization and to structural crowding of the branching unit (benzene-1,3,5-tricarbonyl trichloride). Thus, the reaction of the remaining acyl chloride moiety was difficult after the first two were consumed, leading to the formation of a large fraction of linear units and, hence, a lower DB. DSC measurements showed no thermal transitions in the hb polymer in both first and second heating cycles. The authors assumed that the hb polymer did not undergo any crosslinking reaction or post-polymerization due to its spatially branched structure, which restricted the probability for the vinyl chloride groups to approach each other. The $T_{d,5\%}$ of ~350°C indicated good thermal stability.
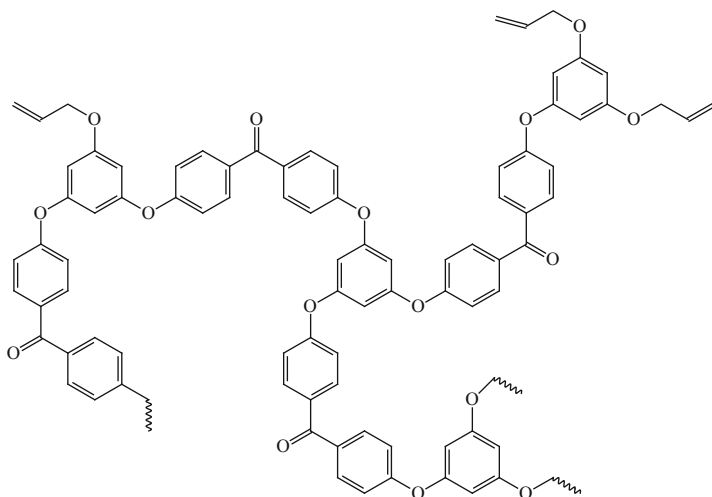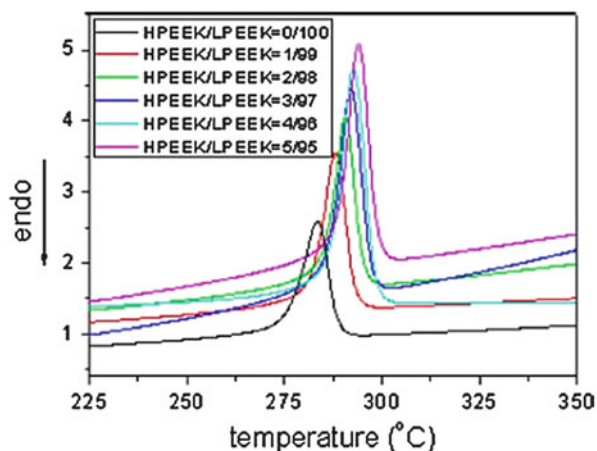
3 Applications

Hyperbranched polymers show lower viscosity and better solubility due to the branching and abundant functional groups and therefore they are good for use as additives. The aromatic hb polymers combine good miscibility and are thermally stable enough to allow melt processing.

3.1 Additives and Rheology Modifier

Schmaljohann et al. [247] used hb polyesters with alkyl-modified end groups as dye carriers in polyolefins. The use of hb polyesters resulted in a reduced melt viscosity of the polyolefin and a much better distribution of the dye in the polyolefin matrix. Jang et al. [248] showed that a small amount of hb polyester with hydroxyl end groups could greatly reduce the relative crystallinity of a semicrystalline polyethylene terephthalate (PET) through hydrogen bonds between the –OH groups of the hb polymer and the carbonyl groups of PET. Simon and coworkers [249] discovered that the lower-generation hb polyesters (Boltorn™-type) showed shear-thinning, whereas higher-generation polyesters exhibited Newtonian dependency, which was also found in the blends if at least one blend component showed Newtonian behavior. The study of Nunez et al. [250] on the rheological behavior of hb polyesters and their blends with linear polymers observed a drastic decrease in viscosity depending on the hb polymer concentration in the blends. More recently, Li et al. [251] employed hb poly(ether ether ketone) (hb-PEEK) at 1–5 wt% as a rheology modifier towards linear poly(ether ether ketone) (LPEEK) for improving the melt processability. Interestingly, the crystallization temperatures (T_c) of LPEEK/hb-PEEK blends were higher than that of pure LPEEK ($T_c = 283°C$), and the T_c of LPEEK/hb-PEEK blends gradually increased from 288 to 294°C with increasing hb-PEEK content in the blends. The increase in T_c of the blends was attributed to the enhanced crystallization capacity of LPEEK because incorporation of branched polymer resulted in a lower melt viscosity of the LPEEK/hb-PEEK blends compared to pure LPEEK, thus improving the mobility of LPEEK segments and leading to the increase in the crystallization capacity of LPEEK. Figure 4 shows the effect of hb-PEEK concentration on nonisothermal crystallization of LPEEK, indicating an increase in the crystallization capacity of LPEEK in the blends due to the presence of hb-PEEK as a rheology modifier in the crystallizing process of LPEEK.

Bismaleimide (BMI) resin is one of the most important thermosetting polymers due to its superior thermal resistance, outstanding dielectric property, and good fatigue resistance at high humidity. However, being a thermosetting resin, original BMI resins suffer from brittleness and poor processing features, such as high melting point and narrow work life, so toughening and improving the processing characteristics have been the main targets of the investigation of BMI resins. Recently, Tang et al. [252] synthesized allyl-terminated hb-PAEK and incorporated it into the BMI matrix with the aim of improving the toughness. BMI resins

Scheme 26 Structure of allyl-terminated hb-PAEK [252]

modified by allyl-terminated hb-PAEK (see structure in Scheme 26) showed good processability, with viscosities below 0.6 Pa s at 110°C. An increase in impact strength from 9.5 kJ/m^2 to about 14 kJ/m^{2}was realized, indicating improvement in the toughness of the cured BMI resins due to the presence of allyl-terminated hb-PAEK.

Aromatic hb polyamides have been used to modify the thermal, dielectric, viscoelastic, and rheological properties of linear polyamides [253, 254]. The characteristic architecture of these macromolecules makes them interesting candidates as a blend component with commercial linear polymers. A hb poly(ether amide) was blended with commercially available polyamide-6 (PA6) by Huber et al. [255] and Clausnitzer and coworkers [256]. The complex melt viscosity of the new materials was reduced, even at small amounts of the hb polymer, whereas the
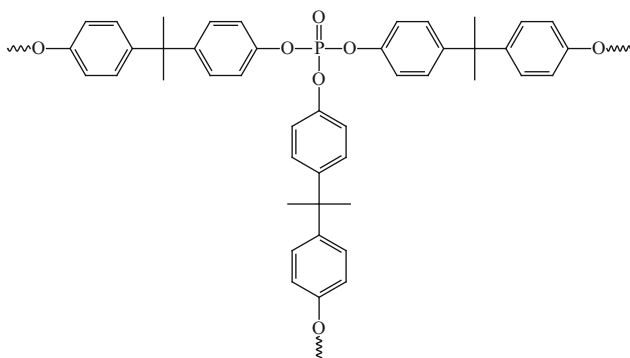
Scheme 27 Structure of dendritic unit of hb polyphosphate ester [258]

mechanical properties of the blends remained nearly constant. This was explained by the formation of hydrogen bonds between the hb polymer with the large number of hydroxyl groups and the polyamide. Hyperbranched polyphenylenes synthesized from AB$_2$ monomers were blended with linear polystyrene (PS) [76]. The resulting materials exhibited a reduced viscosity at high temperatures and an improved thermal stability compared with pure PS.

PA6 is one of the most important engineering plastics and is widely used as fibers, molded articles, and binders for composites. However, the applications of PA6 are still restricted in many fields owing to its poor flame retardant property and low limiting oxygen index (LOI) ~21, and because it burns easily. Fang et al. [257] synthesized hb polyphosphate bisphenol-S ester to improve the flame retardancy of PA6. Chen et al. [258] synthesized hb polyphosphate ester (Scheme 27) and used it as curing agent and flame retardant in epoxy resins.

Polypropylene shows an interesting set of mechanical and physical properties but it lacks dyeability and is not usually regarded as a textile fiber. Many efforts have been made to improve the dyeability of polypropylene. Recently, Sari et al. [259] utilized a poly(ester amide)-based hb polymer (Scheme 28) in fiber-grade polypropylene (PP) to study the nanostructure of the hb-modified PP and its correlation with macromechanical behavior. The study revealed an enhancement in mechanical properties due to the grafting reactions of hb poly(ester amide), leading to the formation of a crosslinked nanostructure of dendritic domains. The domains were capable of penetrating into the amorphous phase of the semicrystalline structure of the PP matrix and behaving as a toughener.

In order to improve the toughness of epoxy materials, hb polymers, having a 3D globular architecture and a large number of functional groups, were used for improving the toughness [260] and reducing the dielectric constant [203] by blending with epoxy resin lacking such qualities.

Qiang et al. used hb polymer with a terminal carboxyl group as an additive in auxiliary tanning of natural leather to improve the moisture absorption and permeability to water vapor of microfiber synthetic leather [261]. Recently, Ren et al. [262] prepared amino-terminated hb polyamide and grafted the same onto the polyamide microfiber synthetic leather employed for clothing, and organic
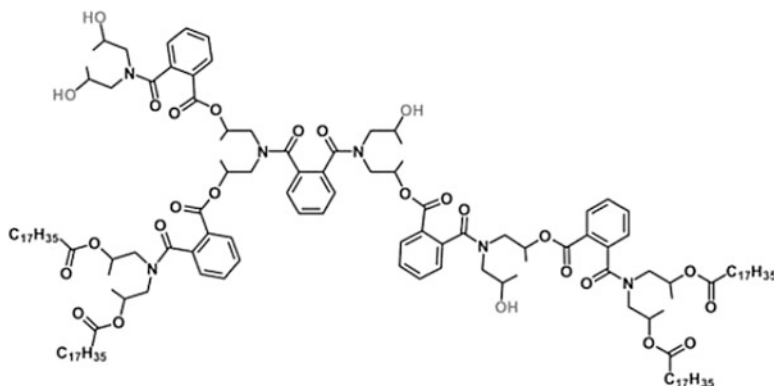
Scheme 28 Structure of hb poly(ester amide) (DSM Hybrane PS2550). Reproduced with permission from [259]

phosphine was used as a crosslinking agent to improve the content of the active groups and enhance the dyeing rate and color fastness. Wang and colleagues [263] synthesized hb poly(aryl ether ketone) terminated with cobalt phthalocyanine (CoPc-hb-PAEK) and studied its catalytic activity in oxidative decomposition of 2,4,6-trichlorophenol (TCP); the results were compared with those for the linear poly(aryl ether ketone) terminated with cobalt phthalocyanine [264, 265]. CoPc-hb-PAEK decomposed 75% of initial TCP within 7 h, whereas linear analogs decomposed only 68–70% within 7 h. This indicated that the efficiency of CoPc-hb-PAEK was better than the linear analogs due to highly branched structure of CoPc-hb-PAEK, followed by the high density and good dispersion of cobalt phthalocyanines compared to the linear analogs.

Hence, because of their unique 3D structure and the large number of functional groups, hb polymers provide high chances for possible interactions and, therefore, are expected to result in novel materials with improved properties upon compounding with other components. Thus, hb polymers are considered good candidates for use as additives and rheology modifiers.

3.1.1 Hyperbranched Phenylene Oxide as a Low Temperature Curing Agent

An epoxy-functionalized hb-PPO (epoxy-hb-PPO) (see structure in Scheme 29) was synthesized by Huang et al. [266] and the effect of adding 2.5–15% of epoxy-hb-PPO on the curing mechanism and kinetics of cyanate ester (CE) was studied.

Each prepolymer showed one exothermic peak; however, interestingly, all peaks of CE/epoxy-hb-PPO prepolymers appeared at a significantly lower temperature than those of CE prepolymer, demonstrating that an additional reaction took place in the CE/epoxy-hb-PPO resin system. The curing mechanism of CE was the cyclotrimerization of CE, whereas that of CE/epoxy-hb-PPO included the cyclotrimerization of CE under the catalytic role of –OH groups in epoxy-hb-PPO, the

Scheme 29 Structure of epoxy-functionalized hb-PPO [266]
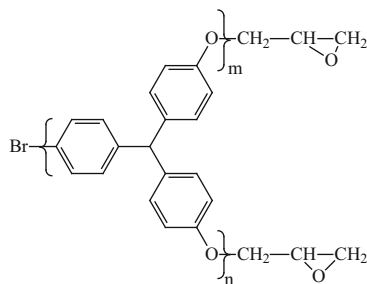
Fig. 5 Overlay plots of tan ∂ versus temperature for cured cyanate ester (*CE*), cured CE resin post-cured at 230°C (*p-CE*), and epoxy-functionalized hyperbranched poly (phenylene oxide) (*CE/ eHBPPO*) resins. Reproduced with permission from [266]
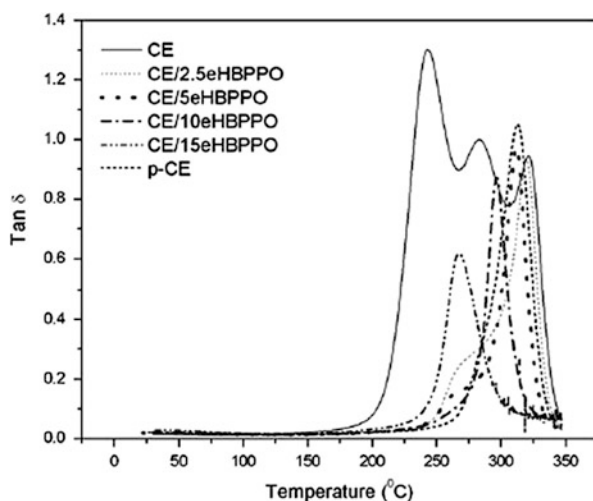
copolymerization between epoxy and –OCN groups as well as triazine rings of CE, and the self-polymerization of epoxy-hb-PPO. Moreover, CE/epoxy-hb-PPO showed a slightly smaller apparent activation energy (55–57 kJ mol^{-1}) than CE (58 kJ mol^{-1}), indicating the ease of the curing reaction of CE/epoxy-hb-PPO with the addition of epoxy-hb-PPO to CE. On the other hand, CE/epoxy-hb-PPO molecules less easily to collide with each other for curing because of the more branched architecture of epoxy-hb-PPO compared with neat CE. The incorporation of 10 and 15% of epoxy-hb-PPO to CE yielded CE/10epoxy-hb-PPO or CE/15epoxy-hb-PPO resin systems and their thermal properties were studied. Because the T_g of the cured CE ranged from 243 to 321°C and was difficult to compare with the resin systems containing epoxy-hb-PPO, the authors compared the thermal properties of the resins with p-CE (cured CE resin post-cured at 230°C), which showed a single T_g value of 314°C, as recorded from the plot of tan ∂ versus temperature. The T_g values observed for CE/10epoxy-hb-PPO and CE/15epoxy-hb-PPO resin system were 296 and 266°C, respectively, which were lower than the T_g value of the p-CE, indicating that the CE/epoxy-hb-PPO resin systems cured at lower temperatures than p-CE. Figure 5 shows the tan ∂–temperature plots for cured CE, p-CE, and CE/eHBPPO resins.
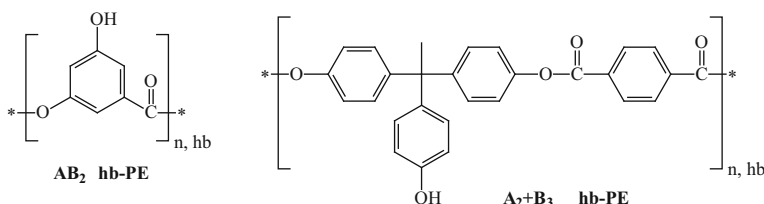
Scheme 30 Structures of hb-PEs from AB_2 and $A_2 + B_3$ approaches [267]

3.1.2 Hyperbranched Poly(aryl ester)s as Rheology Modifiers for Linear Polyamides

Voit and coworkers utilized high T_g hb aromatic polyesters [115] as additives for modification of the most important engineering thermoplastics, namely polyamides, in terms of their thermal properties and melt rheological behavior by blending. A lowering of the melt viscosity and, thus, an improvement in the processing properties is of high interest, especially for the partially aromatic polyamide PA6T/6, which requires a processing temperature above 310°C. Different amounts of the two hb polyesters, from 1 up to 20 wt%, were added to the linear thermoplastic polyamides by melt mixing. Two different polyamide grades, either partly aromatic polyamide-6 (PA6) or aliphatic polyamide-6 T-type (PA6T/6), were used for blending with hb aromatic polyesters [267]. Scheme 30 shows the structures of the AB_2 and $A_2 + B_3$-type polyesters that were used for blending. The influence of the addition of AB_2 and $A_2 + B_3$-type polyesters on the rheological behavior of linear polyamides was investigated. Miscible blends were formed in all cases, as was confirmed by a single T_g in DSC measurements.

The –OH group density in AB_2 hb polyesters (hb-PEs) was higher than that of $A_2 + B_3$ hb-PEs. The hb-PEs were compounded in the melt with the partly aromatic polyamide PA6 and the aliphatic polyamide PA6T/6 to obtain polyamide blends. Melt mixing was carried out at 320°C for PA6T/6 and at 250°C for PA6. As control samples, pure matrix polyamides and pure hb polyesters were also processed under the same conditions for comparison with the blends. All of the blends showed both T_g and T_m, indicating the semicrystalline nature of the polymer blends. The T_m as well as the crystallinity of the blends of PA6T/6 and hb-PE containing the AB_2 hb-PE was decreased from 297 to 258°C with increasing the amount of hb polymer from 1 to 20 wt%. The T_m as well as the crystallinity of the PA6/hb-PE blends containing the AB_2 hb-PE was decreased from 221 to 205°C with increasing the amount of hb polymer from 1 to 20 wt%. The T_g of the blends increased from 103 to 119°C for polyamide PA6T/6 as matrix material and from 56 to 72°C in the blends for polyamide PA6 as matrix material with increasing the content of AB_2 hb-PE from 1 to 20 wt% in the blends. With respect to the structures of the hb polyester and the polyamides, the increase in T_g was favored due to the formation of strong hydrogen bonding between the hydroxyl groups of AB_2 hb-PE and the carbonyl groups of the polyamides.

The addition of 1–10 wt% of $A_2 + B_3$ hb-PEs to polyamide PA6T/6 showed negligible effect on the T_g of the blends, the value of 101°C being the same as that for the polyamide PA6T/6. This was attributed to the influence of the temperature selected for compounding. At high processing temperatures (320°C) for the PA6T/6 blends, the $A_2 + B_3$ hb-PEs might undergo side reactions such as post-polymerization, leading to crosslinking, which prevent the formation of miscible blends. Gas chromatography/mass spectrometry (GC/MS) investigations of $A_2 + B_3$ hb-PE showed a release of phenol at temperatures above 250°C due to decomposition of terminal groups derived from the B_3 monomer [115], thus reducing the number of free phenolic groups responsible for the interactions with the polyamide.

The modification of PA6T/6 with AB_2 hb-PE led to a reduction in the complex viscosity, even at low concentrations of AB_2 hb-PE. After adding 1 wt% of AB_2 hb-PE, the zero-shear viscosity of PA6T/6 changed from 500 Pa s (0 wt% of AB_2 hb-PE) to 340 Pa s (1 wt% of AB_2 hb-PE). By increasing the amount of AB_2 hb-PE in the blends, a continuous reduction in the viscosity was observed until a concentration of 10 wt% was reached. Further increase in the AB_2 hb-PE content of the blends did not further affect the complex viscosity. The decreased melt viscosity of the resulting blends indicated improved processability of polyamides by the addition of AB_2 hb-PE. Adding 1 wt% of $A_2 + B_3$ hb-PE to PA6T/6 resulted in a comparable complex viscosity to that of the processed matrix polyamide. However, a larger amount of $A_2 + B_3$ hb-PE (10 wt%) in the blends resulted in a reduction in viscosity, especially in the region of higher frequencies. Generally, for the same concentration (e.g., 10 wt%) of hb polymers in the blends, the addition of AB_2 hb-PE resulted in a much more significant reduction in the complex viscosity of the final material than addition of $A_2 + B_3$ hb-PE.

All of the blends of PA6 and the hb polyesters exhibited Newtonian behavior. Only at a high content of AB_2 hb-PE was a decrease in the complex viscosity of the blends observed. The addition of $A_2 + B_3$ hb-PE to PA6 resulted in a continuously increased zero-shear viscosity from 380 to 920 Pa s with increase in the content of $A_2 + B_3$ hb-PE from 0 to 15 wt% in the blends, which is in contrast to previous findings [49, 247, 254, 268]. This was attributed to the existence of a heterogeneous system in which a phase with a higher viscosity ($A_2 + B_3$ hb-PE) was dispersed in the continuous phase (PA6) possessing a lower complex viscosity, and this was also manifested in the scanning electron microscopy (SEM) images. The hb polymer phase behaved like reactive filler. Also, $A_2 + B_3$ hb-PE distributed in the blend might behave as a coupling agent, connecting the polyamide chains at different positions through strong physical interactions that result in effects similar to a material being reinforced, causing an increase in the complex viscosity. In general, the addition of AB_2 hb-PE to the polyamides showed a more pronounced effect on the improvement of T_g and the processability of both the polyamides. However, the gelation tendency of $A_2 + B_3$ hb-PE at higher processing temperatures and the larger nonpolar branching unit and lower branching density lead to a lower miscibility of $A_2 + B_3$ hb-PE within the polyamide matrix. Besides, the lower density of –OH groups in $A_2 + B_3$ hb-PE induce a lower possibility for hydrogen bonding between $A_2 + B_3$ hb-PE and polyamides. Hence, AB_2 hb polyesters show a much higher
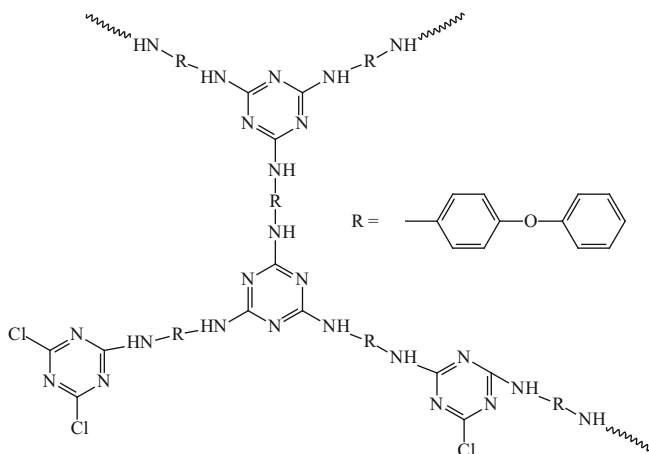
Scheme 31 Representative structure of hb-PAm used as flame retardant for PA6 [269]

potential for use as processing additives in linear thermoplastic polyamides compared to $A_2 + B_3$ hb polyesters because of the potential post-polymerization at the processing temperatures.

3.1.3 Hyperbranched Poly(aryl amine) as Flame Retardant for PA6

A hb polyamine (hb-PAm) was prepared by Ke et al. [269] utilizing the $A_2 + B_3$ approach where s-triazine was the B_3 monomer and ODA was the A_2 monomer. The representative hb-PAm structure is shown Scheme 31. The resulting hb-PAm acted as a hb charing and foaming agent (HCFA) in combination with ammonium polyphosphate (APP) to form a new intumescent flame retardant (IFR) system for PA6, abbreviated as IFR-PA6. The effect of HCFA on the flame retardance and thermal degradation properties of IFR-PA6 was investigated by the limiting oxygen index (LOI), UL-94 vertical burning, cone calorimetry, and thermogravimetric analysis (TGA).

The experimental results of UL-94 vertical burning indicated that all the IFR-PA6 composites gave a V-0 rating when the weight ratio of HCFA to APP was between 1:3 and 3:2. The IFR system showed the most effective flame retardancy in PA6 when the weight ratio of HCFA to APP was 1:2. The LOI value of IFR-PA6 could reach 36.5 with a V-0 rating when the IFR loading was 30 wt%. Additionally, even with 25 wt% loading of the IFR (where HCFA: APP = 1:2), a V-0 rating could be still maintained with an LOI value of 31. The interaction between APP and HCFA improved the char formation ability of the IFR system. Much more char was formed for the PA6/HCFA/APP composite than for the PA6/APP system, indicating better flame retardancy with incorporation of HCFA. The char acted as a barrier that prevented the transfer of gas and heat flow during combustion and, hence, the flame retardancy of PA6 resin was greatly

improved by adding HCFA to the system. The average heat release rate (Av-HRR), peak heat release rate (PHRR), and total heat release (THR) values were recorded by a cone calorimeter. In general, for effective flame retardant materials, the heat release in tests should reduce drastically. The results of cone calorimetry also showed HCFA/APP as an effective IFR system for PA6. Neat PA6 showed the following values: Av-HRR 310 KW/m^2, PHRR 490 KW/m^2, and THR 106.5 MJ/m^2. For the PA6/APP system, the values were reduced: Av-HRR 133 KW/m^2, PHRR 420 KW/m^2, and THR 43.7 MJ/m^2. The PA6/HCFA/APP showed Av-HRR 76 KW/m^2, PHRR 343 KW/m^2, and THR 31 MJ/m^{2}values, which were lower than the values recorded for neat PA6 and indicated that PA6/HCFA/APP is an effective flame retardant system. TGA results showed higher char residue at 700°C for the PA6/HCFA/APP composite system (24% char residue) compared to the PA6/APP composite system (15% char residue) because when HCFA was added the polyphosphoric acid not only interacted with PA6 but also with HCFA, decreasing the amount of evaporated excess polyphosphoric acid and enhancing the char formation ability.

3.1.4 Hyperbranched Polyphenylene Sulfide as Textile Dyeing Agent for Polypropylene

The hb-PPS prepared from previously synthesized AB$_2$ monomer [206] was utilized for studying the dye uptake by PP in the presence of a monoazo-type of disperse dye, namely CI Disperse Red 202 [270]. The hb-PPS at various concentrations was added to PP granules followed by melt mixing to form hb-PPS/PP spun fibers. Due to the presence of polar groups and aromatic rings in hb-PPS, the hb-PPS/PP spun fibers showed the potential to interact with the dye. The neat PP fibers were dyed to a pale depth and the modified PP fibers were dyed to a deeper depth, indicating the presence of hb-PPS in the modified PP. In the case of the modified PP fibers, the dye uptake increased with increased hb-PPS content from 1 to 3 w/w%, which was attributed to the increased introduction of polar groups and aromatic rings that acted as active sites for the dye molecules. With hb-PPS dispersed in PP matrix, the chlorides formed intermolecular hydrogen bonding with the proton-supplying groups (such as −OH and −NH$_2$) present in the dye structure. Aromatic rings, present in hb-PPS, formed π bonds with the groups in the dye molecules supplying protons, which also helped to produce deeper shades of color. There was no increase in the depth of shade in hb-PPS modified PP fibers with increasing the dye concentration from 4 to 6%, which Yan's group attributed to the saturation of dye sites in hb-PPS-modified PP fiber. The hb-PPS/PP blends showed only one T_g, corresponding to the T_g of PP, because of the very low content of hb-PPS present in the blend. Interestingly, with increasing the hb-PPS content, the T_g of the PP phase showed a tendency to shift towards higher temperatures, indicating that the blends were partially miscible.

3.2   Membranes

Aromatic hb polymers have been found to fulfill the broad material needs for membrane-based separation applications due to their large free volume. Some selected examples will be highlighted to demonstrate the potential of hb polymers for membrane-based applications.

In recent years, there has been increasing interest in reverse osmosis (RO) membranes for desalination. Thin film composite polyamide membranes are currently used in commercial RO membranes [271]. Among these materials, m-phenylenediamine- and trimesoyl chloride-based polyamides prepared by interfacial polymerization are available as commercial products [272, 273]. Ideally, RO membranes should possess high flux and high salt rejection, in addition to excellent chlorine and fouling resistance, mechanical durability, and low cost. Chiang et al. [274] synthesized nanofiltration membranes based on hb polyethyleneimine ($M_w = 2,000$ Da) with two acyl chlorides, namely trimesoyl chloride and terephthaloyl chloride. They observed that highly branched polyamides showed higher flux and higher salt rejection to sodium chloride, which the authors attributed to the presence of pendant amine groups that interact with the ions in the pathway and thus hinder ion transport. Recently, Park et al. [275] prepared hb aromatic polyamide-grafted silica and disulfonated 4,4-bis(3-aminophenoxy)phenyl sulfone composite membranes to enhance the chlorination resistance of RO membranes for desalination. After the chlorination test, salt rejection was decreased by 36.2% and water permeation was increased by only 5.6% compared with performance before chlorination measurement.

Fuel cells are regarded as efficient and clean energy sources as alternatives to limited fossil fuel resources. For proton exchange membranes for fuel cell (PEMFC) applications, high proton conductivity, mechanical properties, and oxidative stability are the basic requirements. DuPont's Nafion is a commercially available perfluoro sulfonated polymer membrane and is the current state-of-the-art proton exchange membrane [276]. However, Nafion has the drawbacks of low operational temperature ($<80°C$) and being very costly due to its complex preparative technique. These deficiencies have produced great research interest in developing alternative polymer electrolyte membranes based on ethoxysiloxane [277]. The proton conductivities of these membranes are comparable to Nafion 115 in humid state. In a separate study, Gode et al. synthesized a novel sulfated hb polymer for the PEMFC [278], such as sulfonated poly[3-ethyl-3-(hydroxy-methyl] oxetane. The hb polymer-containing PEMFC showed higher proton conductivity compared to Nafion 117 in humid state. The hb sulfonated poly(3-ethyl-3-(hydroxy-methyl) oxetane-modified membrane was more flexible and exhibited better mechanical properties than the chemically crosslinked membranes, such as the Nafion series. Recently, Itoh et al. synthesized two novel hb polymers with sulfonic acid or acryloyl groups at the end of chains [279]. It was reported that the ionic conductivity of these two novel hb polymers increased with increasing

temperature and that the thermal stability of these materials was perfect up to 200°C.

Membrane-based gas separation has attracted much attention during the last two decades. Compared with traditional separation processes it has many significant advantages, such as low investment cost, low energy consumption, simple operation, etc. Gas separation processes using polyimide gas separation membranes have been developed and are of great interest because of their excellent thermal, mechanical, and gas transport properties [280]. The high gas permeability of polyimides is generally attributed to the large fractional free volume, which is closely related to their highly rigid structure, whereas the high selectivity is due to the high diffusion selectivity and/or the high solubility selectivity. On the other hand, it is reported that there are many open and accessible cavities in a rigid hb polymer that are formed due to the periphery of neighboring branches. These cavities may function as the pathways for the transport of gas molecules, resulting in high gas permeability [281–286].

3.2.1   Sulfonated hb Poly(aryl ether ketone) for PEMFC

Wang et al. [287] prepared sulfonated linear poly(aryl ether ketone) (S-LPAEK)/ sulfonated hb poly(aryl ether ketone)s (S-hb-PAEKs) blend membranes and focused on the influence of the IEC and the content of S-hb-PAEKs on the properties of the blend membranes. The S-LPAEK membranes with varying content of sulfonated groups were synthesized and characterized. Three S-hb-PAEKs were synthesized based on varying degrees of sulfonation by post-functionalization of fluoro-terminated hb poly(aryl ether ketone) (F-hb-PAEK) with concentrated sulfuric acid at different temperatures and reaction times to afford S-hb-PAEKs with three different ion exchange capacities (IECs); these were named S-hb-PAEK-20, S-hb-PAEK-40, and S-hb-PAEK-60. The monomer combinations for the synthesis of S-LPAEK and S-hb-PAEK are shown in Scheme 32. The, S-hb-PAEKs and S-LPAEKs were blended and cast into membranes. The blend membranes were prepared using DMAc as solvent and S-hb-PAEK content was 15, 20, 25, and 30 wt% in the S-hb-PAEK/S-LPAEK blends.

The T_g of F-hb-PAEK was 124°C, whereas no T_g was found up to 300°C for S-hb-PAEKs due to the ionic effects that produced increased intermolecular interaction, followed by the difficulty of the internal rotations. The thermal stability of F-hb-PAEK was better than that of the S-hb-PAEKs, and the thermal stability of S-hb-PAEKs gradually decreased with increasing IEC value because of the increase in sulfonated groups.

The T_g values of all S-hb-PAEK/S-LPAEK blend membranes were lower than 214°C (the T_g of the sulfonated linear analog, S-LPAEK was 214°C) and gradually decreased with the increase in S-hb-PAEK content. The T_g values of these membranes were 214, 199, 188, 184, and 180°C for blend composition S-hb-PAEK-XX/ S-LPAEK with S-hb-PAEK-XX contents of 0, 15, 20, 25, and 30 wt%, respectively. Besides, S-hb-PAEK-40/S-LPAEK and S-hb-PAEK-60/S-LPAEK membranes
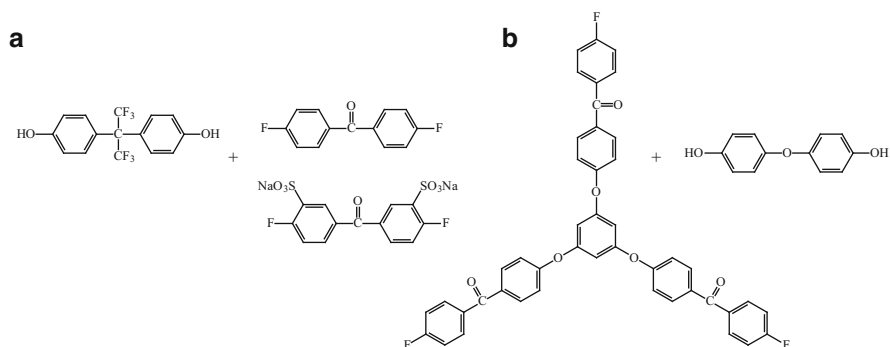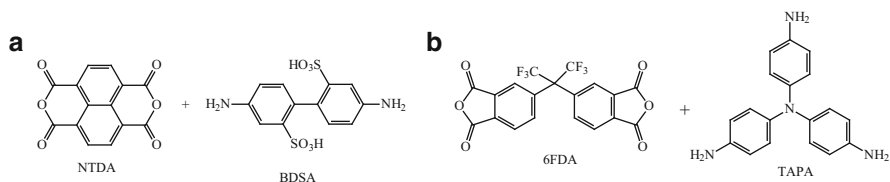
Scheme 32 (**a**) Monomer combinations for the synthesis of S-LPAEK. (**b**) Monomer combination for the synthesis of S-hb-PAEK [287]

showed similar a trend. The blend membranes exhibited second and third weight loss at ~350°C and 500°C, corresponding to the loss of sulfonated groups and the actual thermal decomposition of the polymer backbone, respectively, indicating high thermal stability. The water uptake and proton conductivity of all the blend membranes increased with the IEC and content of S-hb-PAEK in the blend membranes compared to neat S-LPAEK. This was a result of the formation of larger and more continuous ion networks as well as an increase in the free volume arising from the introduction of the branched structure. The membranes exhibited enhanced proton conductivity at lower temperatures (20 and 40°C).

3.2.2 Sulfonated Star Hyperbranched Polyimide for PEMFC

Suda et al. [288] reported the synthesis and characterization of a series of sulfonated star-hb polyimides (S-hb-PIs) without any crosslinking for use as proton exchange membranes. Sulfonated anhydride-terminated polyimides with different molecular weights (M_w = 59,000, 200,000 and 300,000 Da) based on monomer combination 1,4,5,8-naphthalene tetracarboxylic dianhydride/4,4′-diaminobiphenyl 2,2′-disulfonic acid (NTDA/BDSA) were synthesized using different molar ratios of BDSA:NTDA. The amine-terminated hb-PI based on monomer combination 4,4-(hexafluoroisopropylidene)diphthalic anhydride/tris(4-aminophenyl)amine (6FDA/TAPA) was also prepared. Scheme 33 shows the monomer combinations used for the preparation of (S-hb-PI).

The amine-terminated polyimide solution in *m*-cresol was added dropwise to sulfonated anhydride-terminated polyimide and stirred following a temperature profile of 70°C for 4 h and 180°C for 24 h to form S-hb-PI with a core–shell structure. The hb polymer based on 6FDA/TAPA formed the core and linear polymer based on NTDA/BDSA formed the shell. The S-hb-PI membranes was soluble in aprotic polar solvents such as in DMAc, DMSO, DMF, and NMP. The

Scheme 33 (**a**) Monomer combination NTDA and BDSA used for the synthesis of sulfonated anhydride-terminated polyimide. (**b**) Monomer combination 6FDA and TAPA used for the synthesis of amine-terminated hb-PI [288]

S-hb-PI membranes showed film-forming ability because of the enhanced entanglement between linear polymers. The M_w values of the S-hb-PI membranes were 320,000, 500,000, and 830,000 Da, respectively, which corresponded to the increase in the molecular weights of sulfonated anhydride terminated polyimides. The onset temperature of decomposition T_d started above 280°C due to the desulfonation of the S-hb-PI membranes. The weight loss above 550°C was due to decomposition of the polymer backbone. The proton conductivities of the S-hb-PI membranes were in the range of 0.34–0.51 S/cm at 80°C and relative humidity ~98%, indicating higher values than that of Nafion (proton conductivity ~0.15 S/cm) under the same conditions. Suda and coworkers suggested that the S-hb-PI membrane containing sulfonic acid groups as a linear hydrophilic domain at the core surface might have formed ionic channels. However, the S-hb-PI membranes broke within 1 h in the presence of Fenton's reagent, indicating that oxidative stability should be improved from an application point of view.

3.2.3 Hyperbranched Polyimide–Silica as a Gas Separation Membrane

The gas transport properties of hb-PI blend membranes of 4,4′-(hexafluoroisopropylidene) diphthalic anhydride/1,3,5-tris(4-aminophenoxy)benzene (6FDA/TAPOB) and 4,4′(hexafluoroisopropylidene) diphthalic anhydride/3,3′-dihydroxybenzidine (6FDA/HAB) blends and their silica hybrid membranes were investigated by Suzuki et al. [289]. The formation of a hb-PI blend silica hybrid membrane is presented in Scheme 34 in a simplified manner. Polymer blending is also a useful approach for combining the advantages of individual components. A number of polyimide-based polymer blends have been studied to develop high-performance gas separation membranes [43, 290–292]. DMAc solutions of the amine-terminated 6FDA/TAPOB-based hb-PAA and 6FDA/HAB hydroxyl-PAA were mixed at room temperature in ratios of 40:60 or 20:80 wt%. Then, 3-(triethoxysilyl)propylsuccinic anhydride (TEOSPSA) was added as a coupling agent and imidization carried out under nitrogen flow to obtain (6FDA/TAPOB)/(6FDA/HAB) blend silica hybrid membranes of 20–25 μm thickness. Neat blended membranes without silica were also prepared in a similar manner for comparison.
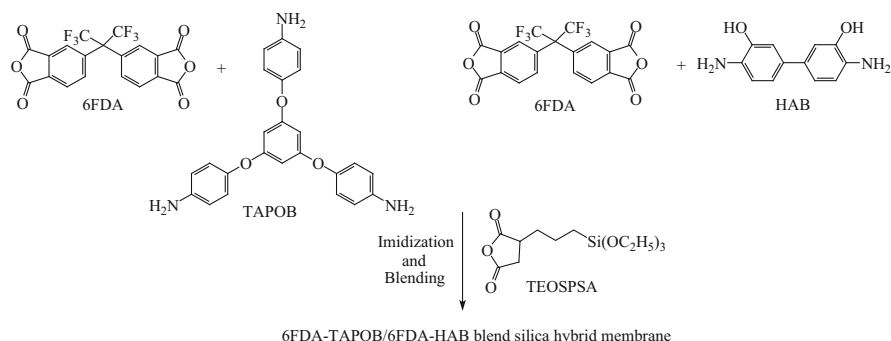
Scheme 34 Monomer combinations used for the formation of hb blend silica hybrid membranes in the presence of coupling agent [289]

In general, gas permeability and selectivity of a binary polymer blend are described by the semilogarithmic additive rule [293]. Gas permeability coefficients of hb-PI (6FDA/TAPOB)/(6FDA/HAB) blend membranes showed positive deviation from the semilogarithmic additive rule. The enhanced gas permeabilities resulted from the increase in free volume elements caused by the intermolecular interaction, disrupting molecular chain packing between terminal amine groups of hb-PI (6FDA/TAPOB) and hydroxyl groups coming from the (6FDA/HAB) backbone. Ideal the CO_2/CH_4 selectivity of hb-PI(6FDA/TAPOB)/(6FDA/HAB) blend silica hybrid membranes showed a tendency to exceed the upper limit for CO_2/CH_4 separation with increasing silica content, that is CO_2 permeability, comparing the results reported by Robeson [294, 295]. The remarkable CO_2/CH_4 separation behavior was considered to be due to the characteristic distribution and interconnectivity of free volume elements created by the incorporation of silica. For the hb-PI (6FDA/TAPOB)/(6FDA/HAB) blend system, the polymer blending and hybridization with silica synergetically induced the enhancement of free volume elements, which provided the prominent CO_2/CH_4 separation ability. This finding was also supported by SEM images, where silica particles showed poor interfacial adhesion with sharp and clear boundaries, indicating the induction of free space around the polymer–silica interfacial area. The T_g values of the hybrid membranes could not be detected by DSC, whereas the blend membranes without silica showed T_g values in the range of 332–329°C. This behavior was attributed to a strong inhibition of segmental mobility of molecular chains by silica. On the other hand, the $T_{d,5\%}$ increased up to 486–496°C with increasing silica content in comparison to the blend membranes without silica that showed values of ~479°C, indicating higher thermal stability by the hybridization with silica. The gas permeability coefficients of the hybrid membranes also increased with increasing silica content.

3.3 Optoelectronic Materials

Photosensitive polymers are well-known polymer materials that play important roles in the field of semiconductor manufacturing as protection and insulation layers. The applications of hb polymers as photoresist materials seem to be very promising. Hyperbranched polymers with compact molecular chains and low chain entanglement offer some advantages over linear polymers for those attempting to pattern feature sizes that are on the order of the molecular dimensions. In addition, the peripheral location of the photosensitive groups at the polymer framework is expected to produce high sensitivity to exposure to light. Fréchet and coworkers [296] reported a hb polymer as the first example of a chemically amplified resist. Ueda and coworkers [297] reported a new negative working photoresist based on resorcinol-terminated hb poly(ether imide) with 4,4′-methylenebis[2,6-bis (hydroxymethyl)]phenol as a crosslinker (**1–50**, Scheme 35) and diphenyliodonium 9,10-dimethoxyanthracene-2-sulfonate as a photoacid generator; it exhibited a feature resolution of 4.5 μm when exposed to 365-nm UV light.

In et al. [298] reported a hydroxy-terminated hb poly(arylene ether phosphine oxide) (**1–51**, Scheme 35) containing 10 wt% diphenyliodonium-9,10-dimethoxyanthracene-2-sulfonate as a photoacid generator and 25 wt% 4,4′-methylenebis-[2,6-bis(hydroxymethylphenyl)phenol] as a crosslinker. It had a sensitivity of 9 mJ/cm^2 and a contrast of 1.6 under 365-nm UV light exposure. Kakimoto and coworkers [299] described a kind of chemically amplified photosensitive polybenzoxazole based on a *tert*-butoxycarbonyl-protected hb poly(*o*-hydroxyamide) (**1–52**, Scheme 35). The resist showed a sensitivity of 115 mJ/cm^2 and a contrast of 2.2 with 365-nm light exposure. A series of benzophenone-containing hb polyimides (hb-PIs) were prepared by Chen and Yin [300, 301] via the end-capping modification of the terminal anhydride groups by *ortho*-alkyl aniline. The hb-PIs were characterized as inherently photosensitive to UV exposure, giving a patterning resolution greater than 3 μm. Chen and Yin [302] also prepared hb-PIs with terminal phenol groups that were modified by acyl chloride compounds (acryloyl chloride, methylacryloyl chloride, and cinnamoyl chloride) to yield photosensitive hb-PIs. Photosensitive property studies revealed good photolithographic properties with a resolution greater than 3 μm and a sensitivity of 650–680 mJ/cm^2. A series of autophotosensitive semi-aromatic hb-PIs end-capped with 3-aminophenylacetylene (**1–53**, Scheme 35) were prepared by Liu et al. [303]. Photosensitivities of hb-PIs were obtained in the range of 80–162 mJ/cm^2, and they showed a clear negative image with a line width of 8 μm when exposed to UV light of 365 nm. Scheme 35 shows some structures of hb polymers used as photoresist materials.

Second-order nonlinear optical (NLO) organic polymer materials have also attracted much attention because of their potential applications in the fields of high-speed electro-optic (EO) modulators, optical data transmission, and optical information processing [304, 305]. Organic polymers have been conceived as a suitable material for these optical devices due to their large optical nonlinearity and
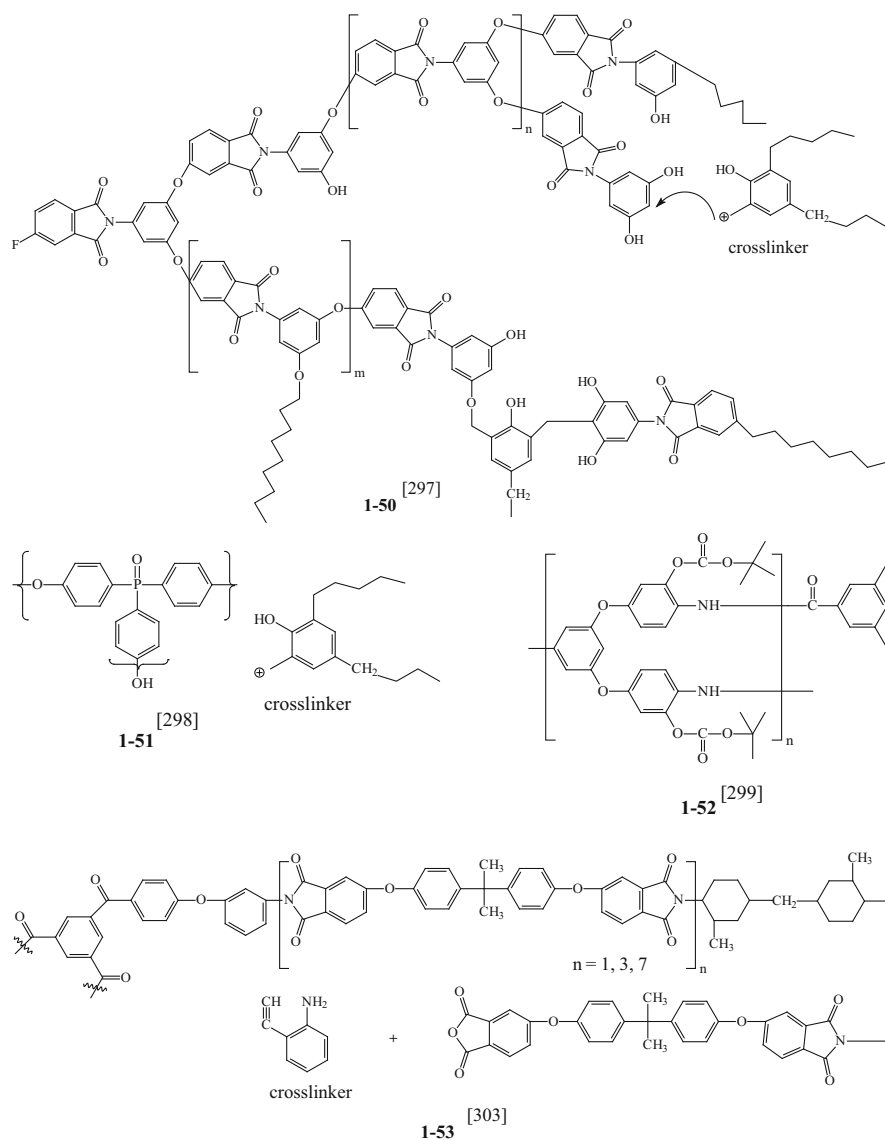
Scheme 35 Representative structures of hb photosensitive polymers

easy fabrication. NLO polymers have many advantages over conventional inorganic polymers, such as light weight, low cost, ultrafast response, wide response wave band, high optical damage threshold, and good processability to form optical devices. A potential NLO polymer must contain highly polarizable conjugated electronic systems and has to be mechanically very strong and thermally stable with a high T_g, together with stabilization of electrically induced dipole alignment.

To exhibit an EO effect, the active moieties (NLO chromophores) should be generally poled under an electric field to form a highly ordered noncentrosymmetric alignment. A proportional relationship between chromophore concentration and optical nonlinearity is observed at low chromophore content. Furthermore, intermolecular dipole interactions at high chromophore content cause obvious decrement in optical nonlinearity. The design of a chemical structure that suppresses the dipole interactions is a promising approach for improving the optical nonlinearity. Hence, there is a need to design and synthesize new chromophores to produce better optical nonlinearity. Hyperbranched polymers with 3D spatial separation of the chromophore moieties endows them with favorable site isolation effects, while their void-rich topological structure could minimize optical loss in the NLO process [306–309]. Therefore, macromolecules with branched architectures are alternative promising candidates for NLO materials with large bulk EO activities. Chang et al. [310] synthesized hb polymers via a ring-opening addition reaction between azetidine-2,4-dione and primary amine. All the obtained polymers showed EO coefficients in the range of 6–16 pm/V with temporal stability at 60°C. The monomer combination used for the synthesis of hb NLO polymer is shown in Scheme 36.

Hyperbranched polymers with methyl ester or epoxy as terminal groups containing pendant azobenzene chromophores (1–54, Scheme 37) were prepared by Xie et al. [311]. The poled films exhibited EO coefficients (>50 pm/V) due to the 3D spatial isolation effect resulting from their highly branched structures. Bai et al. [312] prepared thermally crosslinkable, hb oligomer containing NLO chromophores and blended it with linear host polymer. They obtained large and stable EO coefficients up to 65 pm/V, which are suitable for device development in terms of improved poling efficiency and temporal stability. Xie et al. [313] synthesized an hb polytriazole (1–55, Scheme 37) and compared the results with a linear analog. The poled film of hb polytriazole showed a much higher second-harmonic coefficient (96.8 pm/V) than the linear analog (23.5 pm/V). They proposed that the 3D spatial isolation effect resulting from the highly branched structure and crosslinking of the terminal acetylene groups at moderate temperature led to the enhancement of optical nonlinearity.

Jiang's group [68] prepared fluorinated hb-PAEK end-capped with nickel phthalocyanine and checked the material for NLO applications. The third-order nonlinear coefficient was found to have a value of 0.98×10^{-11} esu, which the authors attributed to the dual contributions of nonlinear absorption and refraction of the molecules. Moreover, the obtained value was found to be almost five times larger than that of other metallophthalocyanines [314] due to presence of the hyperbranched structure, the aromatic backbone, and the number of end-functionalities.

Hyperbranched polymers, are good candidates for both core and cladding materials in photonic device applications [315, 316] due to excellent processability and good optical properties in terms of low optical losses, low birefringence and high T_g. Gao et al. [317] developed ZnO/hb-PI nanohybrid films and investigated the optical properties and fluorescence mechanisms. An efficient energy transfer from
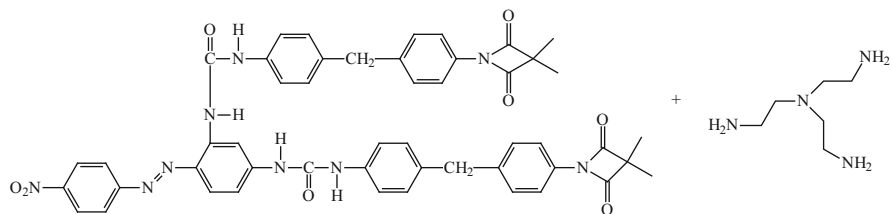
Scheme 36 Monomer combination used for the synthesis of hb NLO polymer [310]

[311]
1-54

[313]
1-55
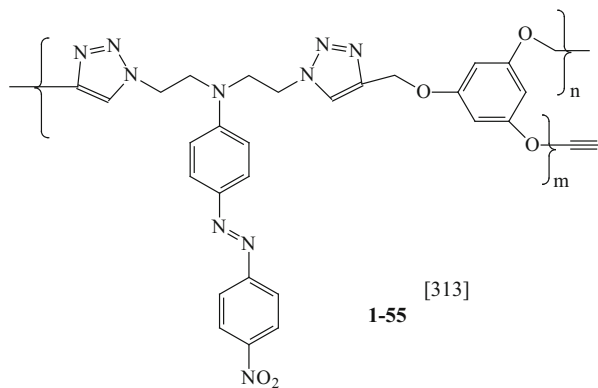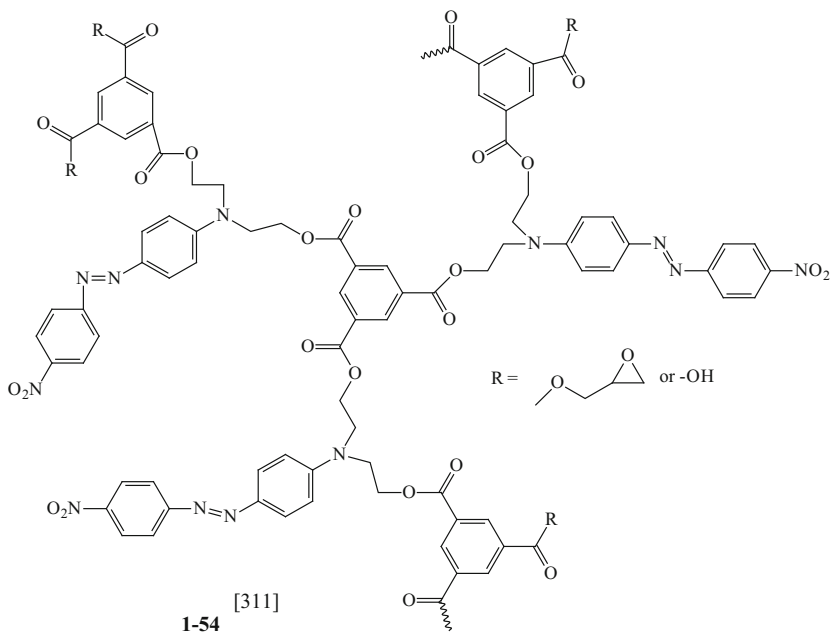
Scheme 37 Representative hb architectures used as NLO polymers

the excited donor (ZnO) to the accepter (hb-PI) occurred in this unique hybrid system and originated from the sufficiently short distance between the ZnO surface and hb-PI chains. All the films exhibited good optical transparency in the range of 450–800 nm, as detected by UV–vis absorption spectra. Chen et al. [137] synthesized both amine- and anhydride-terminated hb-PIs and investigated them using UV–vis spectra and fluorescence spectroscopy. The hb-PIs showed UV–vis absorptions in the region 200–400 nm and also displayed strong purple and blue fluorescence at 400 and 460 nm, respectively, indicating their possible utilization in organic photoluminescence and photoelectricity. Zhang and colleagues [142] prepared hb-PIs end-capped with metallophthalocyanines that showed different colors in chloroform ($CHCl_3$) solution depending on the type of metal present in the hb-PI, i.e., brown, dark green, and green colored for Cu, Zn, and Ni, respectively. The absorption maxima as detected by UV–vis spectra of the three polymers in chloroform solution were 672, 701, and 665 nm, respectively. A fluoro-terminated hb poly (aryl ether ketone) end-capped by azobenzene chromophores was prepared by Jiang et al. [318]. The UV-visible absorption spectrum of azo-hb-PAEK in DMF solution exhibited two absorption bands in the range of 300–650 nm, centered around 347 and 445 nm, which revealed the π–π^* and n–π^* electronic transitions of the azo-chromophoric moieties. The azo-hb-PAEK films were investigated for surface relief grating (SRG) and birefringence measurements. The SRGs of the azo-hb-PAEK film showed good thermal shape stability and could not be totally erased by even heating up to 300°C, which the authors attributed to the rigidity of the azo-hb-PAEK structure. The azo-hb-PAEK showed a large photoinduced birefringence intensity and good reversible optical storage upon irradiation with 532 nm light using a Nd:YAG laser. Such azo-hb-PAEKs show potential application in holographic memory, reversible high-density optical storage, optical switches, and other photodriven devices.

Multilevel interconnection technology is essential for realization of high density and ultralarge scale integrated circuits (ULSIs). The interlayer dielectric film technology is one of the most important keys for fabrication of multilevel interconnections [319]. Dielectric materials must meet stringent material property requirements for successful integration into the interconnect structures. The desired electrical properties are low dielectric constant, high T_g, high thermal and chemical stability, and good mechanical properties. The linear polyimide made from PMDA and ODA was the first to be commercialized by DuPont under the trade name Kapton®, and it is still the most widely used dielectric material in microelectronics. It has a high T_g of 377–400°C and dielectric constant of 3.1–3.5. With microelectronic devices becoming smaller and lighter during the past decades, a low dielectric constant has become one of the most crucial factors for minimizing electrical power loss and delay in signal transmission in microelectronic applications and, hence, there is a great need for materials exhibiting low dielectric constants for application as insulating materials around the interconnecting wires in these devices [320].

One of the developments in low-dielectric-constant polymers has been an increase in the free volume in the structure. Dubois et al. prepared hb carbosiloxane

thin films by sol–gel processing and reported dielectric constants ranging from 2.6 to 3.1. The Dow Chemical Company has already commercialized a polyphenylene-based product under the trade name SiLK™ with dielectric constant value of 2.65 [321]. Somboonsub et al. [322] prepared multilayer hb-PI/POSS nanocomposites synthesized by the incorporation of POSS into the side chains of polyimide. The lowest dielectric constant value attained was 2.54 in the hb-PI/POSS nanocomposite because of the large free volume and loose polyimide structures. The fluorinated hb poly(aryl ether)s (F-hb-PAEs) synthesized [143, 197] could be used for dielectric coatings, which require crosslinked films on a substrate after high-temperature baking. The dielectric constant values ($\varepsilon = 2.67 \pm 0.2$) obtained for the analogous linear poly(aryl ether)s [323] support the fact that these F-hb-PAEs exhibit even lower dielectric constants due to the increased free volume arising from the highly branched architecture and to the $-CF_3$ pendant groups on these polymers. Hyperbranched polyphenylenes have been shown to exhibit low dielectric constants due to their branched and twisted nonpolar all-phenylene structure. Hyperbranched PPhs are promising candidates for application as insulating materials in microelectronics, where features like high thermal stability, good processability and solubility, and low moisture absorption are required. The dielectric constant value of the synthesized hb-PPh from an AB_2 monomer prepared by Voit and colleagues showed a value of 2.1 [232] at low frequencies, indicating that hb-PPh is a very promising insulating material, even without the presence of pores. The introduction of nanopores into a low dielectric matrix [324, 325] can offer further advantages because a very low dielectric value might be obtained in combination with greater mechanical strength and greater thermal conductivity.

3.3.1   Hyperbranched Poly(arylene ethynylene) as NLO Material

A hb poly(arylene ethynylene) was prepared by Li et al. [326] via a Sonogashira coupling reaction, in which the chromophore moieties were in the main chain rather than in the side chains. The structure of the hb poly(arylene ethynylene) is shown in Scheme 38. A linear analog was also prepared for comparison.

Both hb and linear poly(aryleneethynylene) exhibited good film-forming ability, and their poled thin films showed second harmonic generation coefficient values (d33) of 144 and 53 pm/V, respectively, at the 1,064 nm fundamental wavelength. The values indicated that the incorporation of hb polymer together with the chromophoric groups in the main chain showed very high d33, implying large optical nonlinearity and high stabilization of dipole moments compared to the linear analog. The onset temperature for decay of hb polymer was found to be 153°C, which was higher than for the linear polymer (onset temperature for decay was 119°C), indicating long term temporal stability of the hb polymer as shown in Fig. 6. These results clearly revealed that the hb polymer had greatly enhanced poling efficiency, making it a promising candidate for optoelectronic applications.
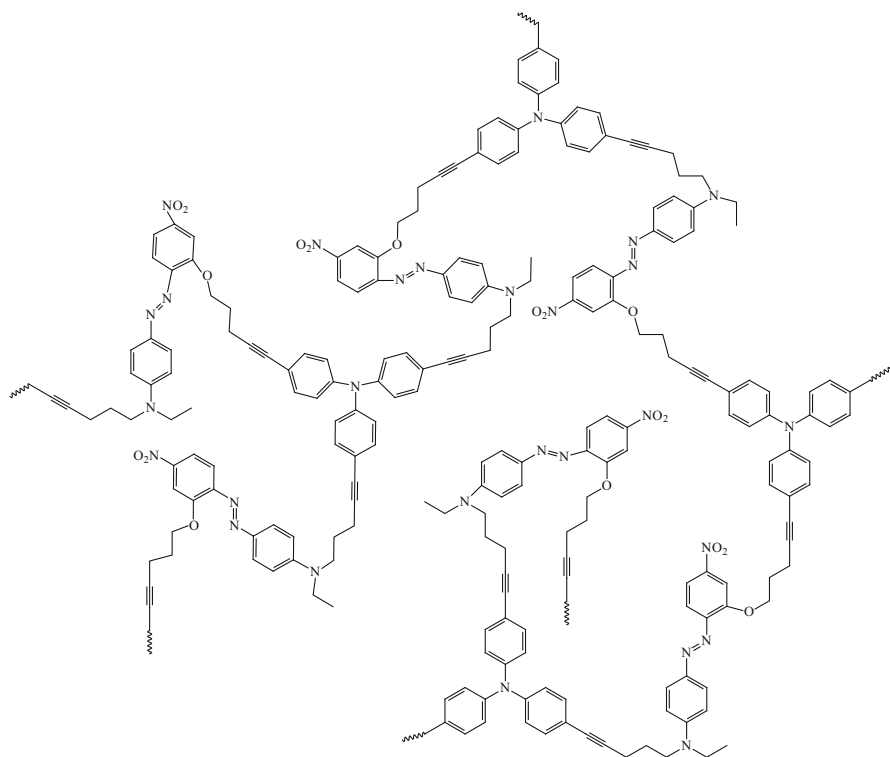
Scheme 38 Structure of hb poly(arylene ethynylene) used as NLO material [326]
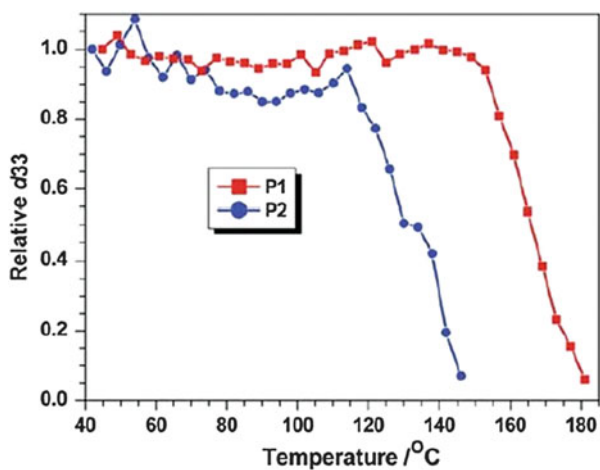
Fig. 6 Decay curves of second harmonic generation (SHG) coefficient of hb poly(arylene ethynylene) (*P1*)and linear poly(arylene ethynylene) (*P2*) as a function of temperature. Reproduced with permission from [326]
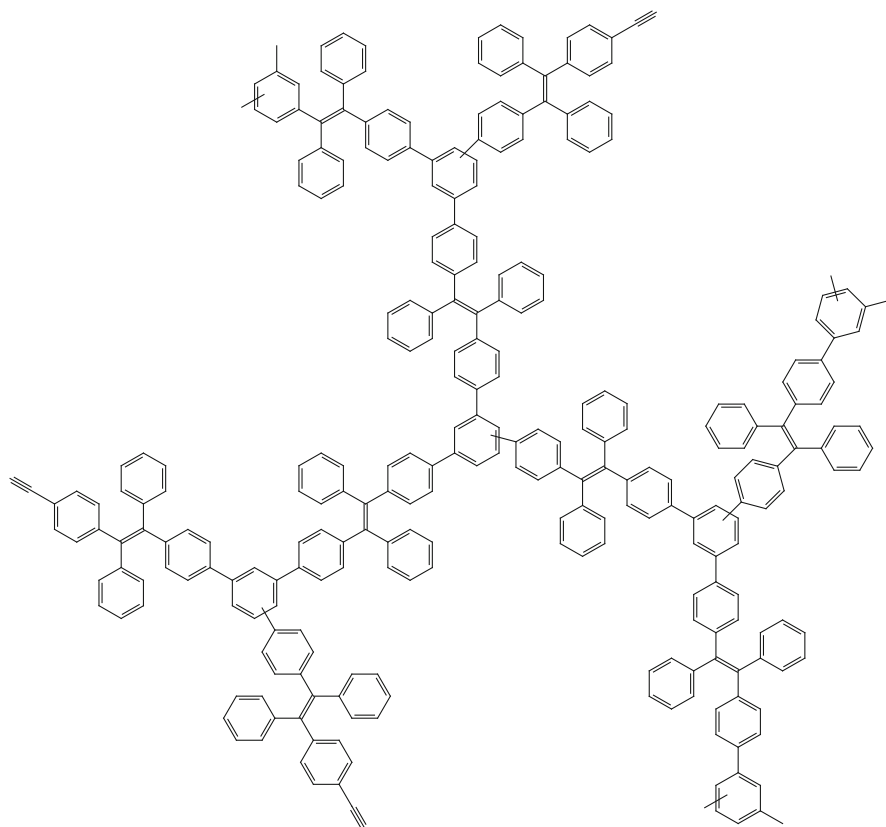
Scheme 39 Structure of hb poly(tetraphenylethene) used as fluorescent chemosensor [327]

3.3.2 Hyperbranched Poly(tetraphenylethene) as Fluorescent Chemosensor for Detection of Explosives

Hu et al. [327] synthesized hb conjugated polymers containing tetraphenylethene units. Tetraphenylethene (TPE) is a well-known building block for aggregation-induced emission (AIE) luminogens. By cyclotrimerization of a TPE-functionalized diyne in the presence of TaBr$_5$ as catalyst, using toluene as solvent at room temperature, hb poly(tetraphenylethene) (hb-TPE) was afforded. The structure of hb-TPE is shown in Scheme 39. The hb-TPE showed good solubility in common organic solvents such as toluene, CH$_2$Cl$_2$, CHCl$_3$, and THF, which the authors attributed to the twisted conformation of the TPE unit, which in turn led to large intermolecular distances and free volume for interaction with the solvent molecules. The hb-TPE also showed good film-forming ability by spin-coating or solution-casting techniques.

The onset decomposition temperatures (T_d) of hb-TPE were 462°C in nitrogen atmosphere and 417°C in air, indicating high thermal stability. The remaining triple

bonds on the periphery of hb-TPE provided suitable sites for photocrosslinking, generating photopatterns. The polymer showed a superamplification effect in the emission quenching of the polymer nanoaggregates by picric acid (used as a model explosive in their work), indicating hb-TPE as a promising fluorescent chemosensor for detection of explosives.

Concluding Remarks

Hyperbranched polymers are characterized by high solubility, low melt and solution viscosity, and excellent thermal properties. They can be tailored for various end-use applications and many of these branched architectures have already been commercialized by the chemical industry. New monomers and hb polymers have been more recently developed to result in materials for various applications, where the branching allows more easy processability and better solubility than the corresponding linear polymers. Typical approaches developed for linear polymers can be used to prepare hb polymers [e.g., poly(aryl ester)s, poly(aryl amide)s, poly(aryl ether), poly(imide)s, and poly(arylene)s] by employing monomers such as AB_2 and A_2B that allow branching and also by copolymerization with AB monomers to adjust the degree of branching. In particular, $A_2 + B_3$-type polymerizations are widely used because of the more easily accessible monomers and the ability to prevent gelation by controlling factors such as the rate of monomer addition, monomer molar ratio, and percentage solid content. New synthetic strategies such as the $AB_2 + A_2$ approach for synthesis of high molecular weight hb poly (aryl ether)s have been identified. The high molecular weight products show significant advantages with regard to thermal stability and film-forming ability. Small amounts of hb polymer can be incorporated into linear polymers to improve the processability, melt flow properties, and various other material properties. For example, hb poly(phenylene sulfide)s exhibits dye-ability in commercially available polypropylene, hence opening a new gateway towards the application of polypropylene as a textile fiber. Triazine-based hb polyamines show good flame retardancy in which the limiting oxygen index value can be tailored by incorporating different moieties in the structure. Sulfonated hb poly(aryl ether ketone)s have been incorporated into linear analogs to prepare blend membranes that could be used as proton exchange membranes. Fluorinated hb poly(arylene ether)s may find application as dielectric materials and as optical waveguide materials. Nanohybrid materials based on hb polyimides have also been explored recently for fluorescence applications. Thus, the future of hb polymers seems to be very promising for a wide range of applications.

References

1. Voit BI, Lederer A (2009) Hyperbranched and highly branched polymer architectures-synthetic strategies and major characterization aspects. Chem Rev 109:5924–5973
2. Voit BI, Komber H, Lederer A (2013) Hyperbranched polymers: synthesis and characterization aspects. Mater Sci Technol. doi:10.1002/9783527603978.mst043
3. Gao C, Yan D (2004) Hyperbranched polymers: from synthesis to applications. Prog Polym Sci 29:183–275
4. Ishizu K, Tsubaki K, Mori A, Uchida S (2002) Architecture of nanostructured polymers. Prog Polym Sci 28:27–54
5. Voit B (2000) New developments in hyperbranched polymers. J Polym Sci A Polym Chem 38:2505–2525
6. Schluter AD, Rabe JP (2000) Dendronized polymers: synthesis, characterization, assembly at interfaces, and manipulation. Angew Chem Int Ed 39:864–883
7. Roovers J, Comanita B (1999) Dendrimers and dendrimer-polymer hybrids. Adv Polym Sci 142:179–228
8. Moore JS (1997) Shape-persistent molecular architectures of nanoscale dimension. Acc Chem Res 30:402–413
9. Newkome GR, Moorefield CN, Vogtle F (2001) Dendrimers and dendrons. Wiley-VCH, Weinheim
10. Peerlings HWI, Meijer EW (1997) Chirality in dendritic architectures. Chem Eur J 3:1563–1570
11. Jang JG, Bae YC (1999) Phase behaviors of hyperbranched polymer solutions. Polymer 40:6761–6768
12. Pirrung FOH, Loen EM, Noordam A (2002) Hyperbranched polymers as a novel class of pigment dispersants. Macromol Symp 187:683–694
13. Striba SE, Frey H, Haag R (2002) Dendritic polymers in biomedical applications: from potential to clinical use in diagnostics and therapy. Angew Chem Int Ed 41:1329–1334
14. Mezzenga R, Boogh L, Manson JAE (2001) A review of dendritic hyperbranched polymer as modifiers in epoxy composites. Compos Sci Technol 61:787–795
15. Haag R (2001) Dendrimers and hyperbranched polymers as high-loading supports for organic synthesis. Chem Eur J 7:327–335
16. Hirao A, Hayashi M, Loykulnant S, Sugiyami K, Ryu SW, Haraguchi N, Matsuo A, Higashihara T (2005) Precise syntheses of chain-multi-functionalized polymers, star-branched polymers, star-linear block polymers, densely branched polymers, and dendritic branched polymers based on iterative approach using functionalized 1,1-diphenylethylene derivatives. Prog Polym Sci 30:111–182
17. Unal S, Long TE (2006) Highly branched poly(ether ester)s via cyclization-free melt condensation of A_2 oligomers and B_3 monomers. Macromolecules 39:2788–2793
18. McKee MG, Park T, Unal S, Yilgor I, Long TE (2005) Electrospinning of linear and highly branched segmented poly(urethane urea)s. Polymer 46:2011–2015
19. Nomura R, Matsuno T, Endo T (1999) Synthesis and polymerization of a self-condensable macromonomer. Polym Bull 42:251–256
20. Yamada B, Konosu O, Tanaka K, Oku F (2000) Preparation of branched polymer by radical polymerization using polymerizable chain transfer agent. Polymer 41:5625–5631
21. Trollsas M, Kelly MA, Claesson H, Seimens R, Hedrik JL (1999) Highly branched block copolymers: design, synthesis, and morphology. Macromolecules 32:4917–4924
22. Peleshanko S, Gunawidjaja R, Petrash S, Tsukruk VV (2006) Synthesis and interfacial behavior of amphiphilic hyperbranched polymers: poly(ethylene oxide)−polystyrene hyperbranches. Macromolecules 39:4756–4766
23. Bernard J, Schappacher M, Viville P, Lazzaroni R, Deffieux A (2005) Synthesis and properties of PS–PEO core–shell amphiphilic dendrigrafts. Polymer 46:6767–6776

24. Ishizu K, Ochi K (2006) Architecture of star−block copolymers consisting of triblock arms via a *N*,*N*-diethyldithiocarbamate-mediated living radical photo-polymerization and application for nanocomposites by using as fillers. Macromolecules 39:3238–3244

25. Kreutzer G, Ternat C, Nguyen TQ, Plummer CJG, Manson JAE, Castelletto V, Hamley IW, Sun F, Sheiko SS, Herrmann A, Ouali L, Sommer H, Fieber W, Velazco MI, Klok HA (2006) water-soluble unimolecular containers based on amphiphilic multiarm star block copolymers. Macromolecules 39:4507–4516

26. Magnusson H, Malmstrom E, Hult A (1999) Synthesis of hyperbranched aliphatic polyethers via cationic ring-opening polymerization of 3-ethyl-3-(hydroxymethyl)oxetane. Macromol Rapid Commun 20:453–457

27. Istratov V, Kautz H, Kim YK, Schubert R, Frey H (2003) Linear-dendritic nonionic poly (propylene oxide)–polyglycerol surfactants. Tetrahedron 59:4017–4024

28. An SG, Cho CG (2004) Synthesis and characterization of Dumbbell type amphiphilic block copolymers via ATRP. Polym Bull 51:255–262

29. Kwak SY, Ahn DU, Choi J, Song HJ, Lee SH (2004) Amelioration of mechanical brittleness in hyperbranched polymer. 1. Macroscopic evaluation by dynamic viscoelastic relaxation. Polymer 45:6889–6896

30. Okrasa L, Zigon M, Zagar E, Czech P, Boiteux G (2005) Molecular dynamics of linear and hyperbranched polyurethanes and their blends. J Non-Cryst Solids 351:2753–2758

31. Seino M, Hayakawa T, Ishida Y, Kakimoto M (2006) Synthesis and characterization of crystalline hyperbranched polysiloxysilane with POSS groups at the terminal position. Macromolecules 39:8892–8894

32. Fanghond G, Tang H, Liu C, Jiang B, Ren Q, Yang Y (2006) Preparation of hyperbranched polymers through ATRP of in situ formed AB* monomer. J Appl Polym Sci 101:850–856

33. Zhu X, Chen L, Yan D, Chen Q, Yao Y, Xiao Y, Hou J, Li J (2004) Supramolecular self-assembly of inclusion complexes of a multiarm hyperbranched polyether with cyclodextrins. langmuir 20:484–490

34. Yan D, Gao C, Frey H (eds) (2011) Hyperbranched polymers: synthesis, properties, and applications. Wiley, Hoboken

35. Peleshanko S, Tsukruk V (2011) Grafting and surface properties of hyperbranched polymers. In: Yan D, Gao C, Frey H (eds) Hyperbranched polymers: synthesis, properties and applications, 1st edn. Wiley, Hoboken, pp 369–386. doi:10.1002/9780470929001.ch14

36. Bruchmann B, Voit B (2011) Applications of hyperbranched polymers in coatings, as additives, and in nanotechnology. In: Yan D, Gao C, Frey H (eds) Hyperbranched polymers: synthesis, properties, and applications. Wiley, Hoboken, pp. 415–440. doi:10.1002/9780470929001.ch16

37. Zhang D, Liang E, Li T, Chen S, Zhang J, Cheng X, Zhou J, Zhang A (2013) Environment-friendly synthesis and performance of a novel hyperbranched epoxy resin with a silicone skeleton. RSC Adv 3:3095–3102

38. Zhu Q, Qiu F, Zhu B, Zhu X (2013) Hyperbranched polymers for bioimaging. RSC Adv 3:2071–2083

39. Wang D, Chen H, Su Y, Qiu F, Zhu L, Huan X, Zhu B, Yan D, Guo F, Zhu X (2013) Supramolecular amphiphilic multiarm hyperbranched copolymer: synthesis, self-assembly and drug delivery applications. Polym Chem 4:85–94

40. Hartmann-Thompson C, Hu J, Kaganove SN, Keinath SN, Keeley DL, Dvornic PR (2004) Hydrogen-bond acidic hyperbranched polymers for surface acoustic wave (SAW) sensors. Chem Mater 16:5357–5364

41. Kricheldorf HR, Stukenbrock T (1998) New polymer syntheses XCIII. Hyperbranched homo- and copolyesters derived from gallic acid and β-(4-hydroxyphenyl)-propionic acid. J Polym Sci A Polym Chem 36:2347–2357

42. Li J, Bo Z (2004) "AB2 + AB" approach to hyperbranched polymers used as polymer blue light emitting materials. Macromolecules 37:2013–2015

43. Robeson LM (2010) Polymer blends in membrane transport processes. Ind Eng Chem Res 49:11859–11865
44. Newkome GR, Moorefield CN, Vogtle F (2008) Dendritic molecules: concepts, syntheses, perspectives. VCH, New York, pp 49–161
45. Astruc D, Chardac F (2001) Dendritic catalysts and dendrimers in catalysis. Chem Rev 101:2991–3024
46. Emrick T, Chang HT, Fréchet JMJ (2000) The preparation of hyperbranched aromatic and aliphatic polyether epoxies by chloride-catalyzed proton transfer polymerization from AB_n and $A_2 + B_3$ monomers. J Polym Sci A Polym Chem 38:4850–4869
47. Fang J, Kita H, Okamoto K (2000) Hyperbranched polyimides for gas separation applications. 1. Synthesis and characterization. Macromolecules 33:4639–4646
48. Kim YH (1992) Lyotropic liquid crystalline hyperbranched aromatic polyamides. J Am Chem Soc 114:4947–4948
49. Monticelli O, Russo S, Campagna R, Voit B (2005) Preparation and characterisation of blends based on polyamide 6 and hyperbranched aramids as palladium nanoparticle supports. Polymer 46:3597–3606
50. Yamakawa Y, Ueda M, Takeuchi K, Asai M (1999) One-pot synthesis of dendritic polyamide. J Polym Sci A Polym Chem 37:3638–3645
51. Yamakawa Y, Ueda M, Takeuchi K, Asai M (1999) One-pot synthesis of dendritic polyamide. 2. Dendritic polyamide from 5-[3-(4-aminophenyl)propionylamino]isophthalic acid hydrochloride. Macromolecules 32:8363–8369
52. Jikei M, Chon SH, Kakimoto MA, Kawauchi S, Imase T, Watanebe J (1999) Synthesis of hyperbranched aromatic polyamide from aromatic diamines and trimesic acid. Macromolecules 32:2061–2064
53. Tabuani D, Monticelli O, Chincarini A, Bianchini C, Vizza F, Moneti S, Russo S (2003) Palladium nanoparticles supported on hyperbranched aramids: synthesis, characterization, and some applications in the hydrogenation of unsaturated substrates. Macromolecules 36:4294–4301
54. Tabuani D, Monticelli O, Komber H, Russo S (2003) Preparation and characterisation of Pd nanoclusters in hyperbranched aramid templates to be used in homogeneous catalysis. Macromol Chem Phys 204:1576–1583
55. Fang J, Kita H, Okamoto K (2001) Gas permeation properties of hyperbranched polyimide membranes. J Membr Sci 182:245–256
56. Yamaguchi N, Wang JS, Hewitt JM, Lenhart WC, Mourey TH (2002) Acid chloride-functionalized hyperbranched polyester for facile and quantitative chain-end modification: one-pot synthesis and structure characterization. J Polym Sci A Polym Chem 40:2855–2867
57. Kricheldorf HR, Hobzova R, Schwarz G (2003) Cyclic hyperbranched polyesters derived from 4,4-bis(4'-hydroxyphenyl)valeric acid. Polymer 44:7361–7368
58. Kricheldorf HR, Zang QZ, Schwarz G (1982) New polymer syntheses: 6. Linear and branched poly(3-hydroxy-benzoates). Polymer 23:1821–1829
59. Moore JS, Stupp SI (1990) Room temperature polyesterification. Macromolecules 23:65–70
60. Blencowe A, Davidson L, Hayes A (2003) Synthesis and characterization of hyperbranched polyesters incorporating the AB_2 monomer 3,5-bis(3-hydroxylprop-1-ynyl)benzoic acid. Eur Polym J 39:1955–1963
61. Kang SH, Luo J, Ma H, Barto RR, Frank CW, Dalton LR, Jen AKY (2003) Hyperbranched aromatic fluoropolyester for photonic applications. Macromolecules 36:4355–4359
62. Jayakannan M, Ramakrishnan S (2001) Recent developments in polyether synthesis. Macromol Rapid Comm 22:1463–1473
63. Miller TM, Neenan TX, Kwock EW, Stein SM (1993) Dendritic analogs of engineering plastics: a general one-step synthesis of dendritic polyaryl ethers. J Am Chem Soc 115:356–357
64. Chu F, Hawker CJ (1993) A versatile synthesis of isomeric hyperbranched polyetherketones. Polym Bull 30:265–272

65. Hawker CJ, Chu F (1996) Hyperbranched poly(ether ketones): manipulation of structure and physical properties. Macromolecules 29:4370–4380

66. Shu CF, Leu CM (1999) Hyperbranched poly(ether ketone) with carboxylic acid terminal groups: synthesis, characterization, and derivatization. Macromolecules 32:100–105

67. Mu JX, Zhang CL, Chen J, Jiang ZH, Kireev VV (2006) Synthesis of functionalized fluorine-containing hyperbranched poly(aryl ether ketones) for optical applications. Polym Sci Ser A 48:1035–1040

68. Wang D, Zhang SL, Zhang YH, Wang H, Mu JX, Wang GB, Jiang Z (2008) Preparation and nonlinear optical characterization of a novel hyperbranched poly(aryl ether ketone) end-functionalized with nickel phthalocyanine. Dyes Pigments 79:217–223

69. Choi JY, Tan LS, Baek JB (2006) Self-controlled synthesis of hyperbranched poly(ether ketone)s from A3 + B2 approach via different solubilities of monomers in the reaction medium. Macromolecules 39:9057–9063

70. Baek JB, Tan LS (2003) Improved syntheses of poly(oxy-1,3-phenylenecarbonyl-1,4-phenylene) and related poly(ether–ketones) using polyphosphoric acid/P_2O_5 as polymerization medium. Polymer 44:4135–4147

71. Baek JB, Park SY, Price GE, Lyons CB, Tan LS (2005) Unusual thermal relaxation of viscosity-and-shear-induced strain in poly(ether-ketones) synthesized in highly viscous polyphosphoric acid/P_2O_5 medium. Polymer 46:1543–1552

72. Martinez CA, Hay AS (1997) Preparation of hyperbranched macromolecules with aryl fluoride and phenol terminal functionalities using new monomers and Cs_2CO_3 or $Mg(OH)_2$ as the condensation agent. J Polym Sci A Polym Chem 35:2015–2033

73. Martinez CA, Hay AS (1998) Synthesis of hyperbranched oligomers with activated aryl chloride and phenol terminal groups. J Macromol Sci Pure Appl Chem 35:57–90

74. Kim YJ, Chung IS, Kim SY (2003) Synthesis of poly(phenylene oxide) containing trifluoromethyl groups via selective and sequential nucleophilic aromatic substitution reaction. Macromolecules 36:3809–3811

75. Kim YJ, Kakimoto MA, Kim SY (2006) Synthesis of hyperbranched poly(arylene ether) from monomer containing nitro group: kinetically controlled growth of polymer chain through dynamic exchange of end functional groups. Macromolecules 39:7190–7192

76. Kim YH, Webster OW (1992) Hyperbranched polyphenylenes. Macromolecules 25:5561–5572

77. Häußler M, Lam JWY, Zheng R, Peng H, Luo J, Chen J, Charles CCW, Tang BZ (2003) Hyperbranched polyarylenes. Chimie 6:833–842

78. Flory PJ (1952) Molecular size distribution in three dimensional polymers. VI. Branched polymers containing A-R-B_{f-1} type units. J Am Chem Soc 74:2718–2723

79. Hawker, CJ, Fréchet, JMJ (1991) One-step synthesis of hyperbranched dendritic polyesters. J Am Chem Soc 113:4583–4588

80. Holter D, Burgath A, Frey H (1997) Degree of branching in hyperbranched polymers. Acta Polym 48:30–35

81. Odian G (1991) Principles of polymerization. Wiley, New York

82. Yang X, Wang L, He X (2010) Kinetics of nonideal hyperbranched $A_2 + B_3$ polycondensation: Simulation and comparison with experiments. J Polym Sci A Polym Chem 48:5072–5082

83. Reisch A (2005) Untersuchungen zur Strukturentwicklung in Hochverzweigten Polymeren auf der Basis von $A_2 + B_3$ Systemen. Diploma Thesis, Technische Universität Dresden, Dresden

84. Reisch A, Komber H, Voit B (2007) Kinetic analysis of two hyperbranched $A_2 + B_3$ polycondensation reactions by NMR spectroscopy. Macromolecules 40:6846–6858

85. Yan DY, Gao C (2000) Hyperbranched polymers made from A_2 and BB'$_2$ type monomers. 1. Polyaddition of 1-(2-aminoethyl)piperazine to divinyl sulfone. Macromolecules 33:7693–7699

86. Gao C, Yan DY (2001) Polyaddition of B$_2$ and BB'$_2$ type monomers to A$_2$ type monomer. 1. Synthesis of highly branched copoly(sulfone–amine)s. Macromolecules 34:156–161

87. Gao C, Tang W, Yan DY, Zhu PF, Tao P (2001) Hyperbranched polymers made from A$_2$, B$_2$ and BB'$_2$ type monomers, 2. Preparation of hyperbranched copoly(sulfone-amine)s by polyaddition of N-ethylethylenediamine and piperazine to divinylsulfone. Polymer 42:3437–3443

88. Gao C, Yan DY, Zhu X, Huang W (2001) Preparation of water-soluble hyperbranched poly (sulfone-amine)s by polyaddition of N-ethylethylenediamine to divinyl sulfone. Polymer 42:7603–7610

89. Liu Y, Chung TS (2002) Facile synthesis of hyperbranched polyimides from A$_2$ + BB'$_2$ monomers. J Polym Sci A Polym Chem 40:4563–4569

90. Chang YT, Shu CF (2003) Synthesis of hyperbranched aromatic poly(amide–imide): Copolymerization of B'B2 monomer with A2 monomer. Macromolecules 36:661–666

91. Abdelrehim M, Komber H, Langenwalter J, Voit B, Bruchmann B (2004) Synthesis and characterization of hyperbranched poly(urea-urethane)s based on AA* and B$_2$B* monomers. J Polym Sci A Polym Chem 42:3062–3081

92. Radke W, Litvinenko G, Müller AHE (1998) Effect of core-forming molecules on molecular weight distribution and degree of branching in the synthesis of hyperbranched polymers. Macromolecules 31:239–248

93. Litvinenko G, Simon PFW, Müller AHE (2001) Molecular parameters of hyperbranched copolymers obtained by self-condensing vinyl copolymerization, 2. Non Equal Rate Constants Macromolecules 34:2418–2426

94. Beginn U, Drohman C, Moller M (1997) Conversion dependence of the branching density for the polycondensation of AB$_n$ monomers. Macromolecules 30:4112–4116

95. Dusek K, Somvarsky J, Smrckova M, Simonsick WJ, Wilczek L (1999) Role of cyclization in the degree-of-polymerization distribution of hyperbranched polymers modelling and experiments. Polym Bull 42:489–496

96. Cameron C, Fawcett AH, Hetherington CR, Mee RAW, McBride FV (1997) Cycles frustrating fractal formation in an AB$_2$ stepgrowth polymerization. Chem Commun 1997(18):1801–1802. doi:10.1039/A703567E

97. Galina H, Lechowicz JB, Kaczmarski K (2001) Kinetic models of the polymerization of an AB2 monomer. Macromol Theory Simul 10:174–178

98. Zhou Z, Jia Z, Yan D (2010) Kinetic analysis of co-polycondensation of AB$_2$ and AB type monomers in presence of multi-functional cores. Polymer 51:2763–2768

99. Voit B (2005) Hyperbranched polymers – all problems solved after 15 years of research? J Polym Sci A Polym Chem 43:2679–2699

100. Liaw DJ, Chang FC, Leung MK, Chou MY, Muellen K (2005) High thermal stability and rigid rod of novel organosoluble polyimides and polyamides based on bulky and noncoplanar naphthalene–biphenyldiamine. Macromolecules 38:4024–4029

101. Scholl M, Kadlecova Z, Klok HA (2009) Dendritic and hyperbranched polyamides. Prog Polym Sci 34:24–61

102. Chao D, He L, Berda EB, Wang S, Jia X, Wang C (2013) Multifunctional hyperbranched polyamide: synthesis and properties. Polymer 54:3223–3229

103. Seike Y, Okude Y, Iwakura I, Chiba I, Ikeno T, Yamada T (2003) Synthesis of polyphenylene ether derivatives: estimation of their dielectric constants. Macromol Chem Phys 204:1876–1881

104. Chiang C, Chang F (1998) Polymer blends of polyamide-6 (PA6) and poly(phenylene ether) (PPE) compatibilized by a multifunctional epoxy coupler. J Polym Sci B Polym Phys 36:1805–1819

105. Wegner G (1981) Polymers with metal-like conductivity-a review of their synthesis, structure and properties. Angew Chem Int Ed Engl 20:361–381

106. Peng H, Dong Y, Jia D, Tang B (2004) Syntheses of readily processable, thermally stable, and light-emitting hyperbranched polyphenylenes. Chinese Sci Bull 49:2637–2639

107. Erber M, Boye S, Hartmann T, Voit B, Lederer A (2009) A convenient room temperature polycondensation toward hyperbranched AB$_2$-type all-aromatic polyesters with phenol terminal groups. J Polym Sci A Polym Chem 47:5158–5168
108. Turner SR, Voit BI, Mourey TH (1993) All-aromatic hyperbranched polyesters with phenol and acetate end groups: synthesis and characterization. Macromolecules 26:4617–4623
109. Schmaljohann D (1998) Funktionalisierung von Hochverzweigten Polyestern fur den Einsatzals Beschichtungs- und Blend material. Ph.D. thesis, TU Munchen, Munchen
110. Schmaljohann D, Komber H, Barratt JG, Appelhans D, Voit B (2003) Kinetics of nonideal hyperbranched polymerizations. 2. Kinetic analysis of the polycondensation of 3,5-Bis (trimethylsiloxy)benzoyl chloride using NMR spectroscopy. Macromolecules 36:97–108
111. Magnusson H, Malmstrom E, Hult A (2000) Structure buildup in hyperbranched polymers from 2,2-Bis(hydroxymethyl)propionic acid. Macromolecules 33:3099–3104
112. Thompson DS, Markoski LJ, Moore JS (1999) Rapid synthesis of hyperbranched aromatic polyetherimides. Macromolecules 32:4764–4768
113. Khalyavina A, Häußler L, Lederer A (2012) Effect of the degree of branching on the glass transition temperature of polyesters. Polymer 53:1049–1053
114. Wooley KL, Hawker CJ, Pochan JM, Frechet JMJ (1993) Physical properties of dendritic macromolecules: a study of glass transition temperature. Macromolecules 26:1514–1519
115. Fan Z, Lederer A, Voit B (2009) Synthesis and characterization of A2 + B3-type hyperbranched aromatic polyesters with phenolic end groups. Polymer 50:3431–3439
116. Lin Q, Long TE (2003) Polymerization of A2 with B3 Monomers: a facile approach to hyperbranched poly(aryl ester)s. Macromolecules 36:9809–9816
117. Unal S, Lin Q, Mourey TH, Long TE (2005) Tailoring the degree of branching: preparation of poly(ether ester)s via copolymerization of poly(ethylene glycol) oligomers (A$_2$) and 1,3,5-benzenetricarbonyl trichloride (B$_3$). Macromolecules 38:3246–3254
118. Schallausky F, Erber M, Komber H, Lederer A (2008) An easy strategy for the synthesis of well-defined aliphatic-aromatic hyperbranched polyesters. Macromol Chem Phys 209:2331–2338
119. Baek JB, Harris FW (2003) Poly(arylether amides) and poly(aryletherketone amides) via aromatic nucleophilic substitution reactions of self-polymerizable AB and AB$_2$ monomers. J Polym Sci A Polym Chem 41:2374–2389
120. In I, Kim SY (2005) Hyperbranched poly(arylene ether amide) via nucleophilic aromatic substitution reaction. Macromol Chem Phys 206:1862–1869
121. Shabbir S, Zulfiqar S, Sarwar MI (2011) Amine-terminated aromatic and semi-aromatic hyperbranched polyamides: synthesis and characterization. J Polym Res 18:1919–1929
122. Ohta Y, Fujii S, Yokoyama A, Furuyama T, Uchiyama M, Yokozawa T (2009) Synthesis of well-defined hyperbranched polyamides by condensation polymerization of AB$_2$ monomer through changed substituent effects. Angew Chem Int Ed 48:5942–5945
123. Liou GS, Lin HY, Yen HJ (2009) Synthesis and characterization of electroactive hyperbranched aromatic polyamides based on A$_2$B-type triphenylamine moieties. Mater Chem 19:7666–7673
124. Liou GS, Chang CW (2008) Highly stable anodic electrochromic aromatic polyamides containing N, N, N′, N′-tetraphenyl-p-phenylenediamine moieties: synthesis, electrochemical, and electrochromic properties. Macromolecules 41:1667–1674
125. Liou GS, Lin KH (2009) Synthesis and characterization of a novel electrochromic aromatic polyamide from AB-type triphenylamine-based monomer. J Polym Sci Part A Polym Chem 47:1988–2001
126. Mittal KL (ed) (2009) Polyimides and other high temperature polymers, vol. 5. VSP/Brill, Leiden
127. Ghosh A, Sen SK, Banerjee S, Voit B (2012) Solubility improvements in aromatic polyimides by macromolecular engineering. RSC Adv 2:5900–5926
128. Kricheldorf HR, Bolender O, Wollheim T (1998) New polymer synthesis 99. Hyperbranched poly(ester-imide)s derived from 4,5-dichlorophthalic acid. High Perform Polym 10:217–229

129. Maier G, Zech C, Voit B, Komber H (1998) An approach to hyperbranched polymers with a degree of branching of 100%. Macromol Chem Phys 199:2655–2664
130. Orlicki JA, Thompson JL, Markoski LJ, Sill KN, Moore JS (2002) Synthesis and character-ization of end-group modified hyperbranched polyetherimides. J Polym Sci A Polym Chem 40:936–946
131. Baek JB, Qin H, Mather PT, Tan LS (2002) A new hyperbranched poly(arylene–ether–ketone − imide): synthesis, chain-end functionalization, and blending with a bis(maleimide). Macromolecules 35:4951–4959
132. Hao J, Jikei M, Kakimoto M (2003) Synthesis and comparison of hyperbranched aromatic polyimides having the same repeating unit by AB2 self-polymerization and A2 + B3 poly-merization. Macromolecules 36:3519–3528
133. Yamanaka K, Jikei M, Kakimoto MA (2000) Synthesis of hyperbranched aromatic polyimides via polyamic acid methyl ester precursor. Macromolecules 33:1111–1114
134. Yamanaka K, Jikei M, Kakimoto MA (2000) Preparation and properties of hyperbranched aromatic polyimides via polyamic acid methyl ester precursors. Macromolecules 33:6937–6944
135. Wang KL, Jikei M, Kakimoto MA (2004) Synthesis of soluble branched polyimides derived from an ABB′ monomer. J Polym Sci A Polym Chem 42:3200–3211
136. Shen J, Zhang Y, Chen W, Wang W, Xu Z, Yeung KWK, Yi C (2013) Synthesis and properties of hyperbranched polyimides derived from novel triamine with prolonged chain segments. J Polym Sci A Polym Chem 51:2425–2437
137. Chen W, Yan W, Wu S, Xu Z, Yeung KWK, Yi C (2010) Preparation and properties of novel triphenylpyridine-containing hyperbranched polyimides derived from 2,4,6-tris (4-aminophenyl)pyridine under microwave irradiation. Macromol Chem Phys 211:1803–1813
138. Gao H, Wang D, Guan S, Wi J, Jiang Z, Gao W, Zhang D (2007) Fluorinated hyperbranched polyimide for optical waveguides. Macromol Rapid Commun 28:252–259
139. Kaino T (1987) Preparation of plastic optical fibers for near-IR region transmission. J Polym Sci A Polym Chem 25:37–46
140. Liu Y, Zhang Y, Guan S, Zhang H, Yue X, Jiang Z (2009) Synthesis of novel fluorinated hyperbranched polyimides with excellent optical properties. J Polym Sci A Polym Chem 47:6269–6279
141. Gao H, Wang D, Jiang W, Guan S, Jiang Z (2008) Gas permeability of fluorinated hyperbranched polyimide. J Appl Polym Sci 109:2341–2346
142. Zhao L, Yao H, Liu Y, Zhang Y, Jiang Z (2013) Synthesis and properties of novel hyperbranched polyimides end-capped with metallophthalocyanines. J Appl Polym Sci 128:3405–3410
143. Banerjee S, Komber H, Häußler L, Voit B (2009) Synthesis and characterization of hyperbranched poly(arylene ether)s from a new activated trifluoro B3 monomer adopting an A2 + B3 approach. Macromol Chem Phys 210:1272–1282
144. Park SJ, Li K, Jin FL (2008) Synthesis and characterization of hyperbranched polyimides from 2,4,6-triaminopyrimidine and dianhydrides system. Mater Chem Phys 108:214–219
145. Peter J, Khalyavina A, Kriz J, Bleha M (2009) Synthesis and gas transport properties of ODPA–TAP–ODA hyperbranched polyimides with various comonomer ratios. Eur Polym J 45:1716–1727
146. Chen Y, Zhang Q, Sun W, Lei XF, Yao P (2014) Synthesis and gas permeation properties of hyperbranched polyimides membranes from a novel (A₂ + B₂B′ + B₂)-type method. J Membr Sci 450:138–146
147. Hawthorne DG, Hodgkin JH (1999) Amine reactivity changes in imide formation from heterocyclic bases. High Perform Polym 11:315–329
148. Riley D, Gungor A, Srinivasan SA, McGrath JE (1997) Synthesis and characterization of flame resistant poly(arylene ether)s. Polym Eng Sci 37:1501–1511

149. Smith CD, Grubbs H, Gungor A, Webster HF, Wightman JP, McGrath JE (1991) Unique characteristics derived from poly(arylene ether phosphine oxide)s. High Perform Polym 3:211–229

150. Yang J, Gibson HW (1999) A polyketone synthesis involving nucleophilic substitution via carbanions derived from bis(α-aminonitrile)s. 5. A new, well-controlled route to "long" bisphenol and activated aromatic dihalide monomers. Macromolecules 32:8740–8746

151. Kricheldorf HR, Vakhtangishvili L, Schwarz G, Kruger RP (2003) Cyclic hyperbranched poly(ether ketone)s derived from 3,5-bis(4-fluorobenzoyl)phenol. Macromolecules 36:5551–5558

152. Morikawa A (1998) Preparation and properties of hyperbranched poly(ether ketones) with a various number of phenylene units. Macromolecules 31:5999–6009

153. Agarwal S, Kumar S, Maken S (2012) Synthesis and characterization of new hyperbranched poly(ether ketones) with various number of phenylene units. J Ind Eng Chem 18:1489–1495

154. Baek JB, Tan LS (2003) Linear-hyperbranched copolymerization as a tool to modulate thermal properties and crystallinity of a *para*-poly(ether-ketone). Polymer 44:3451–3459

155. Choi JY, Oh SJ, Lee HJ, Wang DH, Tan LS, Baek JB (2007) In-situ grafting of hyperbranched poly(ether ketone)s onto multiwalled carbon nanotubes via the $A_3 + B_2$ approach. Macromolecules 40:4474–4480

156. Li X, Zhang S, Wang H, Pang J, Sun D, Mu J, Wang G, Jiang Z (2010) Facile synthesis and characterization of hyperbranched poly(aryl ether ketone)s obtained via an $A_2 + BB'_2$ approach. Polym Int 59:1360–1366

157. Himmelberg P, Fossum E (2005) Development of an efficient route to hyperbranched poly (arylene ether sulfone)s. J Polym Sci A Polym Chem 43:3178–3187

158. Jikei M, Uchida D, Haruta Y, Takahashi Y, Matsumoto K (2012) Synthesis and properties of hyperbranched poly(ether sulfone)s prepared by self-polycondensation of novel AB_2 monomer. J Polym Sci A Polym Chem 50:3830–3839

159. Imai Y, Ishikawa H, Park KH, Kakimoto M (1997) A facile cesium fluoride-mediated synthesis of aromatic polyethers from bisphenols and activated aromatic dihalides. J Polym Sci Part A Polym Chem 35:2055–2061

160. Kricheldorf HR, Vakhtangisgvili L, Fritsch D (2002) Synthesis and functionalization of poly (ether sulfone)s based on 1,1,1-tris(4-hydroxyphenyl)ethane. J Polym Sci Part A Polym Chem 40:2967–2978

161. Lin Q, Unal S, Fornof AR, Yilgor I, Long TE (2006) Highly branched poly(arylene ether)s via oligomeric A2 + B3 strategies. Macromol Chem Phys 207:576–586

162. Osano K, Force L, Turner SR (2010) Synthesis and properties of linear poly(ether sulfone)s with hyperbranched terminal groups. Ind Eng Chem Res 49:12098–12103

163. Grunzinger SJ, Hayakawa T, Kakimoto MA (2008) Synthesis of multiblock hyperbranched-linear poly(ether sulfone) copolymers. J Polym Sci Part A Polym Chem 46:4785–4793

164. Lee HS, Takeuchi M, Kakimoto MA, Kim SY (2000) Hyperbranched poly(arylene ether phosphine oxide)s. Polym Bull 45:319–326

165. Lin Q, Long TE (2000) Synthesis and characterization of a novel AB_2 monomer and corresponding hyperbranched poly(arylene ether phosphine oxide)s. J Polym Sci A Polym Chem 38:3736–3741

166. Bernal DP, Bankey N, Cockayne RC, Fossum E (2002) Fluoride-terminated hyperbranched poly(arylene ether phosphine oxide)s via nucleophilic aromatic substitution. J Polym Sci A Polym Chem 40:1456–1467

167. Bernal DP, Bedrossian L, Collins K, Fossum E (2003) Effect of core reactivity on the molecular weight, polydispersity, and degree of branching of hyperbranched poly(arylene ether phosphine oxide)s. Macromolecules 36:333–338

168. Czupik M, Fossum E (2003) Manipulation of the molecular weight and branching structure of hyperbranched poly(arylene ether phosphine oxide)s prepared via an $A_2 + B_3$ approach. J Polym Sci A Polym Chem 41:3871–3881

169. Sennet L, Fossum E, Tan LS (2008) Branched poly(arylene ether ketone)s with tailored thermal properties: effects of AB/AB_2 ratio, core (B_3) percentage, and reaction temperature. Polymer 49:3731–3736
170. Fossum E, Tan LS (2005) Geometrical influence of AB_n monomer structure on the thermal properties of linear-hyperbranched ether–ketone copolymers prepared via an $AB + AB_n$ route. Polymer 46:9686–9693
171. Wang DH, Baek JB, Tan LS (2005) Phthalonitrile-terminated hyperbranched poly(arylene-ether-ketone-imide): synthesis and its blending with 4,4'-bis(3,4-dicyanophenoxy)biphenyl, phthalonitrile-terminated hyperbranched poly(arylene-ether-ketone-imide): synthesis and its blending with 4,4'-Bis(3,4-dicyanophenoxy)biphenyl. Polym Prepr 46:727–728
172. Yu Z, Fossum E, Wang DH, Tan LS (2008) Alternative approach to an AB_2 monomer for hyperbranched poly(arylene ether ketone imide)s. Syn Commun 38:419–427
173. Gong ZH, Leu CM, Wu FI, Shu CF (2000) Hyperbranched poly(aryl ether oxazole)s: synthesis, characterization, and modification. Macromolecules 33:8527–8533
174. Schmaljohann D, Haussler L, Potschke P, Voit BI, Loontjens TJA (2000) Modification with alkyl chains and the influence on thermal and mechanical properties of aromatic hyperbranched polyesters. Macromol Chem Phys 201:49–57
175. Wu FI, Shu CF (2001) Synthesis and characterization of new hyperbranched poly(aryl ether oxadiazole)s. J Polym Sci A Polym Chem 39:3851–3860
176. Fu Y, Oosterwijck CV, Vandendriessche A, Kowalczuk-Bleja A, Zhang X, Dworak A, Dehaen W, Smet M (2008) Hyperbranched poly(arylene oxindole)s with a degree of branching of 100% for the construction of nanocontainers by orthogonal modification. Macromolecules 41:2388–2393
177. Kowalczuk A, Vandendriessche A, Trzebicka B, Mendrek B, Szeluga U, Cholenwiński G, Smet M, Dworak A, Dehaen W (2009) Core-shell nanoparticles with hyperbranched poly (arylene-oxindole) interiors. J Polym Sci A Polym Chem 47:1120–1135
178. Colquhoun H, Zolotukhin M, Khalolov L, Dzhemilev U (2001) Superelectrophiles in aromatic polymer chemistry. Macromolecules 34:1122–1124
179. Baek JB, Harris FW (2005) Hyperbranched polyphenylquinoxalines from self-polymerizable AB_2 and A_2B monomers. Macromolecules 38:297–306
180. Baek JB, Harris FW (2005) Fluorine- and hydroxyl-terminated hyperbranched poly (phenylquinoxalines) (PPQs) from copolymerization of self-polymerizable AB and AB_2, BA, and BA_2 monomers. Macromolecules 38:1131–1140
181. Baek JB, Tan LS (2006) Hyperbranched poly(phenylquinoxaline–ether–ketone) synthesis in poly(phosphoric acid)/P_2O_5 medium: optimization and some interesting observations. Macromolecules 39:2794–2803
182. Dhara M, Banerjee S (2010) Fluorinated high-performance polymers: poly(arylene ether)s and aromatic polyimides containing trifluoromethyl groups. Prog Polym Sci 35:1022–1077
183. Labadie JW, Hedrick JL (1990) Perfluoroalkylene-activated poly(aryl ether) synthesis. Macromolecules 23:5371–5373
184. Yang H, Hay AS (1993) Fluorine substitutent effects on poly(2,6-diphenylphenylene ether). J Polym Sci A Polym Chem 31:2015–2029
185. Maier G, Hecht R (1995) Poly(aryl ether thiazole)s with pendent trifluoromethyl groups. Macromolecules 28:7558–7565
186. Park SK, Kim SY (1998) Synthesis of poly(arylene ether ketone)s containing trifluoromethyl groups via nitro displacement reaction. Macromolecules 31:3385–3387
187. Mohanty AK, Sen SK, Ghosh A, Maji S, Banerjee S (2010) Synthesis, characterization, and comparison of properties of new fluorinated poly(arylene ether)s containing phthalimidine moiety in the main chain. Polym Adv Technol 21:767–773
188. Aggarwal M, Maji S, Sen SK, Dasgupta B, Chatterjee S, Ghosh A, Banerjee S (2009) New poly(arylene ether)s containing phthalimidine group in the main chain. J Appl Polym Sci 112:1226–1233

189. Salunke AK, Ghosh A, Banerjee S (2007) Synthesis and characterization of novel poly (arylene ether)s based on 9,10-bis-(4-fluoro-3-trifluoromethylphenyl) anthracene and 2,7-bis-(4-fluoro-3-trifluoromethylphenyl) fluorine. J Appl Polym Sci 106:664–672

190. Digal AK, Ghosh A, Banerjee S (2008) Synthesis and characterization of novel poly(Arylene Ether)s from 4,4′-thiodiphenol. J Macromol Sci A Pure and Appl Chem 45:212–217

191. Banerjee S, Maier G, Dannenberg C, Spinger J (2004) Gas permeabilities of novel poly (arylene ether)s with terphenyl unit in the main chain. J Membr Sci 229:63–71

192. Xu ZK, Dannenberg C, Springer J, Banerjee S, Maier G (2002) Novel poly(arylene ether) as membranes for gas separation. J Membr Sci 205:23–31

193. Ghosh A, Banerjee S (2009) Synthesis and characterization of new fluorinated polyimides derived from 9, 10-bis[3′-trifluoromethyl-4′ (4″-aminobenzoxy) benzyl] anthracene. High Perform Polym 21:173–186

194. Banerjee S (2007) Synthesis and characterization of novel hyperbranched poly(arylene ether) from a AB$_2$ monomer. J Polym Mater 24:247–254

195. Satpathi H, Ghosh A, Banerjee S, Komber H, Voit B (2011) Synthesis and characterization of new semifluorinated linear and hyperbranched poly(arylene ether phosphine oxide)s through B$_2$ + A$_2$ and AB$_2$ approaches. Eur Polym J 47:196–207

196. Herbert CG, Bass RG, Watson KA, Connell JW (1996) Preparation of poly(arylene ether pyrimidine)s by aromatic nucleophilic substitution reactions. Macromolecules 29:7709–7716

197. Ghosh A, Banerjee S, Komber H, Voit B (2010) Extremely high molar mass hyperbranched poly(arylene ether)s from a new semifluorinated AB$_2$ monomer by an unusual AB$_2$ + A$_2$ polymerization approach. Macromolecules 43:2846–2854

198. Dusek K, Duskova-Smrckova M, Voit B (2005) Highly-branched off-stoichiometric functional polymers as polymer networks precursors. Polymer 46:4265–4282

199. Mahapatra SS, Karak N (2007) Hyperbranched aromatic polyamines with *s*-triazine rings. J Appl Polym Sci 106:95–102

200. Zhang J, Wang H, Li X (2006) Novel hyperbranched poly(phenylene oxide)s with phenolic terminal groups: synthesis, characterization, and modification. Polymer 47:1511–1518

201. Lv J, Meng Y, He L, Qiu T, Li X, Wang H (2013) Novel epoxidized hyperbranched poly (phenylene oxide): synthesis and application as a modifier for diglycidyl ether of bisphenol A. J Appl Polym Sci 128:907–914

202. Theil F (1999) Synthesis of diaryl ethers: a long-standing problem has been solved. Angew Chem Int Ed 38:2345–2347

203. Luo L, Qiu T, Meng Y, Guo L, Yang J, Li Z, Cao X, Li X (2013) A novel fluoro-terminated hyperbranched poly(phenylene oxide) (FHPPO): synthesis, characterization, and application in low-*k* epoxy materials. RSC Adv 3:14509–14520

204. Ghosh A, Chatterjee S, Banerjee S, Komber H, Voit B (2011) Linear and hyperbranched poly (arylene ether)s from a new semifluorinated AB monomer. J Macromol Sci A Pure and Appl Chem 48:509–517

205. Frey H, Holter D (1999) Degree of branching in hyperbranched polymers. 3 Copolymerization of AB$_m$-monomers with AB and AB$_n$-monomers. Acta Polym 50:67–76

206. Mellace A, Hanson JE, Griepenburg J (2005) Hyperbranched poly(phenylene sulfide) and poly(phenylene sulfone). Chem Mater 17:1812–1817

207. Brandrup J, Immergut EH, Grulke EA (eds) (1999) Polymer handbook, 4th edn. Wiley, New York

208. De Girolamo Del Mauro A, Loffredo F, Venditto V, Longo P, Guerra G (2003) Polymorphic behavior of syndiotactic poly(*p*-chlorostyrene) and styrene/*p*-chlorostyrene cosyndiotactic random copolymers. Macromolecules 36:7577–7584

209. Bo Y, Yanmo C, Hao Y, Bin S, Meifang Z (2009) Kinetics of the thermal degradation of hyperbranched poly(phenylene sulfide). J Appl Polym Sci 111:1900–1904

210. Day M, Budgell DR (1992) Kinetics of the thermal degradation of poly(phenylene sulfide). Thermochim Acta 203:465–474

211. Yang MH (2002) On the thermal degradation of poly(styrene sulfone)s. V Thermogravimetric kinetic simulation of polyacrylamide pyrolysis. J Appl Polym Sci 86:1540–1548
212. Li XG, Huang MR (1999) Thermal decomposition kinetics of thermotropic poly (oxybenzoate-co-oxynaphthoate) Vectra copolyester. Polym Degrad Stab 64:81–90
213. Popescu C (1996) Integral method to analyze the kinetics of heterogeneous reactions under non-isothermal conditions A variant on the Ozawa–Flynn–Wall method. Thermochim Acta 285:309–323
214. Sun JT, Huang YD, Gong GF, Cao HL (2006) Thermal degradation kinetics of poly (methylphenylsiloxane) containing methacryloyl groups. Polym Degrad Stab 91:339–346
215. Núñez L, Fraga F, Núñez MR, Villanueva M (2000) Thermogravimetric study of the decomposition process of the system BADGE ($n=0$)/1,2 DCH. Polymer 41:4635–4641
216. Montserrat S, Málek J, Colomer P (1998) Thermal degradation kinetics of epoxy–anhydride resins: I.: influence of a silica filler. Thermochim Acta 313:83–95
217. Xu R, Liu H, Liu S, Li Y, Shi W (2008) Effect of core structure on the fluorescence properties of hyperbranched poly(phenylene sulfide). J Appl Polym Sci 107:1857–1864
218. Zeng Q, Li Z, Dong Y, Di C, Qin A, Hong Y, Ji L, Zhu Z, Jim CKW, Yu G, Li Q, Li Z, Liu Y, Qin J, Tang BZ (2007) Fluorescence enhancements of benzene-cored luminophors by restricted intramolecular rotations: AIE and AIEE effects. Chem Commun 2007(1):70–72. doi:10.1039/B613522F
219. Lam JWY, Chen J, Law CCW, Peng H, Xie Z, Cheuk KKL, Kwork HS, Tang BZ (2003) Silole-containing linear and hyperbranched polymers: synthesis, thermal stability, light emission, nano-dimensional aggregation, and optical power limiting. Macromol Symp 196:289–300
220. Tang BZ (2008) Construction of functional polymers from acetylenic triple-bond building blocks. Macromol Chem Phys 209:1303–1307
221. Haussler M, Qin A, Tang BZ (2007) Acetylenes with multiple triple bonds: a group of versatile A_n-type building blocks for the construction of functional hyperbranched polymers. Polymer 48:6181–6204
222. Peng H, Lam JWY, Tang BZ (2005) Hyperbranched poly(aryleneethynylene)s: synthesis, thermal stability and optical properties. Macromol Rapid Commun 26:673–677
223. Hong Y, Lam JWY, Tang BZ (2009) Aggregation-induced emission: phenomenon, mechanism and applications. Chem Commun 2009(29): 4332–4353. doi:10.1039/B904665H
224. Qin A, Lam JWY, Tang BZ (2010) Click polymerization. Chem Soc Rev 39:2522–2544
225. Mukamal H, Harris FW, Stille JK (1967) Diels–Alder polymers. III. Polymers containing phenylated phenylene units. J Polym Sci A Polym Chem 5:2721–2729
226. Loi S, Butt HJ, Hampel C, Bauer R, Wiesler UM, Müllen K (2002) Two-dimensional structure of self-assembled alkyl-substituted polyphenylene dendrimers on graphite. Langmuir 18:2398–2405
227. Andreitchenko EV, Clark CG Jr, Bauer RE, Lieser G, Müllen K (2005) Pushing the synthetic limit: polyphenylene dendrimers with "exploded" branching units—22-nm-diameter, monodisperse, stiff macromolecules. Angew Chem Int Ed 44:6348–6354
228. Tasdelen MA (2011) Diels–Alder "click" reactions: recent applications in polymer and material science. Polym Chem 2:2133–2145
229. Xu K, Peng H, Sun Q, Dong Y, Salhi F, Luo J, Chen J, Huang Y, Zhang D, Xu Z, Tang BZ (2002) Polycyclotrimerization of diynes: synthesis and properties of hyperbranched polyphenylenes. Macromolecules 35:5821–5834
230. Dong H, Zheng R, Lam JWY, Häussler M, Tang BZ (2005) A new route to hyperbranched macromolecules: syntheses of photosensitive poly(aroylarylene)s via 1,3,5-regioselective polycyclotrimerization of bis(aroylacetylene)s. Macromolecules 38:6382–6391
231. Stumpe K, Komber H, Voit B (2006) Novel branched polyphenylenes based on A_2/B_3 and AB_2/AB monomers via Diels–Alder cycloaddition. Macromol Chem Phys 207:1825–1833

232. Stumpe K, Eichhorn KJ, Voit B (2008) Characterisation of thin composite films from hyperbranched polyphenylene and thermolabile hyperbranched polycarbonate. Macromol Chem Phys 209:1787–1796
233. Pötzsch R, Voit B (2012) Thermal and photochemical crosslinking of hyperbranched polyphenylene with organic azides. Macromol Rapid Commun 33:635–639
234. Pötzsch R, Komber H, Stahl BC, Hawker CJ, Voit BI (2013) Radical thiol-yne chemistry on diphenylacetylene: selective and quantitative addition enabling the synthesis of hyperbranched poly(vinyl sulfide)s. Macromol Rapid Commun 34:1772–1778
235. Liu JG, Ueda M (2009) High refractive index polymers: fundamental research and practical applications. J Mater Chem 19:8907–8919
236. Pötzsch R, Stahl BC, Komber H, Hawker CJ, Voit BI (2014) High refractive index polyvinylsulfide materials prepared by selective radical mono-addition thiol–yne chemistry. Polym Chem 5:2911–2921
237. Lam JWY, Tang BZ (2005) Functional polyacetylenes. Acc Chem Res 38:745–754
238. Schluter AD, Wegner G (1993) Palladium and nickel catalyzed polycondensation – the key to structurally defined polyarylenes and other aromatic polymers. Acta Polym 44:59–69
239. Tour JM (1994) Soluble oligo- and polyphenylenes. Adv Mater 6:190–198
240. Watson MD, Fechtenkotter A, Mullen K (2001) Big is beautiful – "aromaticity" revisited from the viewpoint of macromolecular and supramolecular benzene chemistry. Chem Rev 101:1267–1300
241. Zheng R, Dong H, Peng H, Lam JWY, Tang BZ (2004) Construction of hyperbranched poly (alkenephenylene)s by Diyne polycyclotrimerization: single-component catalyst, glycogen-like macromolecular structure, facile thermal curing, and strong thermolysis resistance. Macromolecules 37:5196–5210
242. Zheng R, Haussler M, Dong H, Lam JWY, Tang BZ (2006) Synthesis, structural character-ization, and thermal and optical properties of hyperbranched poly(aminoarylene)s. Macro-molecules 39:7973–7984
243. Liu J, Zheng R, Tang Y, Haussler M, Lam JWY, Qin A, Ye M, Hong Y, Gao P, Tang BZ (2007) Hyperbranched poly(silylenephenylenes) from polycyclotrimerization of A2-type diyne monomers: synthesis, characterization, structural modeling, thermal stability, and fluorescent patterning. Macromolecules 40:7473–7486
244. Haussler M, Liu J, Zheng R, Lam JWY, Qin A, Tang BZ (2007) Synthesis, thermal stability, and linear and nonlinear optical properties of hyperbranched polyarylenes containing carba-zole and/or fluorene moieties. Macromolecules 40:1914–1925
245. Shi J, Jim CJW, Mahtab F, Liu J, Lam JWY, Sung HHY, Williams ID, Dong Y, Tang BZ (2010) Ferrocene-functionalized hyperbranched polyphenylenes: synthesis, redox activity, light refraction, transition-metal complexation, and precursors to magnetic ceramics. Mac-romolecules 43:680–690
246. Liu J, Deng C, Tseng NW, Chan CYK, Yue Y, Ng JCY, Lam JWY, Wang J, Hong Y, Sung HHY, Williams ID, Tang BZ (2011) A new polymerisation route to conjugated polymers: regio- and stereoselective synthesis of linear and hyperbranched poly(arylene chlorovinylene)s by decarbonylative polyaddition of aroyl chlorides and alkynes. Chem Sci 2:1850–1859
247. Schmaljohann D, Pötschke P, Haussler R, Voit BI, Froehling PE, Mostert B, Loontjens JA (1999) Blends of amphiphilic, hyperbranched polyesters and different polyolefins. Macro-molecules 32:6333–6339
248. Jang J, Hak Oh J, Moon SI (2000) Crystallization behavior of poly(ethylene terephthalate) blended with hyperbranched polymers: the effect of terminal groups and composition of hyperbranched polymers. Macromolecules 33:1864–1870
249. Hsieh TT, Tiu C, Simon GP (2001) Rheological behaviour of polymer blends containing only hyperbranched polyesters of varying generation number. Polymer 42:7635–7638
250. Nunez CM, Chiou BS, Andrady AL, Khan SA (2000) Solution rheology of hyperbranched polyesters and their blends with linear polymers. Rheological behaviour of polymer blends

containing only hyperbranched polyesters of varying generation number. Macromolecules 33:1720–1726

251. Li X, Zhang S, Wang H, Zhang C, Pang J, Mu J, Ma G, Wang G, Jiang Z (2011) Study of blends of linear poly(ether ether ketone) of high melt viscosity and hyperbranched poly(ether ether ketone). Polym Int 60:607–612

252. Tang H, Fan X, Shen Z, Zhou Q (2013) One-pot synthesis of hyperbranched poly(aryl ether ketone)s for the modification of bismaleimide resins. Polym Eng Sci 54:1675–1685

253. Hakme C, Stevenson I, Fulchiron R, Seytre G, Clement F, Odoni L, Rochat S, Varlet J (2005) Dielectric studies of hyperbranched aromatic polyamide and polyamide-6,6 blends. J Appl Polym Sci 97:1522–1537

254. Monticelli O, Oliva D, Russo S, Clausnitzer C, Potschke P, Voit B (2003) On blends of polyamide 6 and a hyperbranched aramid. Macromol Mater Eng 288:318–325

255. Huber T, Pötschke P, Pompe G, Häßler R, Voit B, Grutke S, Gruber F (2000) Blends of hyperbranched poly(ether amide)s and polyamide-6. Macromol Mater Eng 280–281:33–40

256. Böhme F, Clausnitzer C, Gruber F, Grutke S, Huber T, Potschke P, Voit B (2001) Hyperbranched poly(ether amide)s via nucleophilic ring opening reaction of oxazolines. High Perform Polym 13:S21–S31

257. Fang K, Li J, Ke C, Zhu Q, Zhu J, Yan Q (2010) Synergistic effect between a novel hyperbranched flame retardant and melamine pyrophosphate on the char forming of polyamide 6. Polym Plastics Technol Eng 49:1489–1497

258. Chen X, Jiao C, Li S, Sun J (2011) Flame retardant epoxy resins from bisphenol-A epoxy cured with hyperbranched polyphosphate ester. J Polym Res 18:2229–2237

259. Sari MG, Stribeck N, Moradian S, Zeinolebadi A, Bastani S, Botta S (2013) Correlation of nanostructural parameters and macromechanical behaviour of hyperbranched-modified polypropylene using time-resolved small-angle X-ray scattering measurements. Polym Int 62:1101–1111

260. Foix D, Ramis X, Ferrando F, Serra A (2012) Improvement of epoxy thermosets using a thiol-ene based polyester hyperbranched polymer as modifier. Polym Int 61:727–734

261. Qiang TT, Wang X (2007) Study on synthesis of hyperbranched polymer with terminal carboxyl and its effect of chrome-tanning assistant. PhD Thesis, Shanxi University of Science and Technology, China

262. Ren L, Zhao G, Qiang T, Wang X, Wang N (2013) Synthesis of amino-terminated hyperbranched polymers and their application in microfiber synthetic leather base dyeing. Textile Res J 83:381–395

263. Lei L, Wang H, Zhang Y, Li X, Mu J, Wang G, Jiang Z, Zhang S (2010) Preparation and characterization of a novel hyperbranched poly(aryl ether ketone) terminated with cobalt phthalocyanine to be used for oxidative decomposition of 2,4,6-trichlorophenol. Macromol Res 18:331–335

264. Zhang YH, Niu YM, Xu R, Wang GB, Jiang ZH (2006) Synthesis and characterization of poly(aryl ether sulfone)s with metallophthalocyanine pendant unit. J Appl Polym Sci 102:3457–3461

265. Zhang YH, Sun XB, Niu YM, Xu R, Wang GB, Jiang ZH (2006) Synthesis and characterization of novel poly(aryl ether ketone)s with metallophthalocyanine pendant unit from a new bisphenol containing dicyanophenyl side group. Polymer 47:1569–1574

266. Huang P, Gu A, Liang G, Yuan L (2012) Synthesis of epoxy-functionalized hyperbranched poly(phenylene oxide) and its modification of cyanate ester resin. J Appl Polym Sci 123:2351–2359

267. Fan Z, Jaehnichen K, Desbois P, Haussler L, Vogel R, Voit B (2009) Blends of different linear polyamides with hyperbranched aromatic AB_2 and $A_2 + B_3$ polyesters. J Polym Sci A Polym Chem 47:3558–3572

268. Mulkern TJ, Beck Tan NC (2000) Processing and characterization of reactive polystyrene/hyperbranched polyester blends. Polymer 41:3193–3203

269. Ke C, Li J, Fang K, Zhu Q, Zhu J, Yan Q (2011) Enhancement of a hyperbranched charring and foaming agent on flame retardancy of polyamide 6. Polym Adv Technol 22:2237–2243
270. Yan H, Chen Y (2010) Blends of polypropylene and hyperbranched poly(phenylene sulphide) for production of dyeable PP fibres. Iran Polym J 19:791–799
271. Lau WJ, Ismail AF, Misdan N, Kassim MA (2012) A recent progress in thin film composite membrane: a review. Desalination 287:190–199
272. Tang CY, Kwon YN, Leckie JO (2007) Probing the nano- and micro-scales of reverse osmosis membranes—a comprehensive characterization of physiochemical properties of uncoated and coated membranes by XPS, TEM, ATR-FTIR, and streaming potential measurements. J Membr Sci 287:146–156
273. Jadav GL, Singh PS (2009) Synthesis of novel silica-polyamide nanocomposite membrane with enhanced properties. J Membr Sci 328:257–267
274. Chiang YC, Hsub YZ, Ruaan RC, Chuang CJ, Tung KL (2009) Nanofiltration membranes synthesized from hyperbranched polyethyleneimine. J Membr Sci 326:19–26
275. Park SY, Kim SG, Chun JH, Chun BH, Kim SH (2012) Fabrication and characterization of the chlorine-tolerant disulfonated poly(arylene ether sulfone)/hyperbranched aromatic polyamide-grafted silica composite reverse osmosis membrane. Desalin Water Treat 43:221–229
276. Peighambardoust SJ, Rowshanzamir S, Amjadi M (2010) Review of the proton exchange membranes for fuel cell applications. Int J Hydrogen Energy 35:9349–9384
277. Colicchio I, Keul H, Sanders D, Simon U, Weirich TE, Moeller M (2006) Development of hybrid polymer electrolyte membranes based on the semi-interpenetrating network concept. Fuel Cells 6:225–236
278. Gode P, Hult A, Jannasch P, Johansson M, Karlsson LE, Lindbergh G, Malmström E, Sandquist D (2006) A novel sulfonated dendritic polymer as the acidic component in proton conducting membranes. Solid State Ionics 177:787–794
279. Itoh T, Hamaguchi Y, Uno T, Kubo M, Aihara Y, Sonai A (2006) Synthesis, ionic conductivity, and thermal properties of proton conducting polymer electrolyte for high temperature fuel cell. Solid State Ionics 177:185–189
280. Ghosh A, Sen SK, Dasgupta B, Banerjee S, Voit B (2010) Synthesis, characterization and gas transport properties of new poly(imide siloxane) copolymers from 4,4′-(4,4′-isopropylidenediphenoxy)bis(phthalic anhydride). J Membr Sci 364:211–218
281. Cornelius CJ, Marand E (2002) Hybrid silica-polyimide composite membranes: gas transport properties. J Membr Sci 202:97–118
282. Hibshman C, Cornelius CJ, Marand E (2003) The gas separation effects of annealing polyimide–organosilicate hybrid membranes. J Membr Sci 211:25–40
283. Hibshman C, Mager M (2004) Marand E (2004) Effects of feed pressure on fluorinated polyimide–organosilicate hybrid membranes. J Membr Sci 229:73–80
284. Suzuki T, Yamada Y (2006) Characterization of 6FDA-based hyperbranched and linear polyimide–silica hybrid membranes by gas permeation and ^{129}Xe NMR measurements. J Polym Sci B Polym Phys 44:291–298
285. Suzuki T, Yamada Y (2007) Effect of end group modification on gas transport properties of 6FDA-TAPOB hyperbranched polyimide—silica hybrid membranes. High Perform Polym 19:553–564
286. Suzuki T, Yamada Y, Itahashi K (2008) 6FDA-TAPOB hyperbranched polyimide-silica hybrids for gas separation membranes. J Appl Polym Sci 109:813–819
287. Wang H, Pang J, Zhou F, Zhang H, Jiang Z, Zhang S (2013) Synthesis and preparation of sulfonated hyperbranched poly(aryl ether ketone)–sulfonated linear poly(aryl ether ketone) blend membranes for proton exchange membranes. High Perform Polym 25:759–768
288. Suda T, Yamazaki K, Kawakami H (2010) Syntheses of sulfonated star-hyperbranched polyimides and their proton exchange membrane properties. J Power Sources 195:4641–4646
289. Suzuki T, Miki M, Yamada Y (2012) Gas transport properties of hyperbranched polyimide/hydroxy polyimide blend membranes. Eur Polym J 48:1504–1512

290. Hosseini SS, Teoh MM, Chung TS (2008) Hydrogen separation and purification in membranes of miscible polymer blends with interpenetration networks. Polymer 49:1594–1603
291. Low BT, Chung TS, Chen H, Jean YC, Pramoda KP (2009) Tuning the free volume cavities of polyimide membranes via the construction of pseudo-interpenetrating networks for enhanced gas separation performance. Macromolecules 42:7042–7054
292. Im H, Kim H, Kim CK, Kim J (2009) Enhancement of gas selectivities of hexafluoroisopropylidene-based polyimides with poly(methylmethacrylate) blending. Ind Eng Chem Res 48:8663–8669
293. Morisato A, Shen HC, Sankar SS, Freeman BD, Pinnau I, Casillas CG (1996) Polymer characterization and gas permeability of poly(1-trimethylsilyl-1-propyne) [PTMSP], poly (1-phenyl-1-propyne) [PPP], and PTMSP/PPP blends. J Polym Sci B Polym Phys 34:2209–2222
294. Robeson LM (1991) Correlation of separation factor versus permeability for polymeric membranes. J Membr Sci 62:165–185
295. Robeson LM (2008) The upper bound revisited. J Membr Sci 320:390–400
296. Trimble AR, Tully DC, Fréchet JMJ, Medeiros DR, Angelopoulos M (2000) Patterning of hyperbranched resist materials by electron-beam lithography. Polym Prepr 41:325–326
297. Okazaki M, Shibasaki Y, Ueda M (2001) New negative-type photosensitive polyimide based on hyperbranched poly(ether imide), a cross-linker, and a photoacid generator. Chem Lett 8:762–763
298. In I, Lee H, Fujigaya T, Okazaki M, Ueda M, Kim SY (2003) A new photoresist based on hyperbranched poly(ary1ene ether phosphine oxide). Polym Bull 49:349–355
299. Hong CS, Jikei M, Kikuchi R, Kakimoto M (2003) Chemically amplified photosensitive polybenzoxazoles based on tert-butoxycarbonyl protected hyperbranched poly (o-hydroxyamide)s. Macromolecules 36:3174–3179
300. Chen H, Yin J (2003) Synthesis of autophotosensitive hyperbranched polyimides based on 3,3′,4,4′-benzophenonetetracarboxylic dianhydride and 1,3,5-tris(4-aminophenoxy)benzene via end capping of the terminal anhydride groups by *ortho*-alkyl aniline. J Polym Sci A Polym Chem 41:2026–2035
301. Chen H, Yin J (2003) Preparation of auto-photosensitive hyperbranched co-polyimide by the condensation of 4,4′-(hexafluoroisopropy1idene)diphthalic anhydride and 3,3′,4,4′-benzophenonetetracarboxylic dianhydride with 1,3,5-tris(4-aminophenoxy)benzene through a stage addition reaction method. Polym Bull 50:303–310
302. Chen H, Yin J (2004) Synthesis and characterization of negative-type photosensitive hyperbranched polyimides with excellent organosolubility from an $A_2 + B_3$ monomer system. J Polym Sci A Polym Chem 42:1735–1744
303. Liu C, Zhao X, Li Y, Yang D, Wang L, Jin L, Chen C, Zhou H (2013) New autophoto-sensitive semiaromatic hyperbranched polyimides with excellent thermal stabilities and low birefringences. High Perform Polym 25:301–311
304. Zyss J (1994) Molecular nonlinear optics: materials, physics and devices. Academic, Boston
305. Li Z, Dong S, Li P, Li Z, Ye C, Qin J (2008) New PVK-based nonlinear optical polymers: enhanced nonlinearity and improved transparency. J Polym Sci A Polym Chem 46:2983–2993
306. Czech P, Okrasa L, Méchin F, Boiteux G, Ulanski J (2006) Investigation of the polyurethane chain length influence on the molecular dynamics in networks crosslinked by hyperbranched polyester. Polymer 47:7207–7215
307. Ren Q, Gong F, Jiang B, Zhang D, Fang J, Guo F (2006) Preparation of hyperbranched copolymers of maleimide inimer and styrene by ATRP. Polymer 47:3382–3389
308. Zhou Z, Yan D (2006) Distribution function of hyperbranched polymers formed by AB_2 type polycondensation with substitution effect. Polymer 47:1473–1479
309. Zhu Z, Li Z, Tan Y, Li Z, Li Q, Zeng Q, Ye C, Qin J (2006) New hyperbranched polymers containing second-order nonlinear optical chromophores: synthesis and nonlinear optical characterization. Polymer 47:7881–7888

310. Chang HL, Chao TY, Yang CC, Dai SA, Jeng RJ (2007) Second-order nonlinear optical hyperbranched polymers via facile ring-opening addition reaction of azetidine-2,4-dione. Eur Polym J 43:3988–3996

311. Xie J, Deng X, Cao Z, Shen Q, Zhang W, Shi W (2007) Synthesis and second-order nonlinear optical properties of hyperbranched polymers containing pendant azobenzene chromophores. Polymer 48:5988–5993

312. Bai Y, Song N, Gao JP, Sun X, Wang X, Yu G, Wang ZY (2005) A new approach to highly electrooptically active materials using cross-linkable, hyperbranched chromophore-containing oligomers as a macromolecular dopant. J Am Chem Soc 127:2060–2061

313. Xie J, Hu L, Shi W, Deng X, Cao Z, Shen Q (2008) Synthesis and nonlinear optical properties of hyperbranched polytriazole containing second-order nonlinear optical chromophore. J Polym Sci B Polym Phys 46:1140–1148

314. He N, Chen Y, Doyle J, Liu Y, Blau WJ (2008) Optical and nonlinear optical properties of an octasubstituted liquid crystalline copper phthalocyanine. Dyes Pigments 76:569–573

315. Zhang Y, Wang L, Wada T, Sasabe H (1996) One-pot synthesis of a new hyperbranched polyester containing 3,6-di-acceptor-substituted carbazole chromophores for nonlinear optics. Macromol Chem Phys 197:667–676

316. Pitois C, Wiesmann D, Lindgren M, Hult A (2001) Functionalized fluorinated hyperbranched polymers for optical waveguide applications. Adv Mater 13:1483–1484

317. Gao H, Yorifuji D, Wakita J, Jiang Z-H, Ando S (2010) In situ preparation of nano ZnO/hyperbranched polyimide hybrid film and their optical properties. Polymer 51:3173–3180

318. Jiang X, Wang H, Chen X, Li X, Lei L, Mu J, Wang G, Zhang S (2010) A novel photoactive hyperbranched poly(aryl ether ketone) with azobenzene end groups for optical storage applications. React Funct Polym 70:699–705

319. Maier G (2001) Low dielectric constant polymers for microelectronics. Prog Polym Sci 26:3–65

320. Volksen W, Miller RD, Dubois G (2010) Low dielectric constant materials. Chem Rev 110:56–110

321. Martin SJ, Godschalx JP, Mills ME, Shaffer EO II, Townsend PH (2000) Development of a low-dielectric-constant polymer for the fabrication of integrated circuit interconnect. Adv Mater 12:1769–1778

322. Somboonsub B, Thongyai S, Praserthdam P (2009) Dielectric properties and solubility of multilayer hyperbranched polyimide/polyhedral oligomeric silsesquioxane nanocomposites. J Appl Polym Sci 114:3292–3302

323. Banerjee S, Maier G, Burger M (1999) Novel poly(arylene ether)s with pendent trifluoromethyl groups. Macromolecules 32:4279–4289

324. Hedrick JL et al (1993) US Patent 5,776,990

325. Zhong B (2001) US Patent 6,197,913

326. Li Z, Wu W, Ye C, Qin J, Li Z (2010) New hyperbranched polyaryleneethynylene containing azobenzene chromophore moieties in the main chain: facile synthesis, large optical nonlinearity and high thermal stability. Polym Chem 1:78–81

327. Hu R, Lam JWY, Liu J, Sung HHY, Williams ID, Yue Z, Wong KS, Yuen MMF, Tang BZ (2012) Hyperbranched conjugated poly(tetraphenylethene): synthesis, aggregation-induced emission, fluorescent photopatterning, optical limiting and explosive detection. Polym Chem 3:1481–1489